NASA TN D-1808

TECHNICAL NOTE

D-1808

INVESTIGATION OF CATALYST BEDS FOR 98-PERCENT-CONCENTRATION HYDROGEN PEROXIDE

By Jack F. Runckel, Conrad M. Willis, and Leland B. Salters, Jr.

Langley Research Center
Langley Station, Hampton, Va.

1

NATIONAL AERONAUTICS AND SPACE ADMINISTRATION
WASHINGTON
June 1963

NATIONAL AERONAUTICS AND SPACE ADMINISTRATION

TECHNICAL NOTE D-1808

INVESTIGATION OF CATALYST BEDS FOR 98-PERCENT-CONCENTRATION HYDROGEN PEROXIDE

By Jack F. Runckel, Conrad M. Willis,
and Leland B. Salters, Jr.

SUMMARY

An investigation of the effect of variation in screen composition and arrangement on the performance of 90- and 98-percent-concentration hydrogen peroxide catalyst beds has been made. Conventional catalyst beds with certain modifications were found to be suitable for use with 98-percent-concentration hydrogen peroxide. Up to 25 silver screens were used without excessive melting of silver provided they were located at the upstream end of the bed. The use of 40-mesh silver screens afforded better starting response characteristics than 20-mesh screens. The use of 2-percent-concentration samarium nitrate, in lieu of 10 percent, was found to be adequate for treatment of silver screens under certain conditions. Bed life was sufficient for reaction-control-rocket missions. The tests covered environmental temperatures from 35° F to 82° F and a chamber pressure range from 100 to 315 pounds per square inch absolute.

INTRODUCTION

Hydrogen peroxide rockets have been widely used as upper atmosphere reaction controls for both aircraft (refs. 1 and 2) and aerospacecraft (refs. 3, 4, and 5). This monopropellant has been utilized because of the simplicity of operation, good response time, reliability, and a well-developed state of the art. (See ref. 6.) These existing systems all operate with a 90 percent by weight concentration of hydrogen peroxide which has been available for a number of years. (See ref. 7.) Recently, higher concentrations of hydrogen peroxide (up to 98 percent) have become available in commercial quantities (ref. 8) and the advantage of the higher specific impulses makes these concentrations attractive for reaction-control systems. (See refs. 3 and 9.) However, for high strength H_2O_2 to be competitive with other high-impulse reaction controls, such as the bipropellant systems, fast response times and reliable operating characteristics are required. (See ref. 10.) One of the problems inherent with 90-percent-concentration H_2O_2 has been poor starting characteristics under low environmental temperature conditions. It was therefore expected that the same difficulty would be encountered with higher strength H_2O_2. The problem is further complicated by the fact that the decomposition temperature of high strength H_2O_2 is of the same order of magnitude

as the melting point of silver, which at the present state of the art is the only catalyst suitable for this type of investigation.

Some preliminary work to define catalysts acceptable for high-strength hydrogen peroxide has been accomplished. (See refs. 6, 11, 12, and 13.) The objective of the present investigation was to study some simple catalyst bed arrangements that would be suitable for use with a 98-percent concentration of hydrogen peroxide in existing H_2O_2 hardware systems. Only commercially available wire screens were used to form the catalysts of the present investigation in order to avoid the complex fabrication and quality control required for plated wire and mixtures of materials such as reported in references 12 and 14. Start and decay times at various temperatures, catalyst deterioration, and catalyst bed efficiencies for four 98-percent H_2O_2 configurations were compared with some conventional 90-percent H_2O_2 catalyst arrangements and a preheat catalyst configuration.

Two decomposition chambers, 1 inch in diameter, were used as gas generators in the investigation. Response times for a similar H_2O_2 reaction-control rocket utilizing a catalyst preheat chamber for 90-percent H_2O_2 are included. Data were obtained at chamber pressures from about 100 to 315 pounds per square inch and at environmental temperatures from 35° F to 82° F. Corresponding thrust values up to 42 pounds were measured. All tests were conducted on static thrust stands with the jets exhausting to sea-level atmospheric pressure.

SYMBOLS

A_j area of nozzle throat, sq in.

D diameter, in.

F jet thrust, lb

F_i ideal thrust for complete isentropic expansion,

$$p_c A_j \sqrt{\left(\frac{2}{\gamma + 1}\right)^{\frac{\gamma+1}{\gamma-1}} \frac{2\gamma^2}{\gamma - 1}\left[1 - \left(\frac{p_a}{p_c}\right)^{\frac{\gamma-1}{\gamma}}\right]}$$

F_{p_c} rated thrust for motor as represented by height of chamber pressure trace, lb

I total impulse for motor as represented by area under the chamber pressure trace, lb-sec

N Nth cycle during cycling operation in which starting delay times have stabilized

p_a ambient pressure, psia

p_c decomposition chamber pressure, psia

p_f feed pressure, psig

p_v void space pressure, psia

Δp pressure drop across catalyst bed and distribution and support plates, psi

T temperature, ^oF

$T_{H_2O_2}$ liquid hydrogen peroxide temperature, ^oF

T_m motor temperature, ^oF

t accumulated run time, min

t_s starting delay time for chamber pressure buildup, sec

$\dot{w}$ propellant flow rate, lb/sec

γ ratio of specific heats of hydrogen peroxide decomposition products

MODEL AND APPARATUS

Decomposition Chambers

Decomposition chamber A.- The 90-percent-concentration hydrogen peroxide catalyst configurations were tested in a decomposition chamber that had been used for a previous hydrogen peroxide catalyst investigation. (See ref. 15.) The case of the original engine was modified to accommodate a shorter length catalyst bed and the chamber volume downstream of the support plate was reduced. A sketch of decomposition chamber A is shown in figure 1(a) and a photograph of the chamber and a typical catalyst is presented in figure 1(b). The nozzle had an expansion ratio of 1.77 which would produce about 20 pounds of thrust at a chamber pressure of 200 pounds per square inch when exhausting to sea-level atmospheric pressure. The catalyst bed loading at this condition was 15.3 lb/min/sq in. for 90-percent H_2O_2. The rocket case, the flanged head, and the support and distribution plates were constructed from 347 series stainless steel because of its compatibility with H_2O_2.

Decomposition chamber B.- Decomposition chamber B, as shown in figure 2, was a rocket motor of the type currently used for reaction control of missile upper stages. (See ref. 5.) The design of this motor was different from the others mainly in that it incorporated a catalyst scroll to initiate the decomposition

process. Hydrogen peroxide entered the motor through a centrally located stem (see fig. 2(a)) and passed out radially through holes in the side of the stem and through the scroll where decomposition began. The partially decomposed H_2O_2 then changed direction from radial to axial, and passed through the distribution plate and main catalyst bed where decomposition was completed. The products of decomposition were exhausted through a convergent-divergent nozzle at right angles to the motor center line. This motor produced about 24 pounds of thrust at a chamber pressure of 200 pounds per square inch absolute. At this condition the bed loading was about 8.7 lb/min/in.^{2}. The nozzle expansion ratio was about 10.0.

Decomposition chamber C.- After the test program had been completed on catalyst beds 1 to 5, it became difficult to prevent leaks of liquid H_2O_2 from decomposition chamber A. A new decomposition chamber "C" was designed by substituting the flared-tube sealing method for the flanges used in chamber A. A sketch and photograph of this unit, which incorporated a convergent nozzle, are shown in figure 3. Decomposition chamber C, which was used with beds 6 and 7, had some increase in void space volume and downstream chamber volume over that of decomposition chamber A. These increases in volume would tend to produce somewhat longer starting and decay times for decomposition chamber C. (See ref. 6.) With 98-percent-concentration hydrogen peroxide, decomposition chamber C would produce a thrust of about 21 pounds at a chamber pressure of 200 pounds per square inch. The catalyst bed loading for this unit at these conditions was 13.2 lb/min/sq in.

Catalyst Beds

Three catalyst beds were tested in decomposition chamber A with 90-percent hydrogen peroxide. A fourth 90-percent H_2O_2 configuration designed for a reaction-control system is included to provide representative data on existing state-of-the-art hydrogen peroxide decomposition systems. Four catalyst configurations designed for decomposition of 98-percent H_2O_2 were investigated to determine how their performance and life compared with typical 90-percent H_2O_2 systems The bed characteristics are presented in table I and the composition of a sample bed is given in figure 4.

Catalyst bed 1.- The first 90-percent H_2O_2 catalyst configuration was made to correspond to an arrangement that had been used by the NASA Langley Research Center for many years in turbojet-exit simulator investigations. (See refs. 16 and 17, for example.) This type of bed consists of a series of sets of one stain less steel to five silver screens over the length of the bed. This design assure complete decomposition of all the hydrogen peroxide and provides a high thrust efficiency. (See ref. 16.) The average life of these beds has been found to be about 2 hours. The silver screen catalyst was activated by oxidizing a 2-percent solution of samarium nitrate on the silver. The packing pressure was 1,000 pound per square inch. Details of the composition of catalyst bed 1 are given in figure 4. The anti-channel baffles were used in this and the other catalyst beds to reduce leakage of H_2O_2 around the edges of the screens.

Catalyst beds 2 and 3.- The compositions of catalyst beds 2 and 3 were based on arrangements that had been previously utilized for reaction controls.

(See ref. 6.) These units contained fewer silver screens than catalyst bed 1 (see table I) and the downstream section was filled with noncatalytic monel screens. The silver screens of bed 2 were treated with a 10-percent solution of samarium nitrate and bed 3 with a 2-percent solution. Beds 2 and 3 were similar in makeup except that bed 3 used flattened silver and regular silver screens alternated and therefore required some additional monel screens to make up the bed length. The flattened screens were formed by pressing the treated disks between two flat plates and reducing the thickness from about 0.026 inch to about 0.014 inch. The screens were flattened to permit more silver to be packed into a given space and also because it seemed probable that forcing the coating particles into the base metal would increase ion exchange during the catalytic decomposition process and thereby improve the response characteristics. Bed 3 was treated with 2-percent samarium nitrate to prevent unnecessary reduction in the size of the open spaces in the flattened screen. Both beds were packed at a pressure of 2,200 pounds per square inch.

Reaction-control-rocket bed.- Decomposition was initiated in the reaction-control-rocket bed by means of a scroll made of nickel screen plated with an alloy of gold and silver. The scroll was not treated with samarium nitrate. The remainder of the bed consisted of seventy-five 20-mesh silver screens followed by 5 monel 10-mesh screens. The silver screens were treated with 2-percent samarium nitrate and packing pressure was about 500 pounds per square inch. This bed and motor represented a typical reaction-control rocket and is presented here as a basis for comparison.

Catalyst beds for 98-percent-concentration H_2O_2.- The decomposition temperature for 90-percent-concentration H_2O_2, as used in the previous tests, is on the order of 1,364° F, whereas, that for 98-percent H_2O_2 is about 1,735° F (ref. 8). Since the melting point for silver is approximately 1,650° F, at the pressures used in this investigation (refs. 18 and 19), the problem of the melting of silver must be considered in the design of catalyst beds for 98-percent H_2O_2. The substitution of other catalysts, with higher melting points, instead of silver was considered, but, at the present state of the art, there appears to be no simple catalyst comparable to silver for overall effectiveness. Therefore, it was necessary to utilize the temperature gradient that exists in the catalyst bed to keep the melting of silver within acceptable limits. The temperature being lowest at the upstream end of the bed, the beds for 98-percent H_2O_2 were designed with silver screens located only at the upstream end of the bed and with a sufficient number of silver screens to initiate the decomposition process. The remainder of the bed consisted of screens made of high-melting-point materials, whose catalytic action, although small, when increased by the high temperature, would complete the decomposition process.

Catalyst bed 4.- In the initial configuration of bed 4, twenty 20-mesh silver screens were used, 55 nickel screens comprising the remainder of the bed. This bed failed to start; therefore the number of silver screens was increased to 35. The resulting bed configuration started easily and performed fairly satisfactorily during the test program; however, losses of silver by melting

were excessive. Exhaust temperatures indicated complete decomposition of H_2O_2. Packing pressure was 4,000 pounds per square inch.

Catalyst bed 5.- Based on experience with bed 4, the number of silver screens used in bed 5 was reduced to 25; however, 40-mesh screens were substituted for 20-mesh screens. The finer mesh screen, although decreasing the thickness of the individual screens and, therefore, also the thickness of the silver portion of the bed, increased the surface area of the silver in contact with H_2O_2. This bed gave good cycling starts even at the low environmental temperatures. The loss of silver due to melting appeared to be small. Exhaust temperatures indicated complete decomposition of H_2O_2. Packing pressure was 4,000 pounds per square inch.

Catalyst bed 6.- As indicated in table I, for bed 6 three 40-mesh silver screens were used at the upstream end followed by fifteen 20-mesh silver screens; 60 nickel screens comprised the remainder of the bed. This bed required a long break-in period and was rather difficult to start at low environmental temperatures; however, it improved gradually with use. This result seemed to indicate the need for more silver screens, especially, since the bed apparently did not completely decompose the H_2O_2. Exhaust temperatures did not exceed 1,650° F during the test program and reached this temperature only during the final tests. The loss of silver was less than that of bed 5. Packing pressure was 5,100 pounds per square inch.

Catalyst bed 7.- As shown in table I, bed 7 contained fourteen 20-mesh silver screens in the upstream part of the bed. The downstream part of the bed was composed of cobalt-coated nickel screens. Half of the total number of coated screens received an additional treatment with a proprietary substance. These screens with the additional coating were alternated with the cobalt-coated screens. Bed 7 required no break-in period and gave excellent starts from the first cycle. Starting response deteriorated rapidly with operating time, however, and became poor as compared with the other beds. This bed appeared to decompose H_2O_2 completely since it provided exhaust temperatures approaching the theoretical values. The loss of silver was small. Packing pressure was 5,100 pounds per square inch.

Test Apparatus

A line diagram of the ambient-temperature test apparatus is presented in figure 5(a). A solenoid valve started and stopped the flow of hydrogen peroxide. For intermittent operation, to simulate the operation of attitude-control rockets the solenoid-valve power circuit was opened and closed at regular intervals by a motor-driven cam. For steady-state operation the cam was not used. A $2\frac{1}{16}$-inch length of tubing was used between the solenoid valve and the motor to reduce feed back of heat from the motor to the valve. Propellant flow rate was measured by a rotating-vane-type flowmeter and was controlled by varying the nitrogen pressure in the feed tank. Temperatures were measured by thermocouples and recorded on strip charts. Thrust was measured by strain-gage-type load cells mounted on a flex-plate-supported platform, and pressures, by pressure transducers.

Propellant flow rate, thrust, and pressures were recorded by means of an oscillograph.

Environmental Control Chamber

An insulated aluminum enclosure cooled by a refrigeration unit comprised the environmental control chamber for low-temperature tests as shown in figure 6. The complete test apparatus including the hydrogen peroxide tank was housed within the chamber. The thrust balance was not used for low-temperature tests; otherwise, the apparatus was the same as that for ambient-temperature tests.

PROCEDURE

Typical oscillograph records are shown in figure 7. Three samples of oscillograph records are presented to illustrate the methods used to measure starting response and tail-off times. For the reaction-control rocket, as shown in figure 7(c), starting delay time was measured from the point at which the electrical signal to the valve was initiated, to the point at which the chamber pressure first reached the stabilized value. The latter point was defined as the intersection of a line tangent to the stabilized part of the curve and the first crossing by the chamber pressure trace. For the other catalyst beds, the terminal point of the starting delay time was defined as the intersection of the two lines as indicated in figure 7(a). Valve opening time was about 0.01 second.

Tail-off thrust which was used as a measure of tail-off delay time was derived from the area under the tail-off part of the chamber pressure trace as shown in figure 7(b). It may be noted that starting delay time and tail-off time both include the valve delay time since they were measured from the point that marked the initiation of the electrical signal to the valve. Valve closing time was about 0.01 second.

The traces for thrust F and propellant flow rate $\dot{w}$, as shown in figure 7(b), were not steady enough to provide coherent data for the cycling tests. The rising trend in the flow-rate trace was caused by lag due to instrumentation inertia. Thrust and flow rate were evaluated only for the steady-state tests, a sample of which is shown in figure 7(e). The lag in void pressure behind chamber pressure is believed to be associated with the change in state of the propellant fluid passing through the catalyst.

Because of its possible influence on the data presented in this paper, it should be noted that the H_2O_2 line to the motor was not blown out before the low environmental temperature tests. This practice is sometimes followed to eliminate the possibility of ice being in the line. An outline of the test program followed for beds 1 to 7 is presented in table II. As explained later, the reaction-control rocket received a warming pulse 10 minutes before data were taken.

RESULTS AND DISCUSSION

Catalysts For 90-Percent-Concentration Hydrogen Peroxide

Catalyst bed 1; decomposition chamber A.- Typical oscillograph records illustrating the starting delay and chamber pressure decay times for catalyst bed 1 are presented in figure 8. The initial start attempt at 35° F environmental temperature is shown in part (a) where it can be seen that no thrust was obtained during the first three cycles (that is, no decomposition took place and liquid H_2O_2 was observed coming out of the nozzle). Only partial chamber pressure was obtained during the fourth cycle, and complete chamber pressure buildup finally occurred on the fifth cycle. Figure 8(b) shows the response characteristics of catalyst bed 1 during the final 35° F environmental temperature run after about 7.3 minutes time on the bed. The unit fired on the second pulse with almost complete chamber pressure buildup. The response characteristics at an ambient temperature of 70° F are shown in figure 8(c).

The starting delay times for catalyst bed 1 are summarized in figure 9 for several environmental temperatures. At the initial 35° F low-temperature run with a start measured from the fourth valve pulse, the starting response time was 0.240 second and decreased to about 0.057 second after many cycles. The final 35° F test data showed improved start times which stabilized at 0.040 second. About the same start delay times of 0.040 second were obtained on the later cycles during the final runs at all environmental temperatures. This improvement is due to the heating of the catalyst and decomposition chamber even though cold propellant is being used.

The decay time for bed 1 is shown in figure 10 as a percent of maximum chamber pressure with time after the valve closing signal. The chamber pressure tail-off lasts about one-third of a second and the long decay time was probably due to the relatively large void and downstream chamber volumes of the decomposition chamber.

Hydrogen peroxide catalyst beds are known to have a limited life which is dependent upon a number of factors which are discussed in reference 6. Indications of deterioration of the catalyst generally are an increase in pressure drop across the bed and decreases in exhaust temperature. The resulting incomplete decomposition will also show up as a decrease in thrust efficiency.

The performance of catalyst bed 1 is presented in figures 11 and 12. The variation of measured and ideal thrust with chamber pressure is given in figure 11. As would be expected for such a short operating time, no loss in thrust with time can be detected for this catalyst bed. The thrust ratios shown in figure 12 also indicate no decrease with time. The thrust efficiency of about 91 percent appears somewhat low (see ref. 16) but is based on idealized weight flow rather than on measured weight flow for the isentropic thrust F_i and the conditions of operation were such that the jet was always underexpanded. Only a slight increase in pressure drop across the bed is apparent with accumulated operation time. The pressure drop for this bed was the highest of the series. The condition of the catalyst screens after 8 minutes of testing time is shown on the

photographs of figure 13. Very little erosion of the silver has occurred; this result is consistent with the bed pressure drop measurements.

Catalyst bed 2; decomposition chamber A.- Sample oscillograph records for catalyst bed 2 are presented in figure 14 and starting delay times in figure 15. The cold start response of bed 2 was superior to that of bed 1 in the initial tests; however, in the final tests the response of both beds was approximately the same because of the marked improvement of bed 1 with increase in operating time. The short initial pulse in figure 14(b) was caused by the failure to "zero" the pulsing cam at the start of the test. In the starting-delay-time figures, throughout this paper, when the lengths of these incomplete initial pulses were considerably shorter than normal, they were weighted as one-half cycle.

As an indication of tail-off response characteristics for bed 2, tail-off thrust over a range of operating conditions is presented in figure 16. These curves are presented for bed 2 only, since they are considered typical for all beds tested. The influence of temperature and operating time on tail-off response characteristics appears to be small.

The performance of catalyst bed 2 is shown in figures 17 and 18. Bed pressure drop and thrust ratio did not change appreciably during 8 minutes of operating time. An insight into the effect of bed design on pressure drop across a catalyst bed may be obtained by comparison of figures 12 and 18 which indicate pressure drop across beds 1 and 2, respectively. These figures show the pressure drop for bed 1 to be some three times as great as that for bed 2. Photographs of bed 2 (fig. 19) after 9 minutes operating time indicate that bed 2 was in good condition.

Catalyst bed 3; decomposition chamber A.- Bed 3 was similar to bed 2 except that half the silver screens were flattened, and that a 2-percent solution of samarium nitrate was used to treat the silver screen instead of a 10-percent solution. (See table I.) Representative oscillograph records are shown in figure 20 and starting response characteristics, in figure 21. Bed 3 required more cycles to start than bed 2, especially at the lower environmental temperatures. At 35° F the start times became longer with use as indicated by the fact that $2\frac{1}{2}$ cycles were required to start the bed initially whereas 8 cycles were required after about 8 minutes operation time. However, at all other test temperatures the starting response improved with increased operating time and the maximum attained was about 0.04 second starting delay times. The thrust performance of bed 3, as shown in figure 22, was almost identical to that of bed 2. Bed pressure drop and thrust ratio indicated no deterioration with operating time as shown in figure 23. Photographs of bed 3 in figure 24 also indicated no deterioration in the bed structure.

Reaction-control-rocket catalyst bed; decomposition chamber B.- Typical oscillograph records for the reaction-control rocket are presented in figure 25 and starting response characteristics, in figure 26. Both figures indicate better starting and more rapid response on all cycles for the reaction-control rocket configuration than for any other bed of this investigation. However, in comparing these data, it should be noted that warming pulses were made prior to all starts

for the reaction-control rocket according to standard practice for this type of rocket. The procedure for these reaction-control rocket tests was to bring the apparatus to the required temperature in the environmental control chamber, pulse the rocket twice, wait for 10 minutes, and then start the test. No warming pulses were made for the other beds before the start of the tests.

Another factor to be considered in comparing these data is the effect of the motor configuration and the design of the test apparatus on the response characteristics. Some aspects of motor and apparatus design which may influence response times are: the size of the void space and the elastic properties of the metal enclosing the void space; the size of the thrust chamber and nozzle; and the location of the fire valve. The rapid buildup and decay in pressures exhibited by this bed and motor, as indicated by the steep slopes of the traces, was probably due to motor design as well as to bed characteristics. Thrust and void pressure data were not obtained for this configuration.

98-Percent-Concentration Hydrogen Peroxide Catalyst Beds

Catalyst bed 4; decomposition chamber A.- As indicated previously, catalyst bed 4 could not be started in its original configuration, which included only 20 silver screens. It now seems probable that the original configuration may have been started, if a rigorous break-in technique, subsequently developed, had been used on bed 4; however, the number of silver screens was increased to 35 and the data presented in this paper were obtained with this second configuration.

Soon after the start of the test program, a white deposit was observed on the thermocouple located in the jet exhaust, and a similar deposit on the inner surface of the nozzle. This condition suggested that the silver catalyst was melting and being carried downstream in the products of decomposition. After 2.15 minutes of operating time on the bed, it was disassembled and inspected. The inspection revealed considerable melting of the silver screens and deposits of silver on the downstream nickel screens, retaining plate, and inner surfaces of the motor and nozzle. Using the same components, the bed was repacked in the motor and the test program was continued to completion.

Sample oscillograph records for bed 4 are shown in figure 27. The large differences in height of the traces between those of figure 27(a) and those of figures 27(b) and 27(c) are not significant, but were due to differences in attenuation settings on the oscillograph. Starting delay times as presented in figure 28, together with figure 27, indicate that the response characteristics of bed 4 with 98-percent H_2O_2 were of the same general type as those of the beds using 90-percent H_2O_2. The final delay time for all temperatures was on the order of 0.04 second.

A marked change in bed pressure drop and thrust performance may be observed between the data obtained before and after the inspection shutdown in figures 29 and 30. Values of $\Delta p/p_v$ averaged about 0.22 before and about 0.16 after the shutdown. Likewise, F/F_i values changed from about 0.93 to about 0.87. Two curves were used in figure 29, one for data before and one for data after

shutdown. The reason for these changes is not known. They did not occur in the other beds which were disassembled and inspected during their test programs. Conditions of the bed and motor at the end of the tests are shown in figures 31, 32, and 33.

Catalyst bed 5; decomposition chamber A.- Representative oscillograph records for catalyst bed 5 are presented in figure 34 and starting delay characteristics in figure 35. Bed 5 indicated perhaps the best overall response characteristics of the series of beds designed for 98-percent hydrogen peroxide, especially at low environmental temperatures. Catalytic action was initiated in this bed by twenty-five 40-mesh silver screens as shown in table I. Each 40-mesh screen afforded about 20 percent more surface area for catalytic action than a 20-mesh screen for the wire sizes used in this investigation. The twenty-five 40-mesh silver screens of bed 5 occupied about half as much bed length as the thirty-five 20-mesh silver screens of bed 4, but still provided about 85 percent as much surface area.

The reason for the better starting characteristics of bed 5, although it contained about 15-percent less catalyst surface area than bed 4, is not known; however, there may be some connection between the excessive erosion of the silver screens of bed 4 and its poorer starting performance. Part of the silver eroded from the screens was deposited downstream on the chamber walls and nickel screens and thereby increased the surface area of silver, but this increase was apparently not sufficient to compensate for the decrease in the samarium oxide coating.

The thrust performance and pressure drop of bed 5 are presented in figures 36 and 37. The fineness of the silver screen probably produced the rather high pressure drop ratio which averaged about 0.28. No significant change in pressure drop is indicated with bed operation time. The efficiency F/F_i started unusually high at about 0.95 but decreased to about 0.90 in 5.75 minutes operating time. It is not certain whether this was due to bed deterioration or to insufficient data points. The bed structure showed some melting, although considerably less than that for bed 4, as shown in photograph of figure 38; however, other than this melting, there was no indication of bed deterioration. The photograph of decomposition chamber A (fig. 39) shows the silver deposit on the inner surface of the nozzle at the end of the tests of bed 5.

Catalyst bed 6; decomposition chamber C.- During the test program it became increasingly difficult to prevent leaks in decomposition chamber A because of warpage in the flanges. Therefore, motor B was designed (fig. 3) with the flare-fitting method for sealing against leakage of the propellant. This motor proved to be satisfactory and was used for beds 6 and 7.

As shown in figure 4, bed 6 contained three 40-mesh silver screens followed by fifteen 20-mesh silver screens; these screens afforded considerably less catalytic surface area than that for bed 5 or bed 4. It was perhaps because of this small catalytic surface area that the break-in period for bed 6 was long and difficult and the exhaust temperatures were lower than those for previous beds at this stage of the tests. Bed 6, however, improved continuously throughout the test program but the exhaust temperatures never reached theoretical decomposition temperatures.

Sample oscillograph records and starting delay response times are presented in figures 40 and 41. The abscissa scale for response time figures was changed for beds 6 and 7 to accommodate the larger number of cycles recorded at the start of the tests. The effect of changing from motor A to motor B on catalyst respons data was not evaluated but it is believed to have been small. Response character istics for bed 6 were not consistent at an environmental temperature of 35° but a the higher temperatures were almost as favorable as those for bed 5.

Thrust performance and pressure drop for bed 6 is shown in figures 42 and 43 Bed pressure drop was about equal to that of bed 5, but thrust efficiency was unusually low, averaging slightly below 0.90. The low thrust efficiency is probably related to the inability of the bed to decompose completely the hydrogen peroxide as indicated by the relatively low exhaust temperatures.

As indicated in figures 44 and 45, the melting of the silver catalyst was less than that for previous beds, as would be expected from a consideration of th smaller number of silver screens used.

Catalyst bed 7; decomposition chamber C.- Bed 7 contained the smallest numbe of silver screens of any bed of this series, namely, fourteen 20-mesh screens. However, the downstream nickel screens were coated with catalytic substances, which apparently augmented the catalytic action of the bed. This bed was unique in that complete decomposition of hydrogen peroxide occurred at the first pulse of the break-in run. However, as shown in subsequent data, the initial good starting characteristics did not continue throughout the test program.

Typical oscillograph records for bed 7 are presented in figure 46 and starting delay characteristics in figure 47. Starting delay response times were greater than 0.04 second throughout the tests, even at ambient environmental temperatures, which indicated that bed 7 had the poorest starting characteristics of any bed tested in this program. In addition, starting times were erratic, as shown in figure 47, by the sudden breaks or shifts in the curves.

Since the previously tested beds having silver screens as the only catalyst did not show any degradation of performance for the short test period, it appears probable that the early decrease in catalytic activity of bed 7 was due to change in the coated nickel part of the bed only. Thrust performance of bed 7 was good, as shown in figures 48 and 49, and the thrust efficiency averaged 0.92. Thrust efficiency is presented for only part of the test, the data for the first part of the test having been lost because of faulty instrumentation. Bed pressure drop was the highest of the 98-percent series, averaging about 0.39 for values of $\Delta p/p_v$.

As indicated in figures 50 and 51, some melting of silver occurred although the number of silver screens was only 14. A further study of this bed may be warranted in view of the excellent initial starting characteristics.

The results of steady-state test points for all the beds are summarized in table III. Run times listed in the table are the accumulated operating times on the catalyst pack before the start of the test point.

Figure 52 presents a comparison of the starting characteristics of the best 90-percent H_2O_2 bed configuration (bed 2) with the best for 98-percent H_2O_2 (bed 5). Circles represent starting delay times at the beginning of a run and the squares, those after the temperatures have become stabilized. These data indicate that bed 5 was more adversely affected by low start temperatures but was slightly superior to bed 2 after temperatures had become stabilized. This result illustrates the fact that satisfactory catalyst beds for 98-percent H_2O_2 may be constructed of conventional materials presently used for 90-percent H_2O_2 beds.

CONCLUDING REMARKS

An investigation has been made of the effects of catalyst bed design and environmental temperatures on reaction-control-type rocket-motor performance and response characteristics using 90- and 98-percent concentrations of hydrogen peroxide. The results of the investigation indicate that a satisfactory catalyst bed may be developed for 98-percent-concentration hydrogen peroxide comparable in response characteristics with conventional 90-percent catalyst beds, but exploiting the inherently greater specific impulse available from 98-percent-concentration hydrogen peroxide.

Although the melting point of silver is in the same temperature range as the decomposition temperature of 98-percent hydrogen peroxide, the excellent low-temperature catalytic power of silver may be utilized to initiate the decomposition process by locating the silver screens at the upstream end of the bed. The remainder of the decomposition was completed by heat in conjunction with inert metal screens. It was indicated that 25 silver screens may be used without excessive melting of the silver and yet provide satisfactory starting characteristics at low environmental temperatures. In providing good response characteristics 40-mesh silver screens appear to be superior to 20-mesh screens. The use of 2-percent concentration samarium nitrate in treating silver screens may be preferable in some cases to the use of 10-percent concentration, in that the former provides adequate catalytic action without unduly increasing pressure drop across the bed. Post-test inspections of the beds indicate that bed life was of sufficient duration for the types of missions required of reaction-control rockets. Of the four catalyst beds designed for use with 98-percent H_2O_2, the best overall performance was exhibited by bed 5.

Langley Research Center,
National Aeronautics and Space Administration,
Langley Station, Hampton, Va., March 27, 1963.

REFERENCES

1. Love, James E., and Stillwell, Wendell H.: The Hydrogen-Peroxide Rocket-Reaction-Control System for the X-1B Research Airplane. NASA TN D-185, 1959.

2. Reisert, Donald, and Adkins, Elmor J.: Flight and Operational Experiences With Pilot-Operated Reaction Controls. ARS No. 1674-61, American Rocket Soc., Mar. 1961.

3. Sanscrainte, Willard: Hydrogen Peroxide Attitude Control Systems. Paper Presented at Fourth Symposium on Ballistic Missile and Space Technology (Los Angeles, Calif.), Aug. 24-27, 1959.

4. Wanhainen, John P., Ross, Phil S., and DeWitt, Richard L.: Effect of Propellant and Catalyst Bed Temperatures on Thrust Buildup in Several Hydrogen Peroxide Reaction Control Rockets. NASA TN D-480, 1960.

5. Anon.: Hydrogen Peroxide Reaction Control Systems for Missile Attitude Control. Rep. No. UNC-230, Walter Kidde & Co., Inc., Nov. 1959.

6. Bollinger, Loren E., Goldsmith, Martin, and Lemmon, Alexis W., Jr., eds.: Liquid Rockets and Propellants. Academic Press, Inc. (New York), 1960, pp. 589-617.

7. Schumb, Walter C., Satterfield, Charles N., and Wentworth, Ralph L.: Hydroge Peroxide. Reinhold Pub. Corp. (New York), c.1955.

8. Bloom, Ralph, Jr., and Brunsvold, Norris J.: Anhydrous Hydrogen Peroxide as a Propellant. Chemical Engineering Progress, vol. 53, no. 11, Nov. 1957, pp. 541-547. (Also available as Bull. No. 93, Becco Chemical Div., Food Machinery and Chemical Corporation.)

9. Anon.: High Strength Hydrogen Peroxide Monopropellant and Bipropellant Performance Data. Bull. No. 107, Becco Chemical Div., Food Machinery and Chemical Corp.

10. Williams, O. S.: Performance and Reliability of Attitude Control Rocket Systems. [Preprint] 952-59, American Rocket Soc., Nov. 1959.

11. Fisher, J. G., and Zeilberger, E. J.: Catalyst Design Keeps Up With H_2O_2 Progress. Space/Aeronautics, vol. 35, no. 5, May 1961, pp. 84-87.

12. Ahlert, Robert C.: Applied Research of Hydrogen Peroxide, Quarterly Progress Report for Period Ending 30 September, 1958. R-1199-P (Contract NOas 56-1052d), Rocketdyne, Nov. 17, 1958.

13. Anon.: State of the Art With Catalyst Packs for Use With Becco 98% H_2O_2 and a Discussion of the Problem. Inorganic Chemicals Div., Food Machinery and Chemical Corp.

14. Gancy, A. B.: Metal Mixtures as Catalysts for the Decomposition of Concentrated Hydrogen Peroxide. Tech. Rep. 224-2 (Contract NOas 59-689c), Central Res. Lab., Food Machinery and Chemical Corp., June 30, 1959.

15. Willis, Conrad M.: The Effect of Catalyst-Bed Arrangement on Thrust Buildup and Decay Time for a 90 Percent Hydrogen Peroxide Control Rocket. NASA TN D-516, 1960.

16. Runckel, Jack F., and Swihart, John M.: A Hydrogen Peroxide Hot-Jet Simulator for Wind-Tunnel Tests of Turbojet-Exit Models. NASA MEMO 1-10-59L, 1959.

17. Swihart, John M., and Mercer, Charles E.: Investigation at Transonic Speeds of a Fixed Divergent Ejector Installed in a Single-Engine Fighter Model. NACA RM L57L10a, 1958.

18. Allen, N. P.: The Effect of Pressure on the Liberation of Gases From Metals (With Special Reference to Silver and Oxygen). Jour. Inst. Metals, vol. 49, no. 2, 1932, pp. 317-340.

19. Brinkley, S. R., Jr., Smith, R. W., Jr., and Edwards, H. E.: Performance Calculations of Hydrogen Peroxide as a Monopropellant - II. Heterogeneous Systems. Rep. PX3-107/14, Bur. Mines, U.S. Dept. Interior, 1953.

16

TABLE I.- CATALYST BED ASSEMBLY CHARACTERISTICS

Bed	Length, in.	Screen arrangement	Number of screens		Motor	Packing pressure, psi
			Active	Total		
90-percent H_2O_2 decomposition						
1	1.38	1 distribution plate 1 antichannel baffle 1 piece 20 mesh, 0.014 stainless-steel screen and 5 pieces 20 mesh, 0.014 silver screen, 2% $Sm(NO_3)_3$ 2 sets, 1 stainless and 5 silver, as above 1 antichannel baffle 15 sets, 1 stainless and 5 silver, as above 8 pieces 20 mesh, 0.014 stainless-steel screen 1 support plate	90	116	A	1,000
2	1.38	2 pieces 20 mesh, 0.014 stainless-steel screen 1 antichannel baffle 20 pieces 20 mesh, 0.014 silver screen, 10% $Sm(NO_3)_3$ 1 antichannel baffle 40 pieces 20 mesh, 0.014 silver screen 2 pieces 24 mesh, 0.014 monel screen 13 pieces 10 mesh, 0.025 monel screen	60	77	A	2,200
3	1.38	2 pieces 20 mesh, 0.014 stainless-steel screen 1 antichannel baffle 20 pieces 20 mesh, 0.014 silver screen, 2% $Sm(NO_3)_3$ (Flattened and regular screens alternated) 1 antichannel baffle 40 pieces 20 mesh, 0.014 silver screen, 2% $Sm(NO_3)_3$ (Flattened and regular screens alternated) 2 pieces 24 mesh, 0.014 monel screen 17 pieces 10 mesh, 0.025 monel screen	60	81	A	2,200
Reaction-control rocket	1.22	1 scroll, 7/16 in. wide, 20 mesh, 0.014 nickel screen plated with a gold and silver alloy 25 pieces 20 mesh, 0.014 silver screen, 2% $Sm(NO_3)_3$ 1 antichannel baffle 25 pieces 20 mesh, 0.014 silver screen, 2% $Sm(NO_3)_3$ 1 antichannel baffle 25 pieces 20 mesh, 0.014 silver screen, 2% $Sm(NO_3)_3$ 5 pieces 10 mesh, 0.025 monel screen	75 plus scroll	80	B	500
98-percent H_2O_2 decomposition						
4	1.50	2 pieces 20 mesh, 0.014 stainless-steel screen 1 antichannel baffle 35 pieces 20 mesh, 0.014 silver screen, 2% $Sm(NO_3)_3$ 1 antichannel baffle 55 pieces 20 mesh, 0.015 nickel screen	35	92	A	4,000
5	1.50	2 pieces 20 mesh, 0.014 stainless-steel screen 1 antichannel baffle 25 pieces 40 mesh, 0.010 silver screen, 2% $Sm(NO_3)_3$ 1 antichannel baffle 60 pieces 20 mesh, 0.015 nickel screen	25	87	A	4,000
6	1.50	1 piece, 14 x 88 mesh, dutch weave stainless-steel screen 1 antichannel baffle 1 piece 20 mesh, 0.014 stainless-steel screen 3 pieces 40 mesh, 0.010 silver screen, 2% $Sm(NO_3)_3$ 15 pieces 20 mesh, 0.014 silver screen, 10% $Sm(NO_3)_3$ 1 piece 20 mesh, 0.015 nickel screen 1 antichannel baffle 65 pieces 20 mesh, 0.015 nickel screen	18	86	C	5,100
7	1.50	1 antichannel baffle 14 pieces 20 mesh, 0.014 silver screen, $Sm(NO_3)_3$ 1 antichannel baffle 1 piece 20 mesh, 0.015 nickel screen with cobalt plate 1 piece 20 mesh, 0.015 nickel screen with proprietary treatment 26 sets of two coated nickel screens as above	14	68	C	5,100

TABLE II.- TEST PROGRAM FOR CATALYST BED CONFIGURATIONS

[Standard feed pressures for 90-percent catalysts: 475 psi for beds 1 and 2, 300 psi for bed 3. Standard chamber pressure for 98-percent catalyst: 200 psi.]

p_f, psi	p_c, psi	T, °F	Duration, sec	Remarks
Break-in runs				
200 to 250		Ambient	5 to 25	Operate at fixed feed pressure and run until jet is dry
350		Ambient	5 to 25	
475 to 500		Ambient	5 to 25	
Initial cold start				
Standard	Standard	35	15	Cycle run[1]
Standard	Standard	45	15	Cycle run[1]
Standard	Standard	60	15	Cycle run[1]
Standard	Standard	35	15	Steady run[2]
Ambient-temperature runs				
Standard	Standard	Ambient	5	Pulse start[1]
200 to 525 in 50-psi steps		Ambient	10 each step	Chamber pressure calibration
Standard	Standard	Ambient	5	Pulse start[1]
Standard	Standard	Ambient	30	Efficiency run
Standard	Standard	Ambient	5	Pulse start[1] (hardware hot)
[3]400	150	Ambient	30	Efficiency run
[3]475	200	Ambient	30	Efficiency run
[3]525	250	Ambient	30	Efficiency run
Standard	Standard	Ambient	5	Pulse start[1]
Standard	Standard	Ambient	30	Pulse start[2]
Standard	Standard	Ambient	15	Cycle run at 1/sec
Standard	Standard	Ambient	15	Cycle run at 2/sec
Standard	Standard	Ambient	15	Cycle run[4] at 5/sec or 10/sec
475	Standard	Ambient	30	Efficiency run[4]
Final cold start runs				
Standard	Standard	35	5	Cycle run[1]
Standard	Standard	35	15	Cycle run[1]
Standard	Standard	45	15	Cycle run[1]
Standard	Standard	60	15	Cycle run[1]
Final ambient run				
Standard	Standard	Ambient	90 to 180	Continuous cycle[2]

[1]Standard 2 cycles/sec run for pulse starts - valve open 250 milliseconds, valve closed 250 milliseconds.

[2]For 98-percent catalysts only.

[3]Noted p_f set when p_c calibration not available at time of run.

[4]For 90-percent catalysts only.

TABLE III.- STEADY-STATE TESTS OF CATALYST CONFIGURATIONS

Run	H_2O_2 temperature, °F	Feed pressure, psi	Void pressure, psi	Chamber pressure, psi	Bed Δp, psi	Flow rate, lb/sec	Measured thrust, lb	F/F_i	Duration, min
Catalyst bed 1									
17-1	74	265	260.8	109.2	151.6	0.093	10.97	0.927	0.55
17-2	74	653	603.8	284.3	319.5		31.18	.877	.60
20-2	66	250	243.2	101.6	141.6	.088	9.56	.878	1.80
20-3	66	300	279.4	115.8	163.6	.103	11.57	.909	1.97
20-4	66	350	316.9	131.7	185.2	.119	13.42	.904	2.13
20-5	66	400	357.1	148.9	208.2	.137	15.75	.920	2.30
20-6	66	440	389.3	164.2	225.1	.151	17.65	.921	2.47
20-7	66	475	423.5	179.2	244.3	.164	19.77	.932	2.63
20-8	66	525	458.3	194.1	264.2	.178	21.24	.914	2.80
21-2	72	475	398.7	195.2	203.5		20.25	.866	3.00
21-4	72	475	339.1	139.5	199.6	.127	14.29	.900	3.50
22-3	64	475	402.0	158.8	243.2	.145	16.40	.889	3.67
22-5	64	475	301.5	121.1	180.4	.108	12.44	.927	4.00
22-6	66	525	408.1	160.0	248.1	.145	16.68	.897	4.08
23-8	68	475	414.8	158.1	256.7	.141	16.46	.897	6.50
23-10	68	475	365.2	148.3	216.9	.131	15.59	.916	6.83
Catalyst bed 2									
31-3	80	250	208.5	164.9	43.6	0.155	16.84	0.875	1.10
31-5	80	300	235.3	187.7	47.6	.181	19.77	.884	1.27
31-7	80	350	258.7	208.9	49.8	.204	22.33	.885	1.43
31-9	80	400	289.6	233.3	56.3	.233	25.58	.893	1.60
31-11	80	440	308.3	250.4	57.9	.250	27.59	.889	1.77
31-13	80	475	308.4	251.4	57.0	.250	27.81	.893	1.93
31-15	80	528	331.8	271.0	60.8	.278	30.75	.907	2.10
32-3	80	475	320.4	262.1	58.3	.260	27.32	.837	2.51
32-4	80	475	313.0	256.1	56.9	.257	26.94	.848	2.52
32-9	80	475	317.0	261.8	55.2	.264	27.97	.858	2.68
32-10	80	475	309.0	254.8	54.2	.261	27.76	.880	3.55
32-15	82	440	292.2	242.1	50.1	.239	26.89	.902	4.38
32-16	82	440	274.1	228.2	45.9	.225	25.53	.916	4.55
32-18	82	525	302.2	251.3	50.9	.253	28.46	.913	5.12
32-19	82	525	270.7	223.1	47.6	.222	25.91	.952	5.29
32-26	75	475	298.3	244.7	53.6	.248	27.92	.925	6.04
32-27	75	475	272.1	223.5	48.6	.231	25.75	.943	6.21
33-2	77		340.6	283.1	57.5	.309	31.18	.875	6.50
33-4	77		338.5	282.4	56.1	.310	31.34	.882	6.58
36-2	86	485	355.2	288.4	66.8	.302	32.37	.891	8.07
36-3	86	485	357.2	286.5	70.7	.310	32.75	.908	8.23

TABLE III.- STEADY-STATE TESTS OF CATALYST CONFIGURATIONS - Continued

Run	H_2O_2 temperature, °F	Feed pressure, psi	Void pressure, psi	Chamber pressure, psi	Bed Δp, psi	Flow rate, lb/sec	Measured thrust, lb	F/F_i	Duration, min
Catalyst bed 3									
37-2	83	475	344.4	280.7	63.7	0.298	31.07	0.880	0.10
37-3	83	350	280.8	225.0	55.8	.226	24.50	.891	.18
39-2	74	250	213.1	170.9	42.2	.166	17.11	.853	1.18
39-4	74	300	248.0	198.4	49.6	.195	21.29	.894	1.35
39-6	74	350	276.8	222.5	54.3	.223	24.34	.897	1.52
39-9	74	400	298.9	245.3	53.6	.257	26.62	.878	1.67
39-11	74	475	342.5	278.9	63.6	.296	31.07	.887	1.83
39-13	74	530	366.6	299.5	67.1	.333	33.95	.894	2.00
39-16	71	295	248.0	194.6	53.4	.190	20.70	.889	2.35
39-17	71	295	242.6	193.4	49.2	.191	20.59	.891	2.52
39-18	71	295	244.0	193.4	50.6	.195	20.97	.907	2.68
40-3	72	295	242.6	194.3	48.3	.195	20.59	.886	3.10
40-4	72	295	242.6	194.6	48.0	.198	20.81	.893	3.27
40-5	72	295	242.6	194.3	48.3	.200	20.81	.895	3.43
41-3	72	325	267.5	205.8	61.7	.219	22.92	.924	3.93
41-19	73	295	236.0	196.9	39.1	.192	21.08	.893	5.68
Catalyst bed 4									
44-1	73	200	183.1	146.0	37.1	0.116	15.21	0.909	0.63
44-2	79	350	297.0	225.5	71.5	.193	26.50	.958	.75
44-3	80	500	398.9	306.2	92.7	.261	36.47	.934	.87
44-4	80	400	337.9	256.2	81.7	.220	30.20	.945	.99
44-5	80	400	335.2	260.0	75.2	.223	30.37	.934	1.23
48-2	77	450	356.6	303.7	52.9	.247	33.25	.859	2.69
48-3	77	400	322.4	269.6	52.8	.224	29.67	.877	2.81
48-4	77	350	277.7	236.7	41.0	.196	25.56	.875	2.93
48-5	77	300	249.2	207.9	41.3	.172	22.21	.881	3.05
48-6	77	250	217.9	177.7	40.2	.147	18.97	.902	3.17
48-7	77	200	178.6	146.9	31.7	.117	15.27	.905	3.29
48-10	77	400	318.9	264.2	54.7	.218	29.03	.877	3.62
49-6	78	305	257.4	215.1	42.3	.171	22.55	.860	4.20
49-10	78	210	176.4	150.1	26.3	.117	14.57	.841	4.70
49-14	78	400	325.5	270.1	55.4	.210	28.22	.831	5.20
51-5	35	305	254.9	217	37.0				6.82

TABLE III.- STEADY-STATE TESTS OF CATALYST CONFIGURATIONS - Continued

Run	H_2O_2 temperature, °F	Feed pressure, psi	Void pressure, psi	Chamber pressure, psi	Bed Δp, psi	Flow rate, lb/sec	Measured thrust, lb	F/F_i	Duration, min
Catalyst bed 5									
54-1	82	200	193.8	131.4	62.4				0.33
54-2	82	250	297.3	211.5	85.8				.47
54-3	82	500	384.8	289.1	95.7				.55
57-1	38	335	292.2	211.1	81.1	0.174			1.47
58-3	72	200	186.4	130.4	56.0	.100	13.82	0.942	2.18
58-5	72	250	235.3	167.7	67.6	.135	18.91	.960	2.35
58-7	72	300	270.8	197.2	73.6	.161	22.21	.935	2.52
58-9	72	350	307.0	227.3	79.7	.185	25.85	.926	2.68
58-12	78	335	297.6	216.5	81.1	.181	24.69	.935	3.20
58-14	78	400	344.5	255.5	89.0	.212	28.51	.894	3.37
58-16	78	450	380.0	279.5	100.5	.236	32.56	.923	3.53
58-18	81	335	293.6	219.7	73.9	.178	24.46	.911	3.62
58-22	81	335	292.9	214.3	78.6	.174	23.83	.913	4.15
59-5	74	270	248.6	174.0	74.6		18.39	.894	5.23
59-9	71	450	377.3	272.5	104.8		31.00	.903	5.73
Catalyst bed 6									
65-2	62	315	274.2	195.3	78.9	0.170	20.70	0.893	2.53
65-3	62	200	187.7	132.6	55.1	.112	13.54	.916	2.70
65-4	62	200	189.1	135.8	53.3	.113	13.82	.910	2.78
65-5	62	250	229.9	163.3	66.6	.140	16.85	.893	2.87
65-6	62	300	264.5	191.8	73.7	.165	19.54	.861	3.03
65-7	62	350	297.6	221.3	76.3	.191	23.64	.882	3.20
65-8	62	400	336.5	247.3	89.2	.218	27.20	.897	3.37
65-10	60	315	370.0	271.6	98.4	.235	29.00	.860	3.61
65-11	60	450	275.5	195.6	79.9	.168	21.10	.909	3.77
65-12	60	315	276.9	199.8	77.1	.171	21.45	.901	3.87
65-13	60	315	276.2	200.7	75.5	.172	21.56	.902	4.04
65-14	60	315	277.5	200.4	77.1	.172	21.70	.910	4.21
65-17	65	315	271.5	196.6	74.9	.169	20.60	.882	4.37
65-18	65	315	274.8	198.5	76.3	.171	20.54	.870	4.62
65-19	65	315	276.2	197.9	78.3	.172	20.75	.882	4.87
66-1	65	230	213.9	147.2	66.7	.128	14.69	.880	5.37
66-2	65	230	215.3	152.6	62.7	.131	14.86	.854	5.62
66-3	65	230	213.9	152.6	61.3	.132	15.67	.901	5.79
66-4	65	400	337.9	241.0	96.9	.214	25.39	.862	5.87
66-5	65	400	337.9	244.1	93.8	.217	26.37	.883	6.12
66-6	65	400	339.9	242.9	97.0	.218	26.66	.898	6.37

TABLE III.- STEADY-STATE TESTS OF CATALYST CONFIGURATIONS - Concluded

Run	H_2O_2 temperature, °F	Feed pressure, psi	Void pressure, psi	Chamber pressure, psi	Bed Δp, psi	Flow rate, lb/sec	Measured thrust, lb	F/F_i	Duration, min
Catalyst bed 7									
80-1	85	200	144.5	84.2	60.3	0.064	7.92	0.925	8.68
80-2	85	250	141.7	84.9	56.8	.065	7.92	.917	8.85
80-3	85	300	162.9	97.4	65.5	.078	9.68	.946	9.18
80-4	85	350	186.4	112.9	73.5	.094	11.18	.915	9.43
80-5	85	400	216.4	129.9	86.5	.110	13.26	.918	9.68
80-6	85	450	240.0	142.4	97.6	.122	14.40	.895	9.93
80-7	82	450	248.5	151.2	97.3	.129	15.65	.908	10.02
80-8	82	500	277.2	170.0	107.2	.146	17.80	.900	10.29
80-9	82	600	324.1	197.5	126.6	.171	20.77	.883	10.54
80-10	82	200	129.0	74.3	54.7	.052	7.01	.958	10.88
80-11	82	300	181.5	107.9	73.6	.087	10.82	.934	11.05

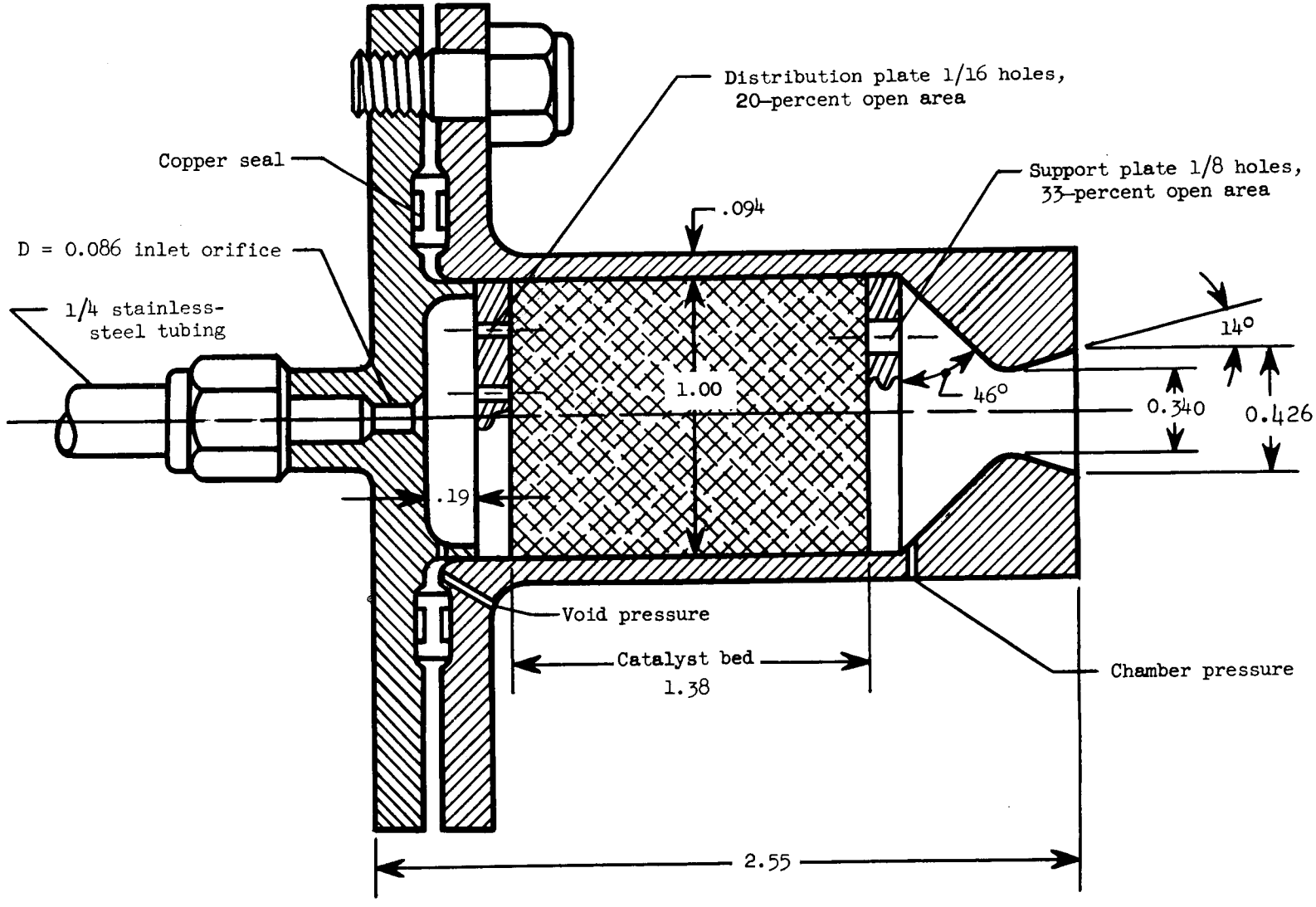

(a) Sketch of decomposition chamber.

Figure 1.- Hydrogen peroxide decomposition chamber A. All linear dimensions are in inches.

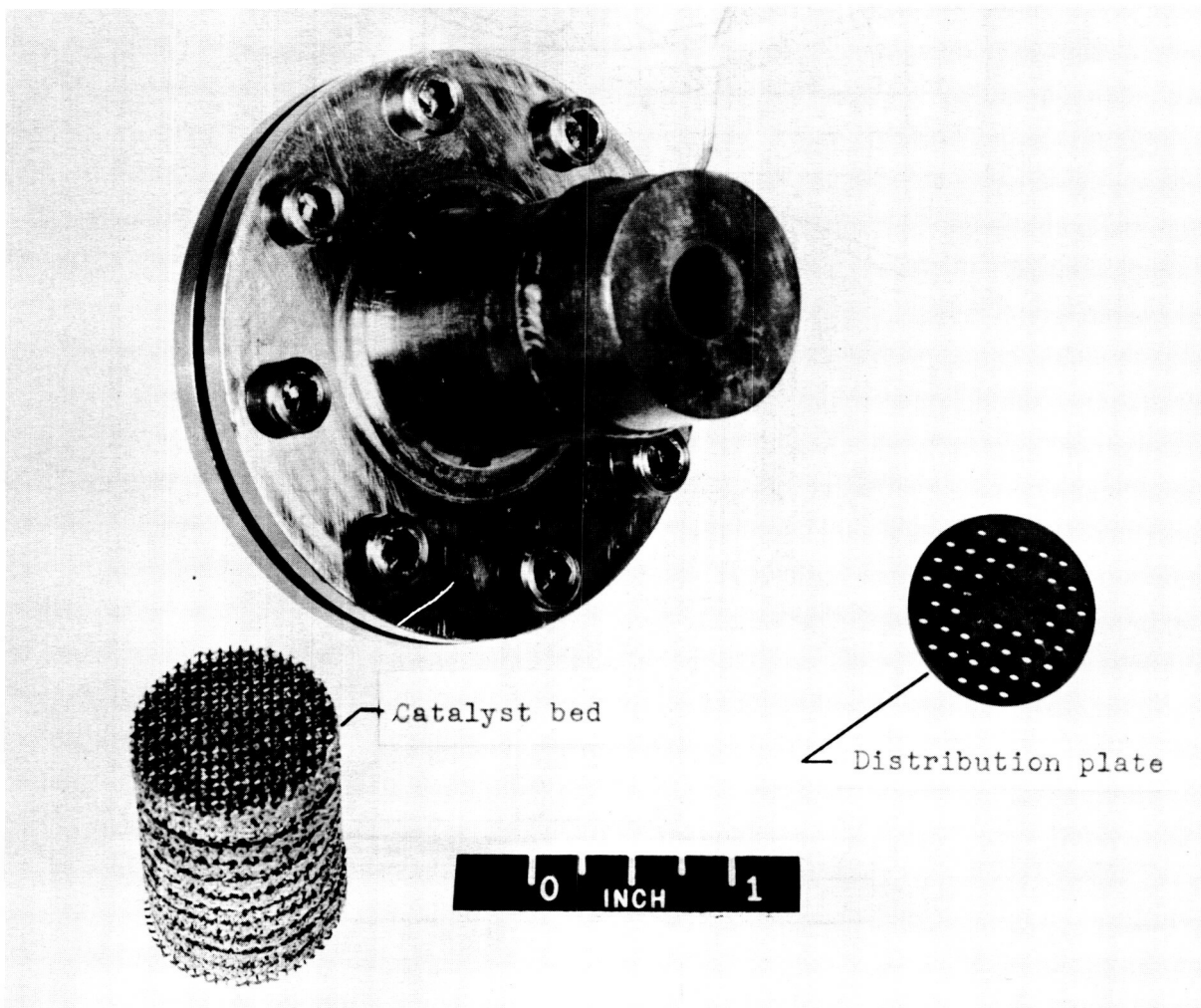

(b) Photograph of decomposition chamber and typical catalyst. L-59-5984.1

Figure 1.- Concluded.

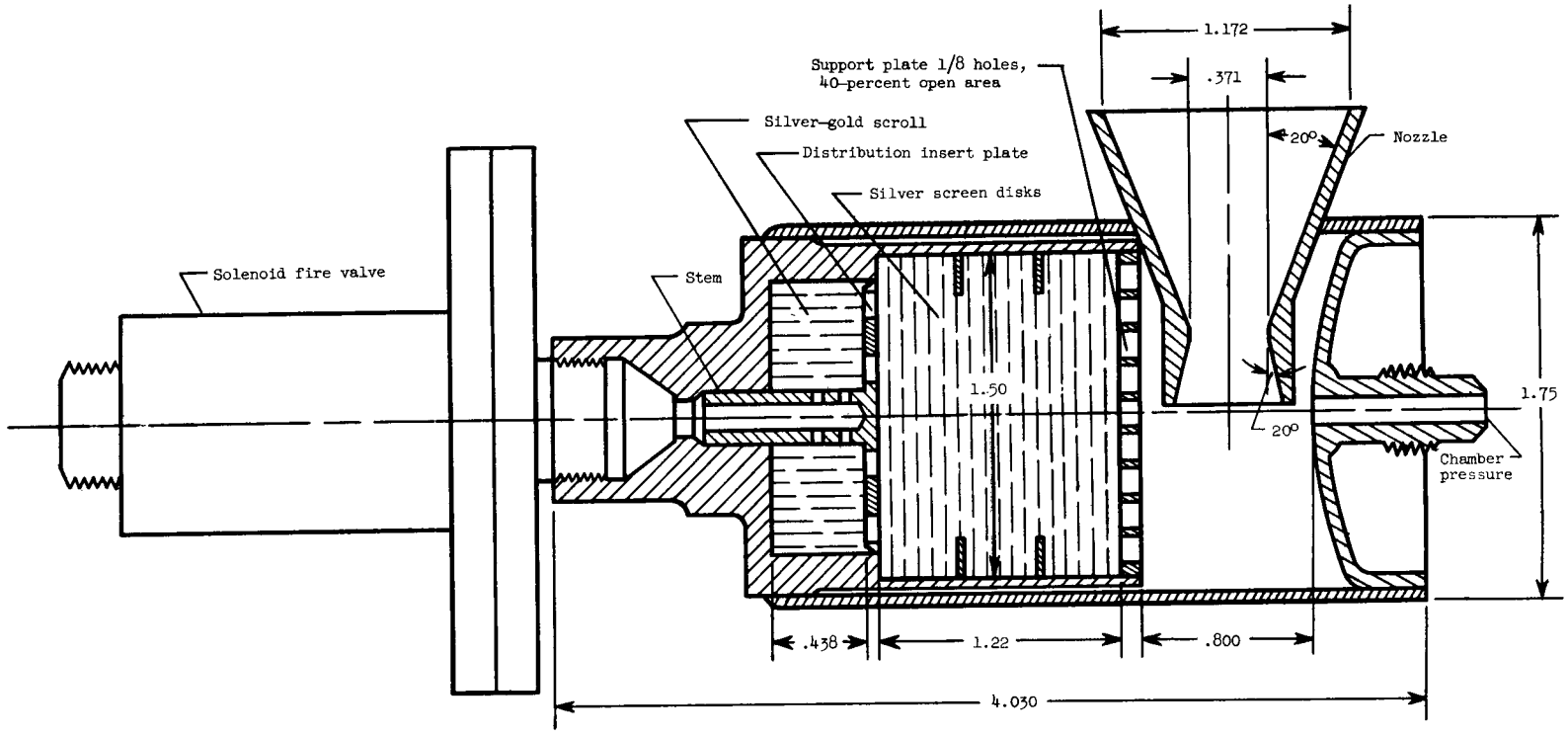

(a) Sketch of reaction-control rocket.

Figure 2.- Hydrogen peroxide decomposition chamber B. All linear dimensions are in inches.

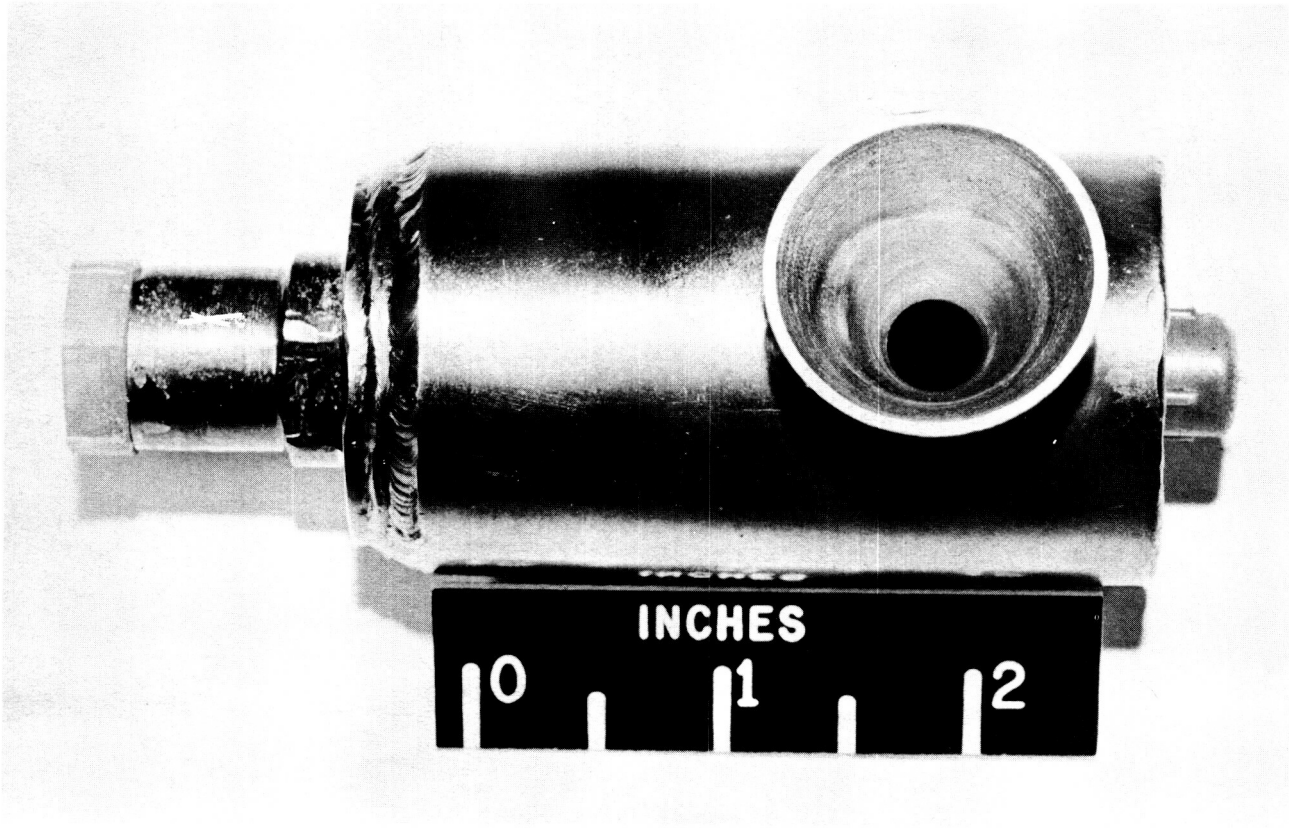

(b) Photograph of reaction-control rocket. L-62-5007

Figure 2.- Concluded.

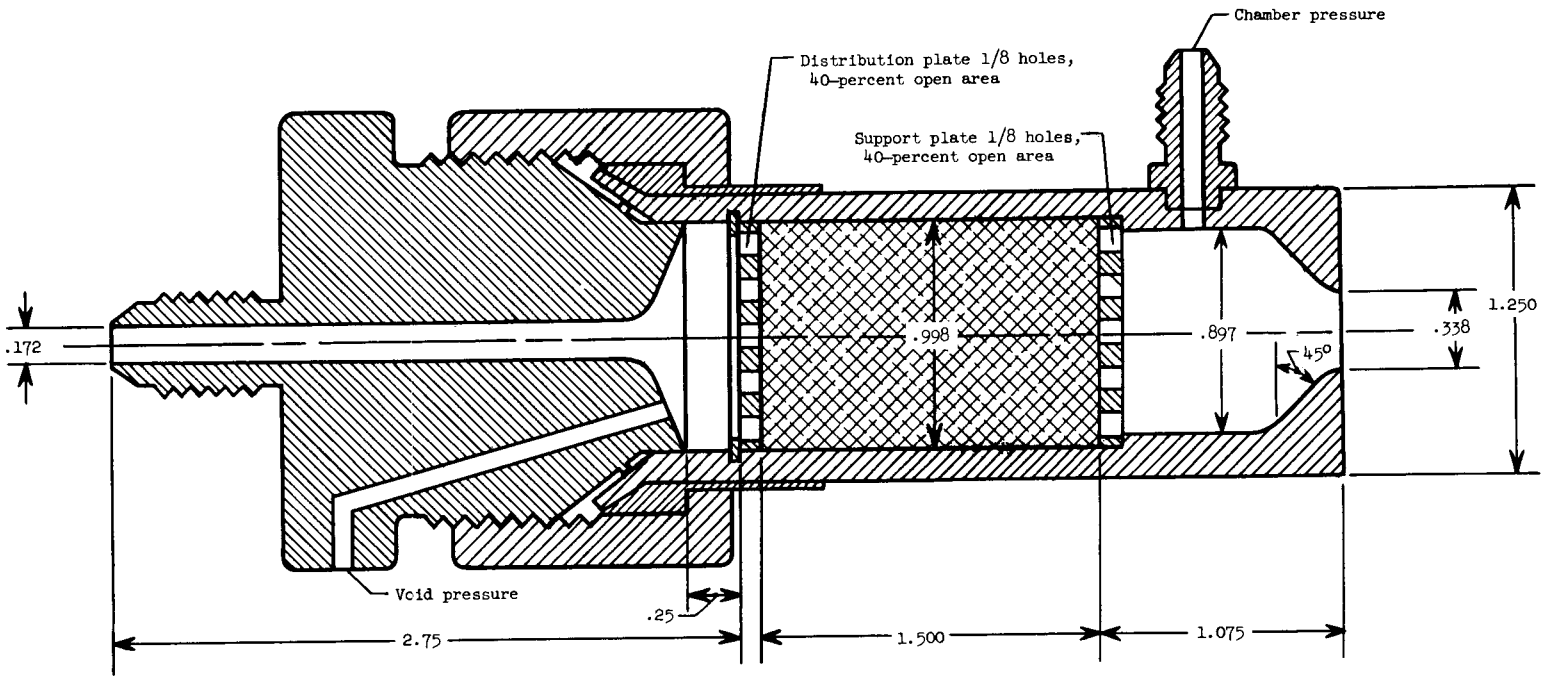

(a) Sketch of decomposition chamber.

Figure 3.- Hydrogen peroxide decomposition chamber C. All linear dimensions are in inches.

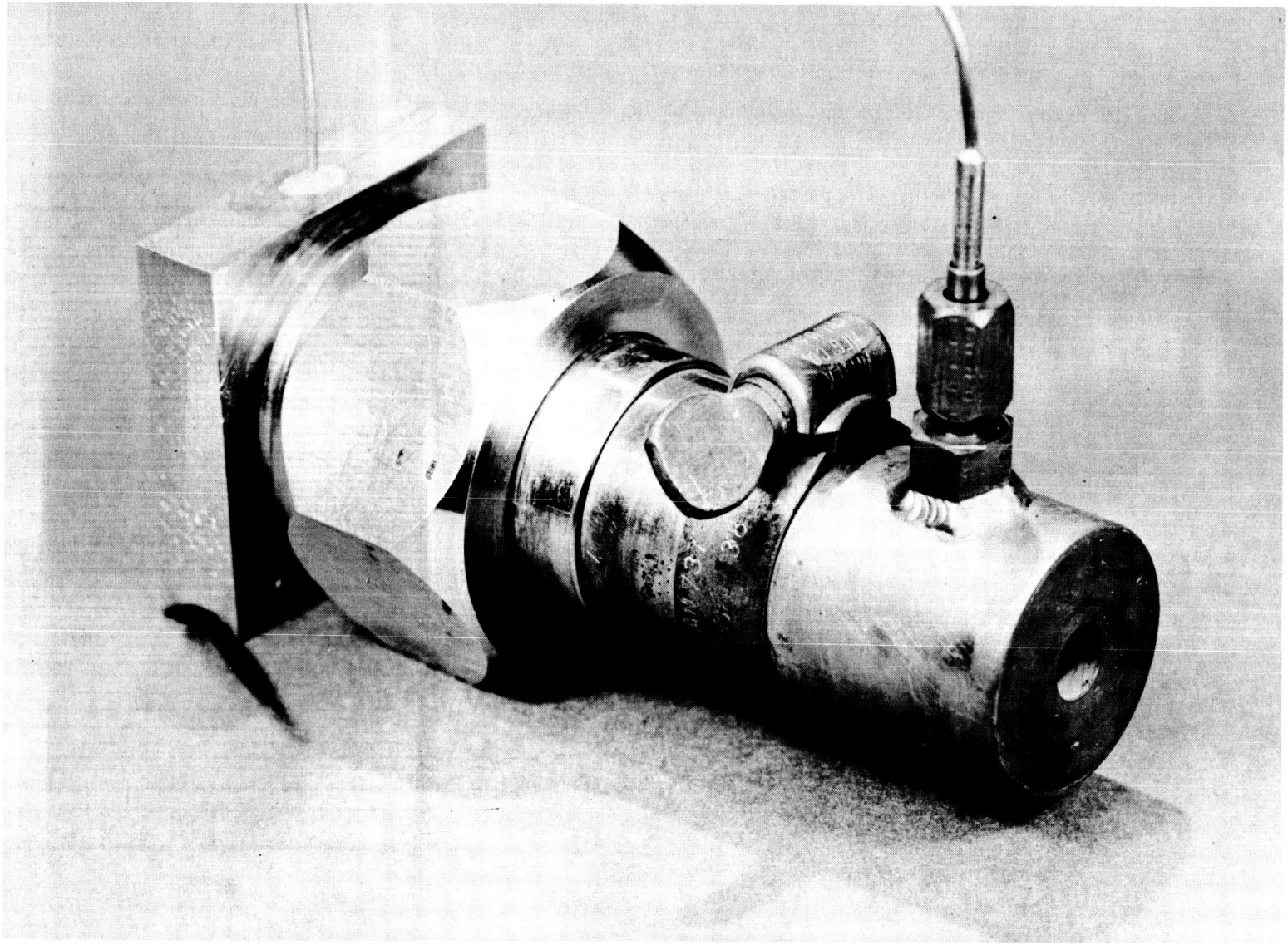

(b) Photograph of decomposition chamber. L-61-8373

Figure 3.- Concluded.

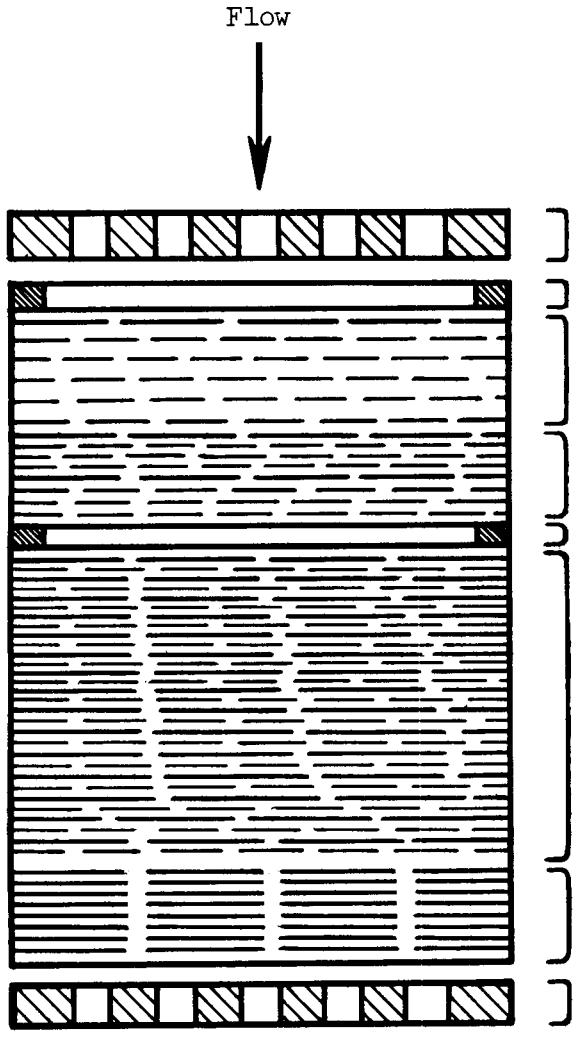

1 distribution plate

1 antichannel baffle

1 piece 20 mesh, .014 stainless-steel screen and
5 pieces 20 mesh, .014 silver screen, 2 % $Sm(NO_3)_3$

2 sets, 1 stainless and 5 silver, as above

1 antichannel baffle

15 sets, 1 stainless and 5 silver, as above

8 pieces 20 mesh, .014 stainless-steel screen

1 support plate

Figure 4.- Sample catalyst bed arrangement. Bed 1.

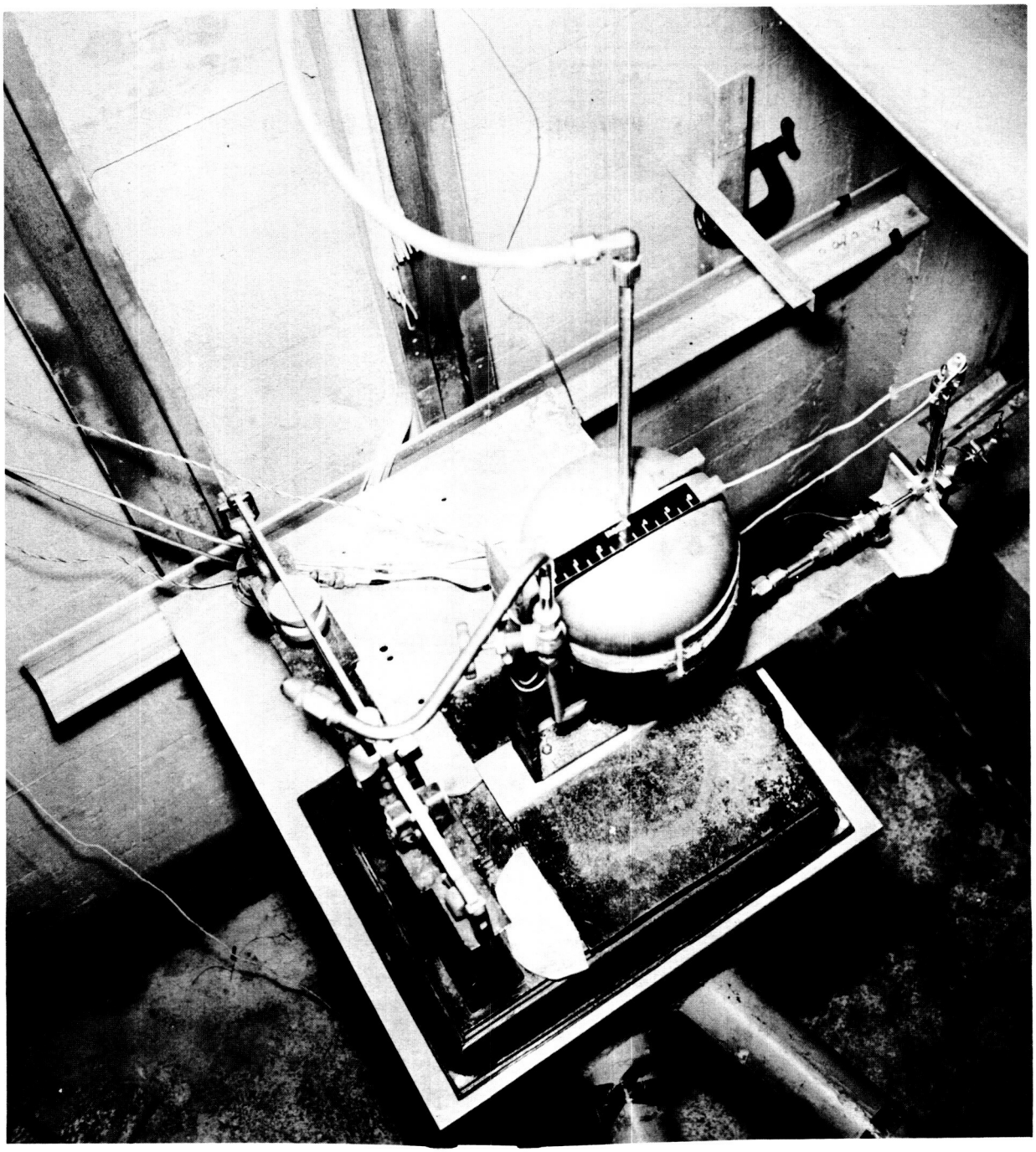

(b) Test equipment with decomposition chamber C. L-61-7578

Figure 5.- Concluded.

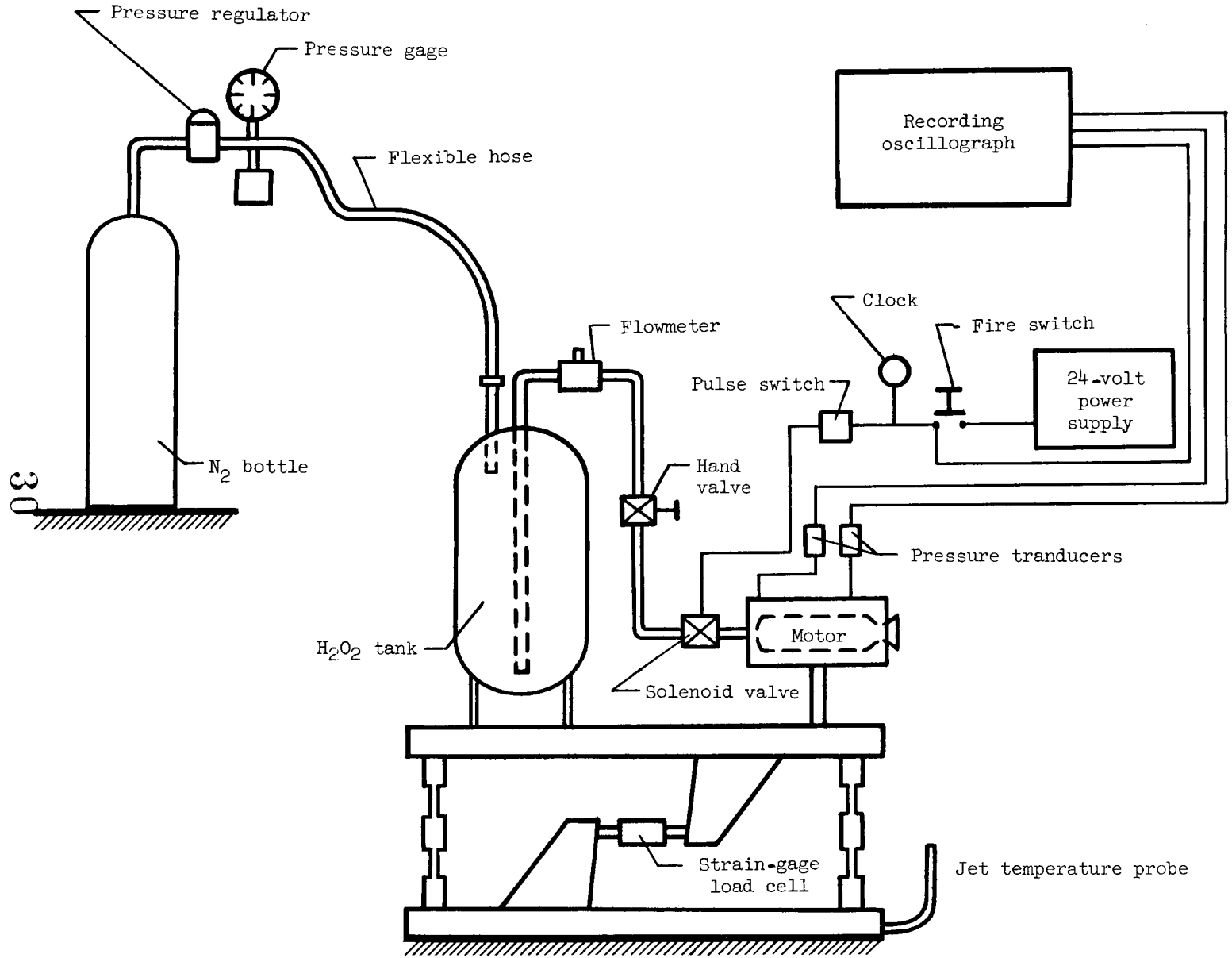

(a) Schematic of test setup.

Figure 5.- Ambient-temperature test apparatus.

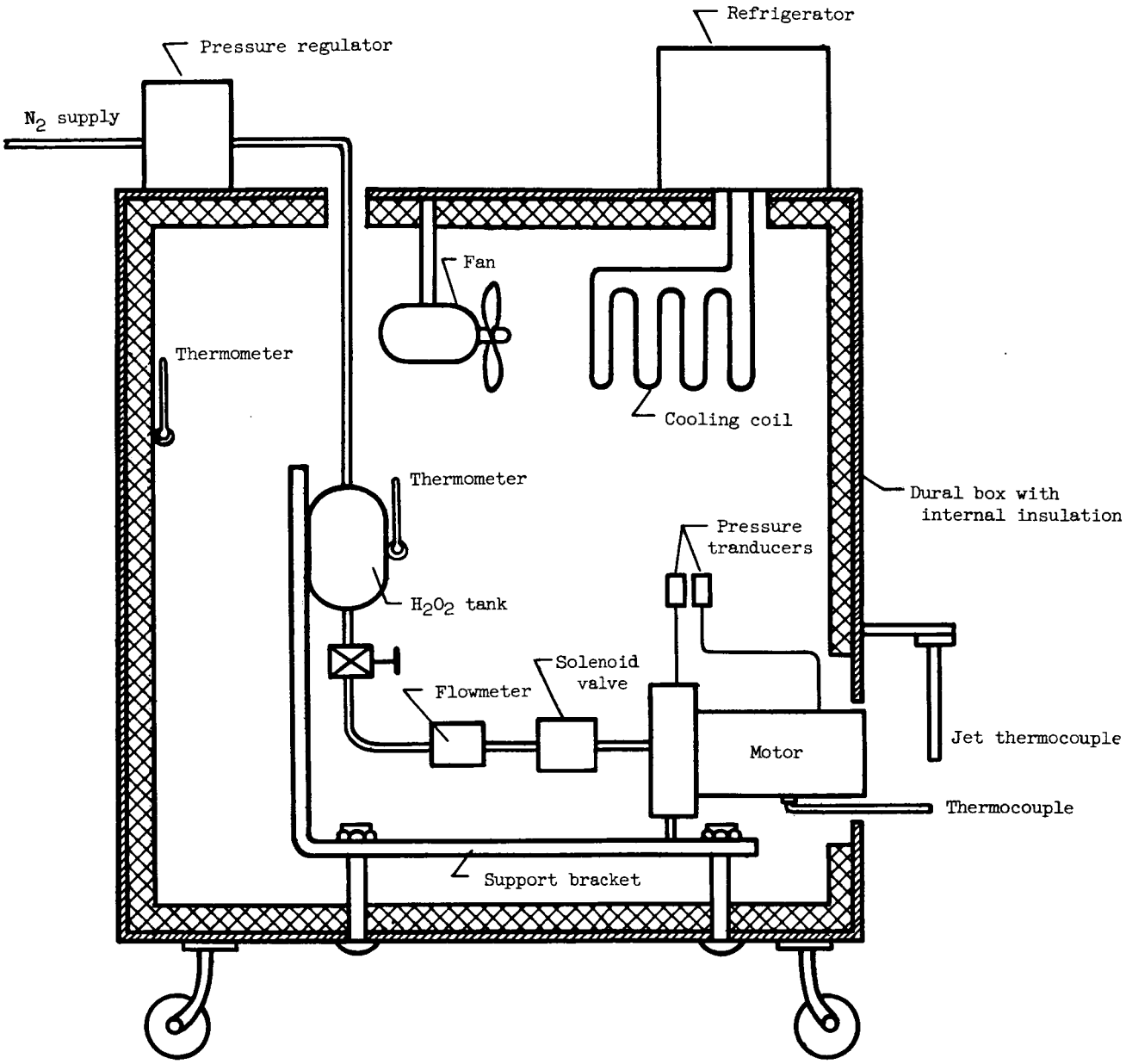

(a) Sketch.

Figure 6.- Environmental test apparatus.

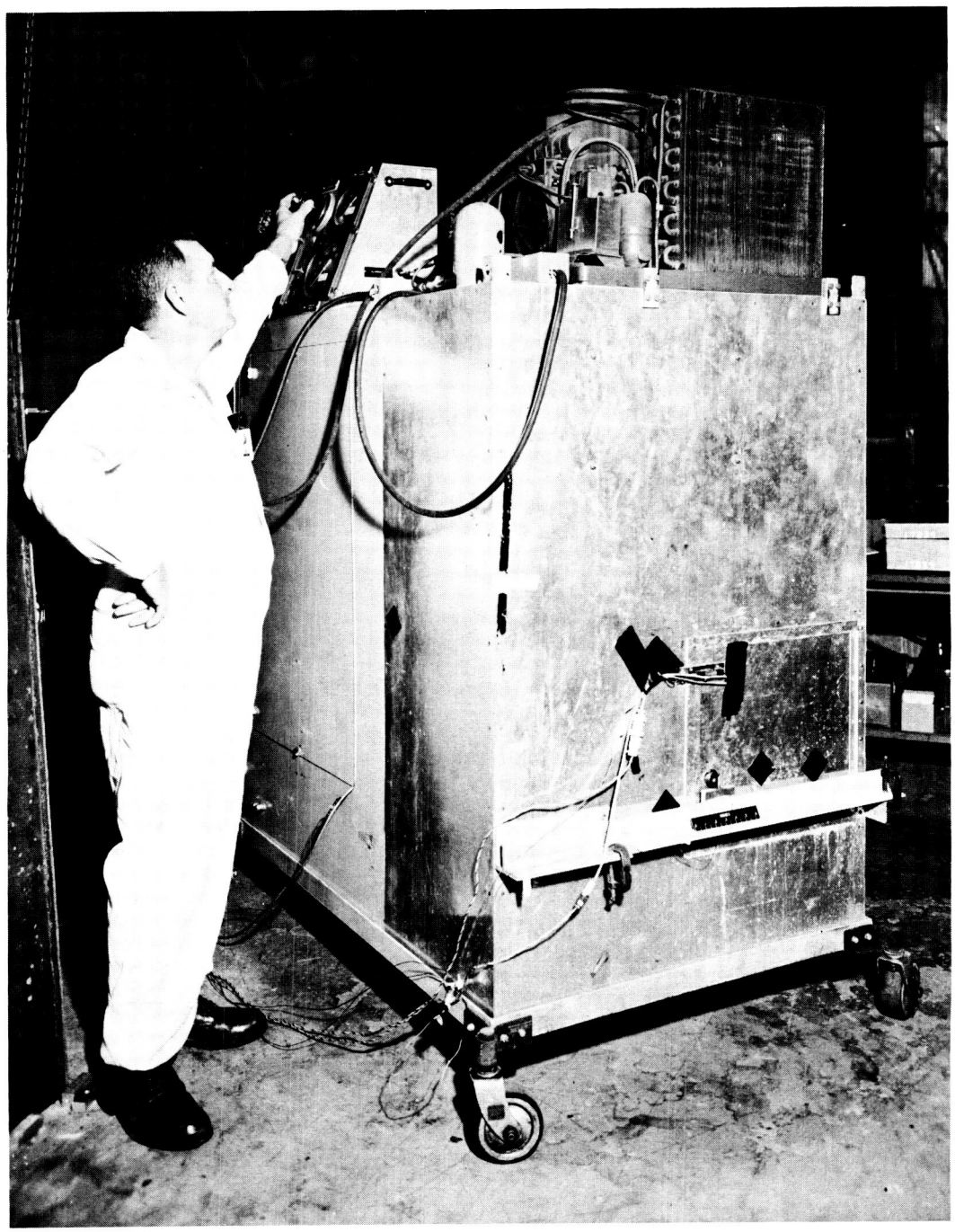

(b) Environmental equipment with decomposition chamber C. L-61-7577

Figure 6.- Concluded.

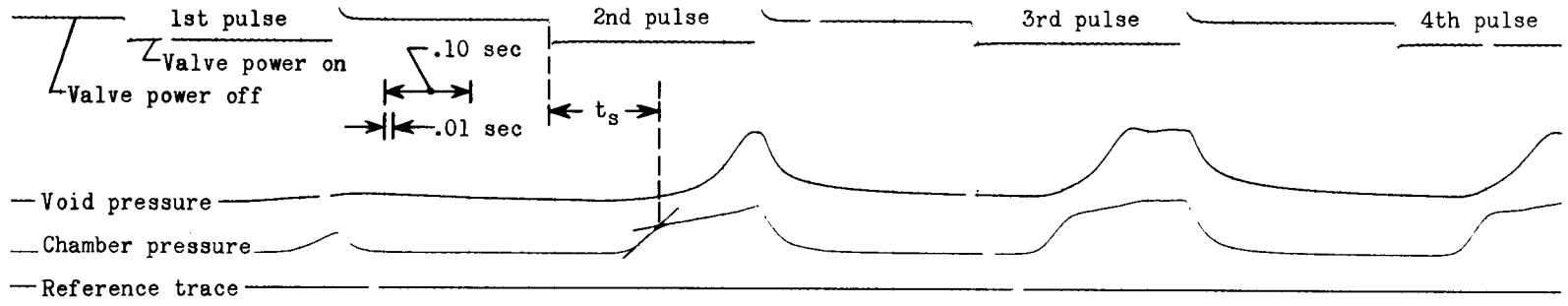

(a) Catalyst bed 1.

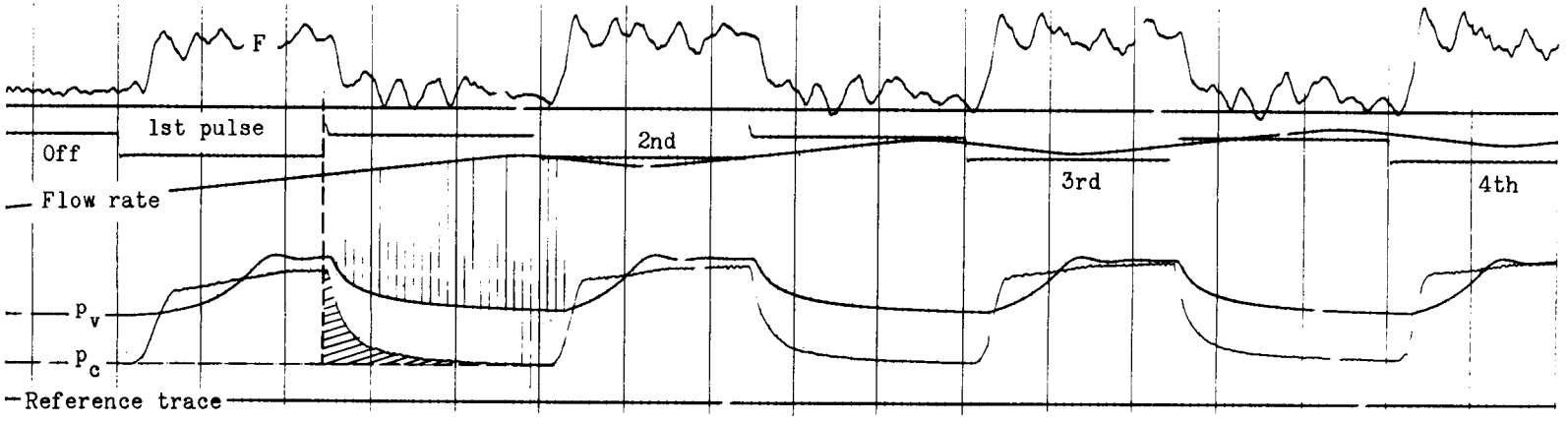

(b) Catalyst bed 2.

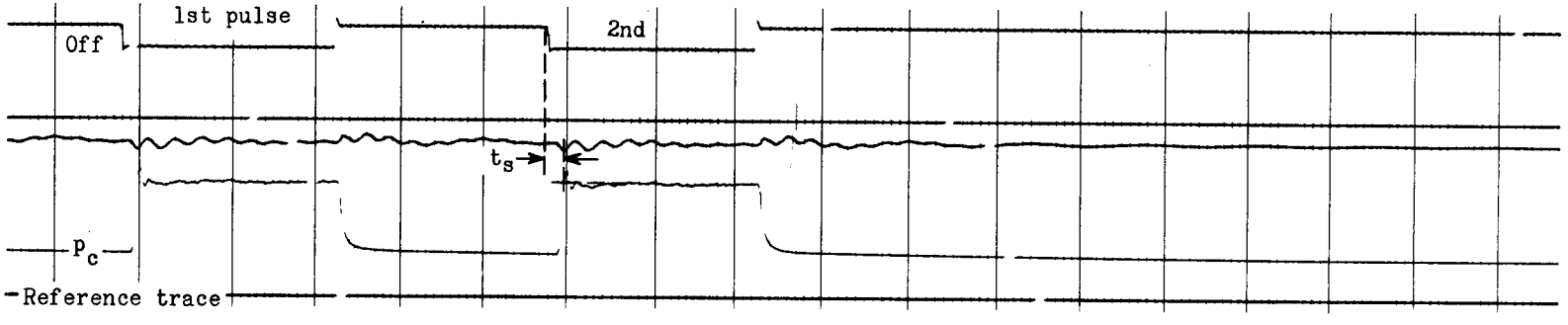

(c) Reaction-control rocket.

Figure 7.- Sample oscillograph records illustrating measurement of starting response and tail-off times.

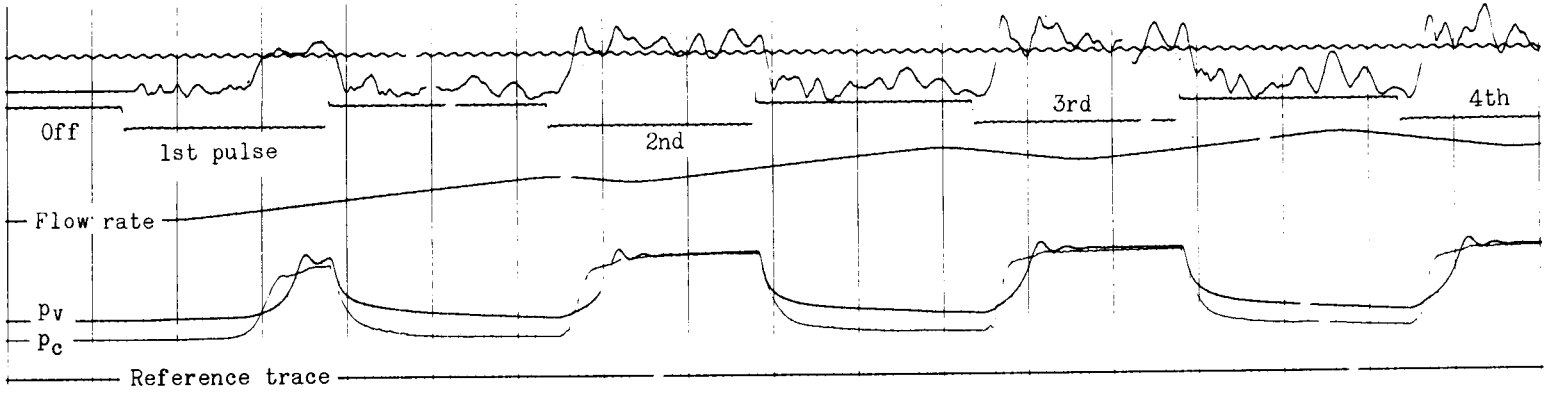

(d) Catalyst bed 5; cycling operation.

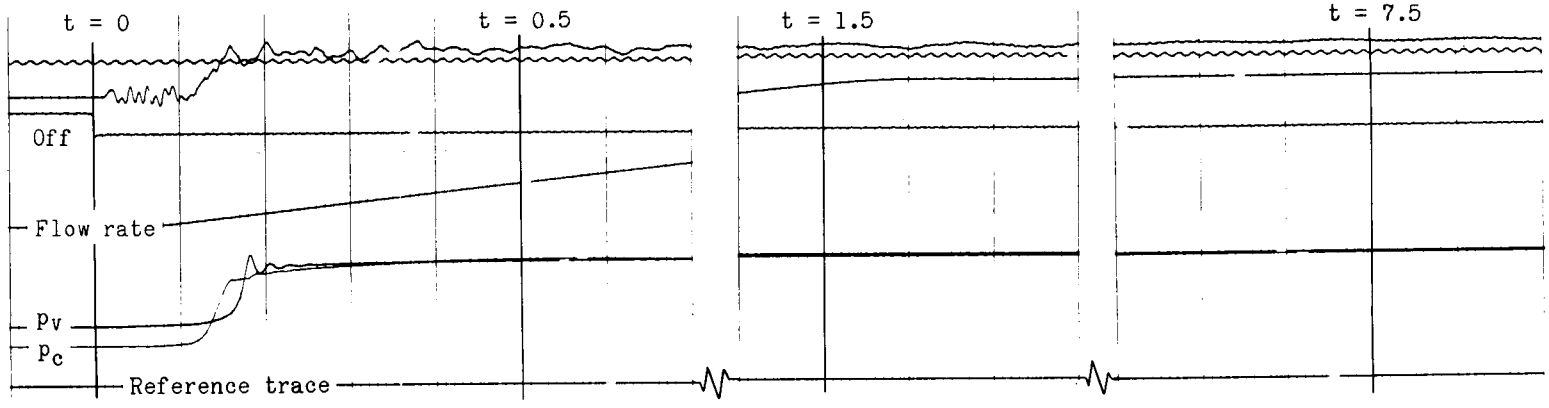

(e) Catalyst bed 5; steady-state operation.

Figure 7.- Concluded.

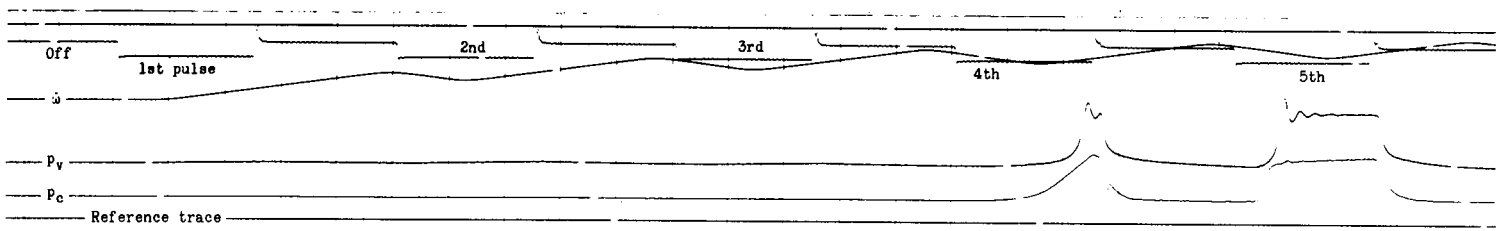

(a) Initial 35° F run.

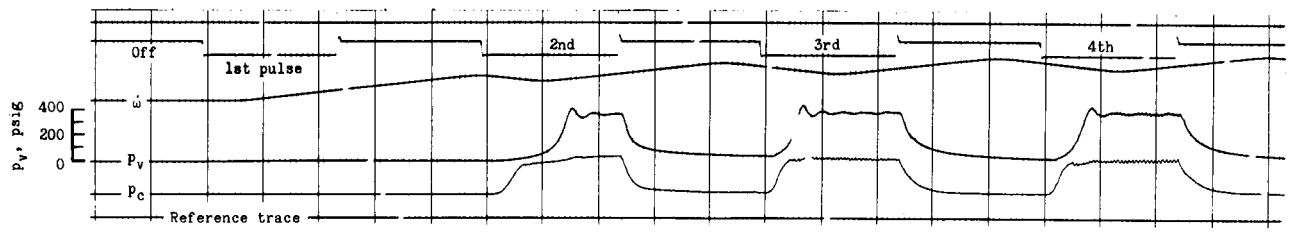

(b) Final 35° F run; t = 7.3 minutes.

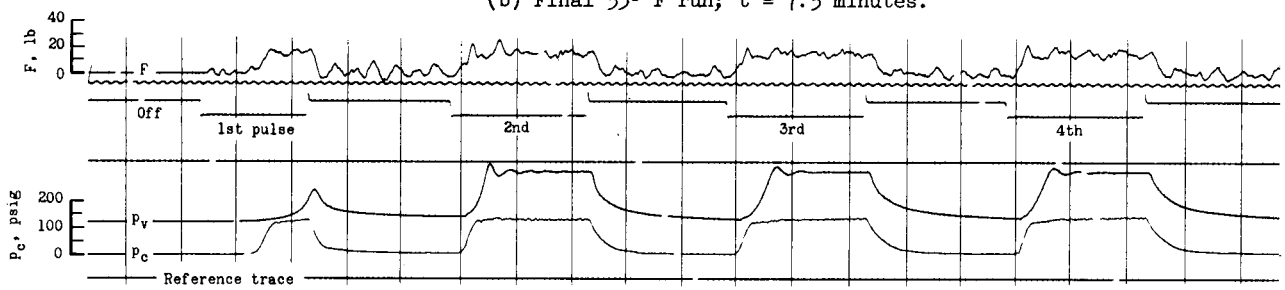

(c) Ambient run; 70° F; t = 5.9 minutes.

Figure 8.- Oscillograph records illustrating delay times for chamber pressure buildup and decay for catalyst bed 1.

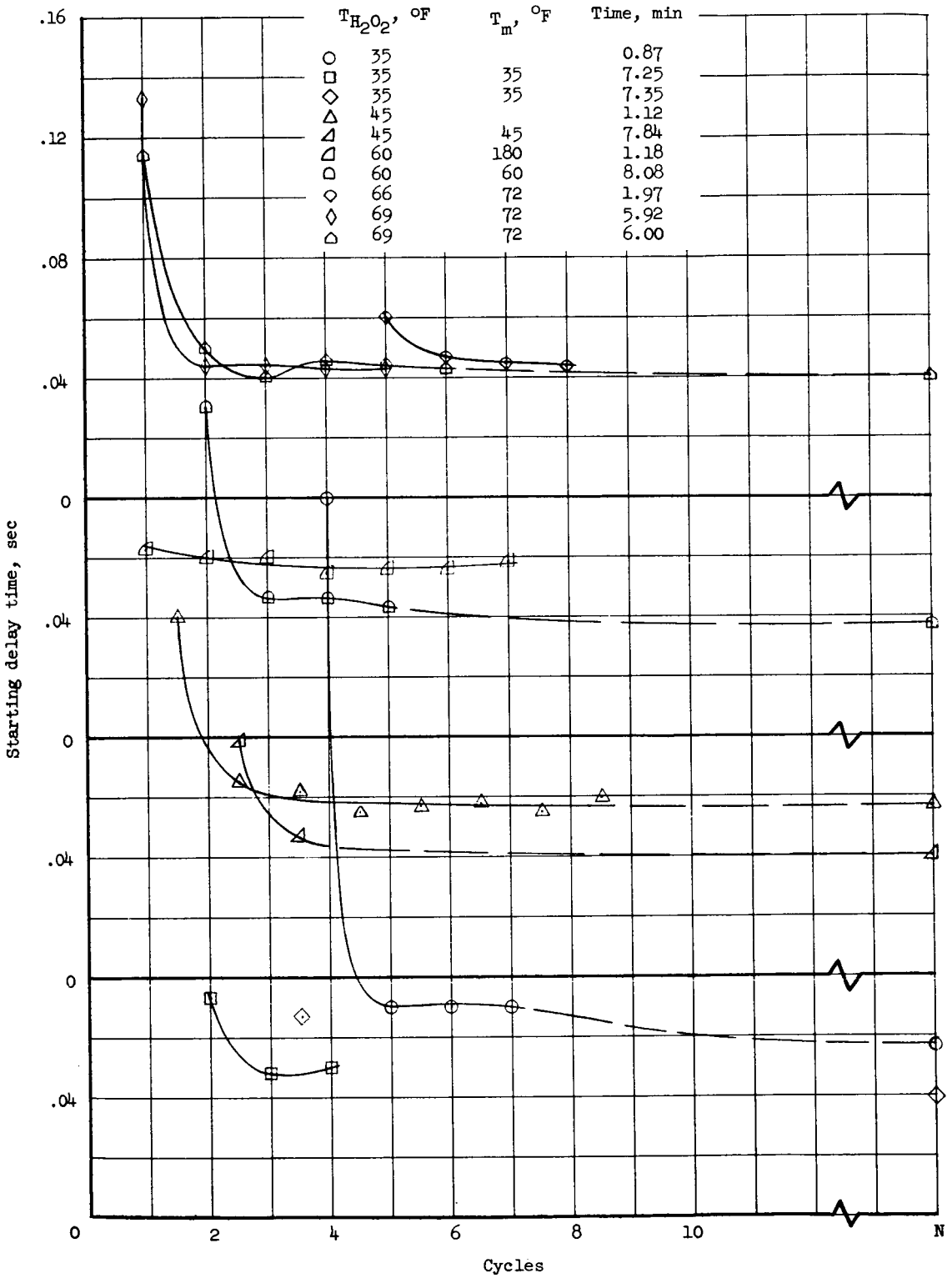

Figure 9.- Starting delay time of catalyst bed 1 during cycling operation.

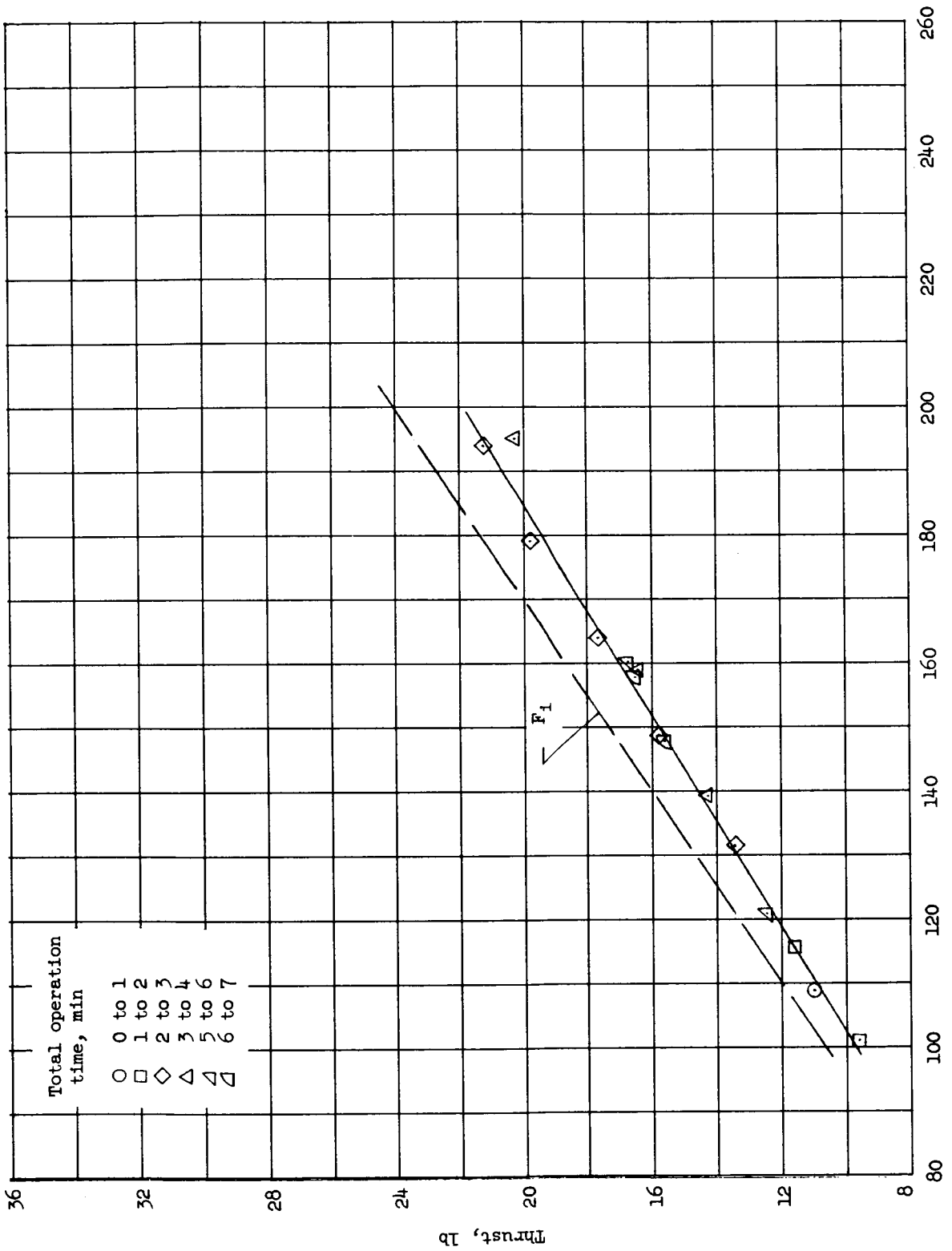

Figure 11.- Variation in thrust with chamber pressure for catalyst bed 1.

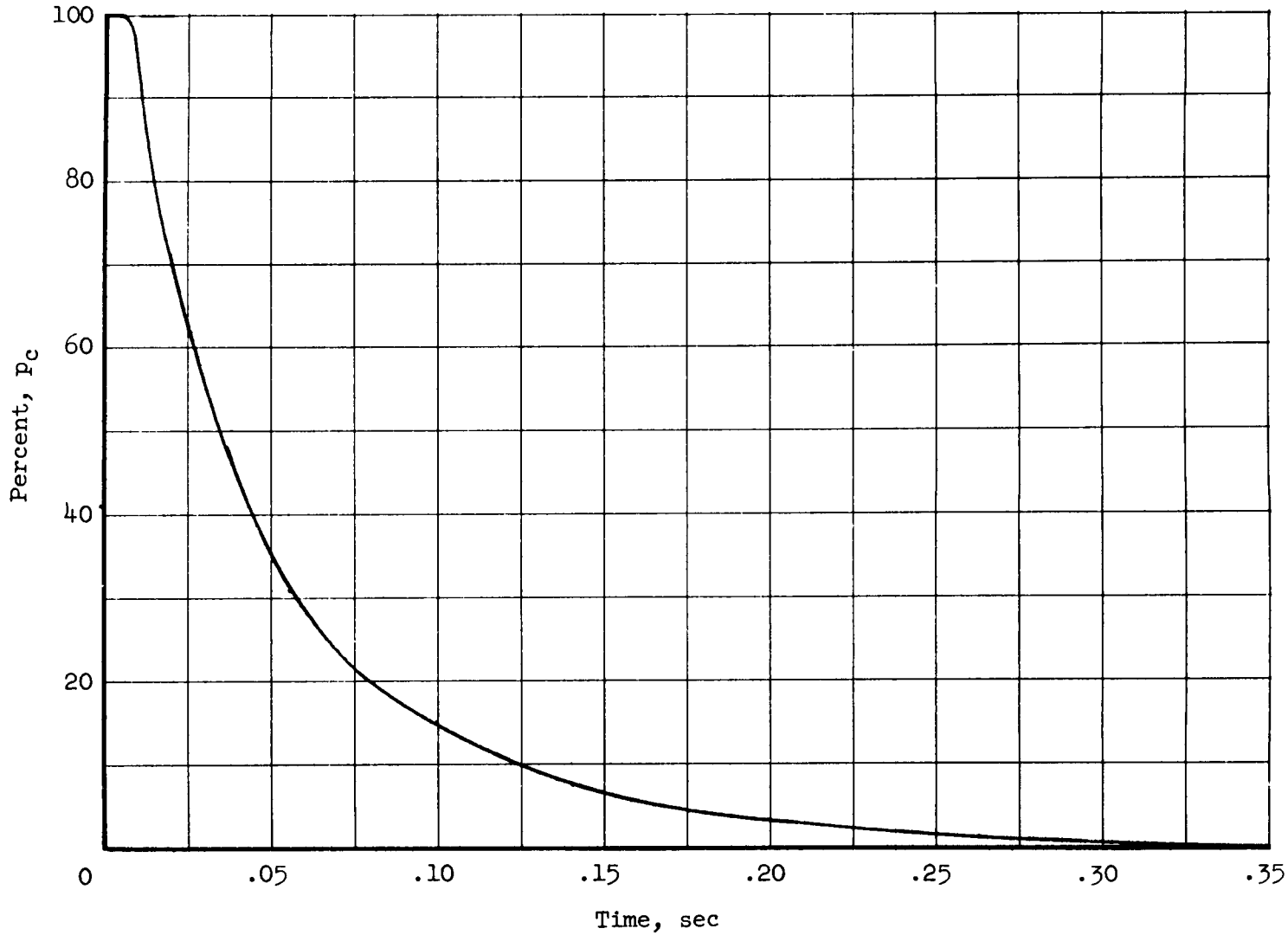

Figure 10.- Typical chamber pressure decay response following valve-closed signal. Bed 1.

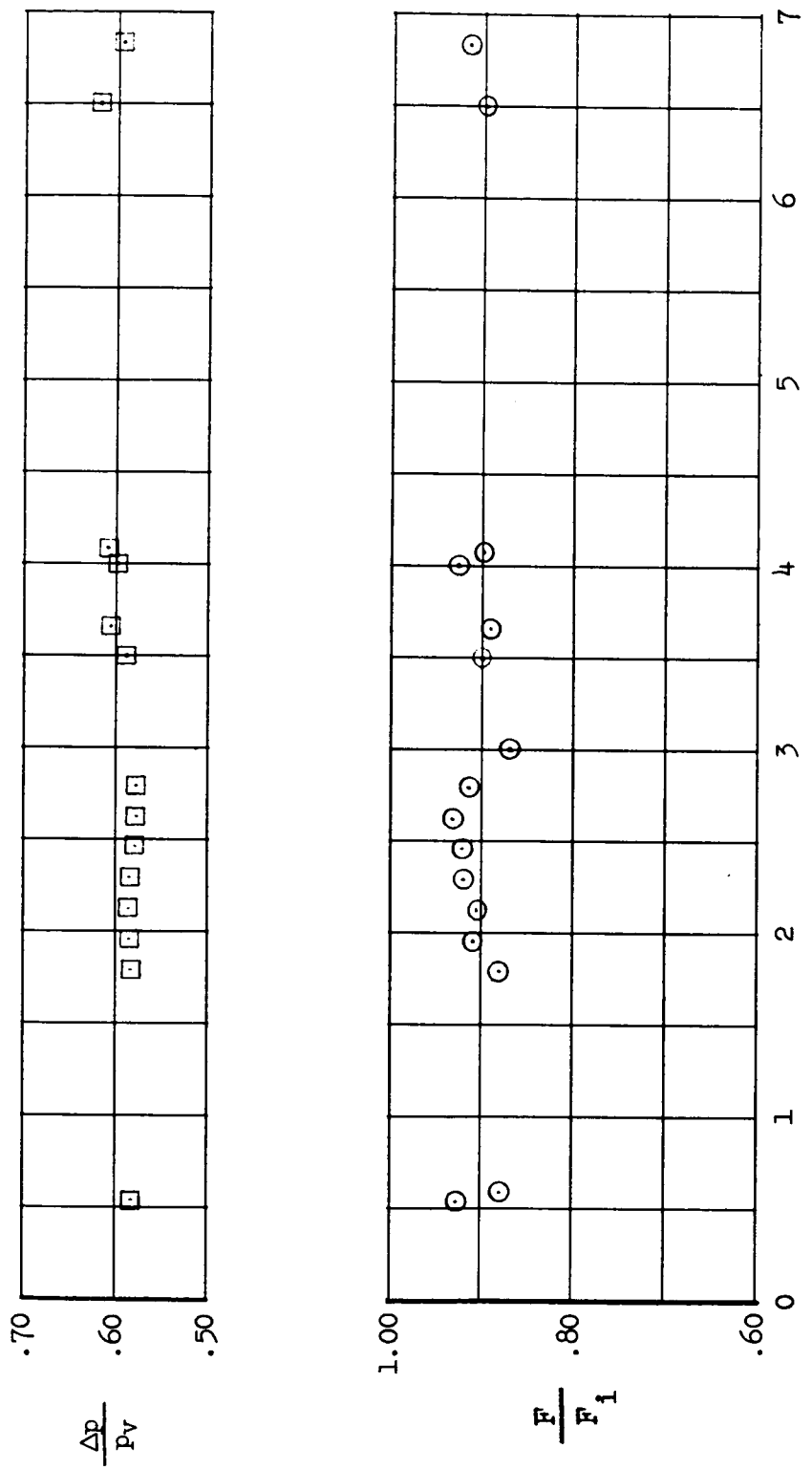

Figure 12.- Variation of thrust ratio and bed pressure drop with operation time for bed 1.

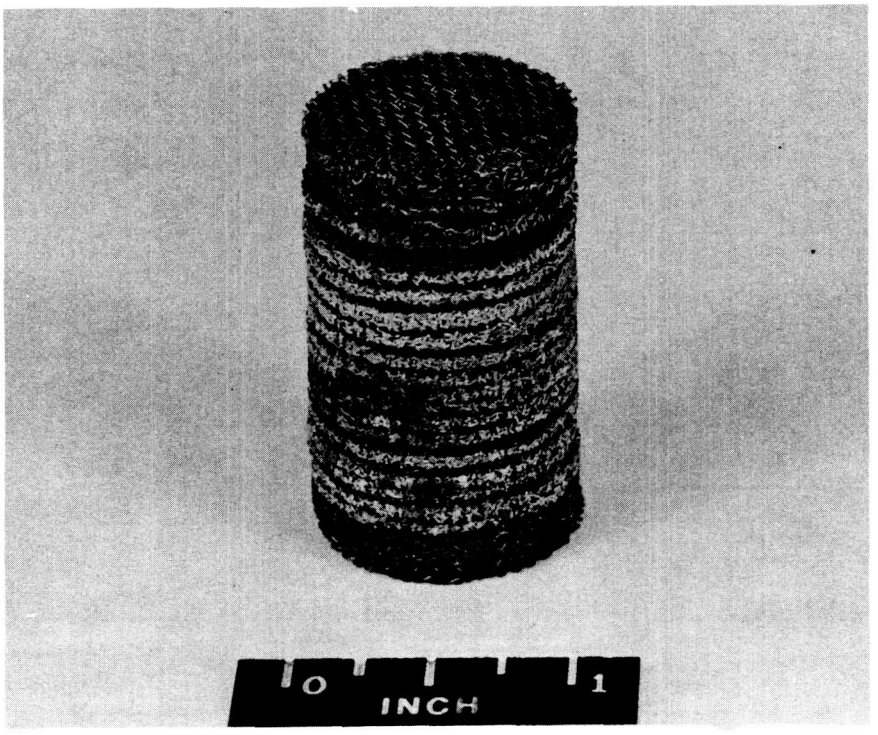

(a) Bed assembly. L-62-565

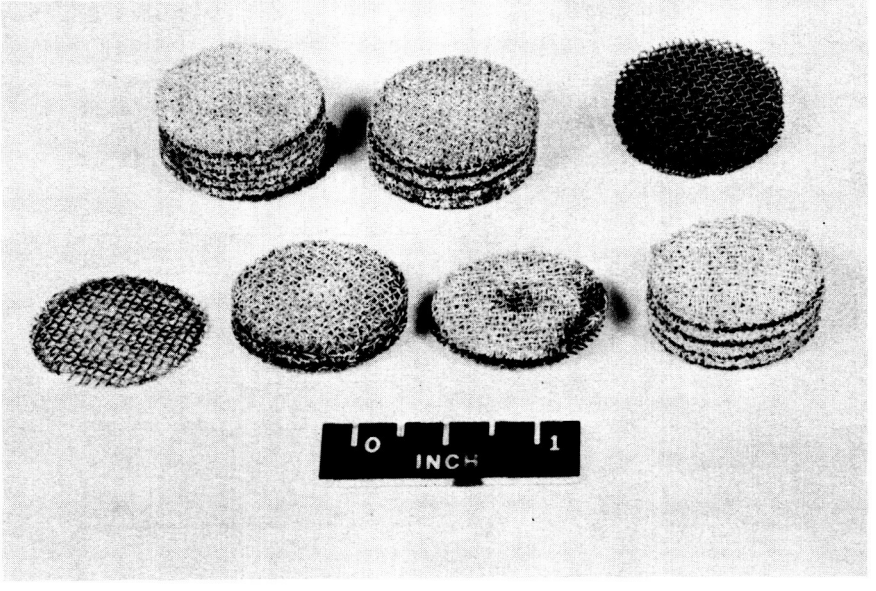

(b) Bed sections. L-62-566

Figure 13.- Catalyst bed 1 after 8.08 minutes run time.

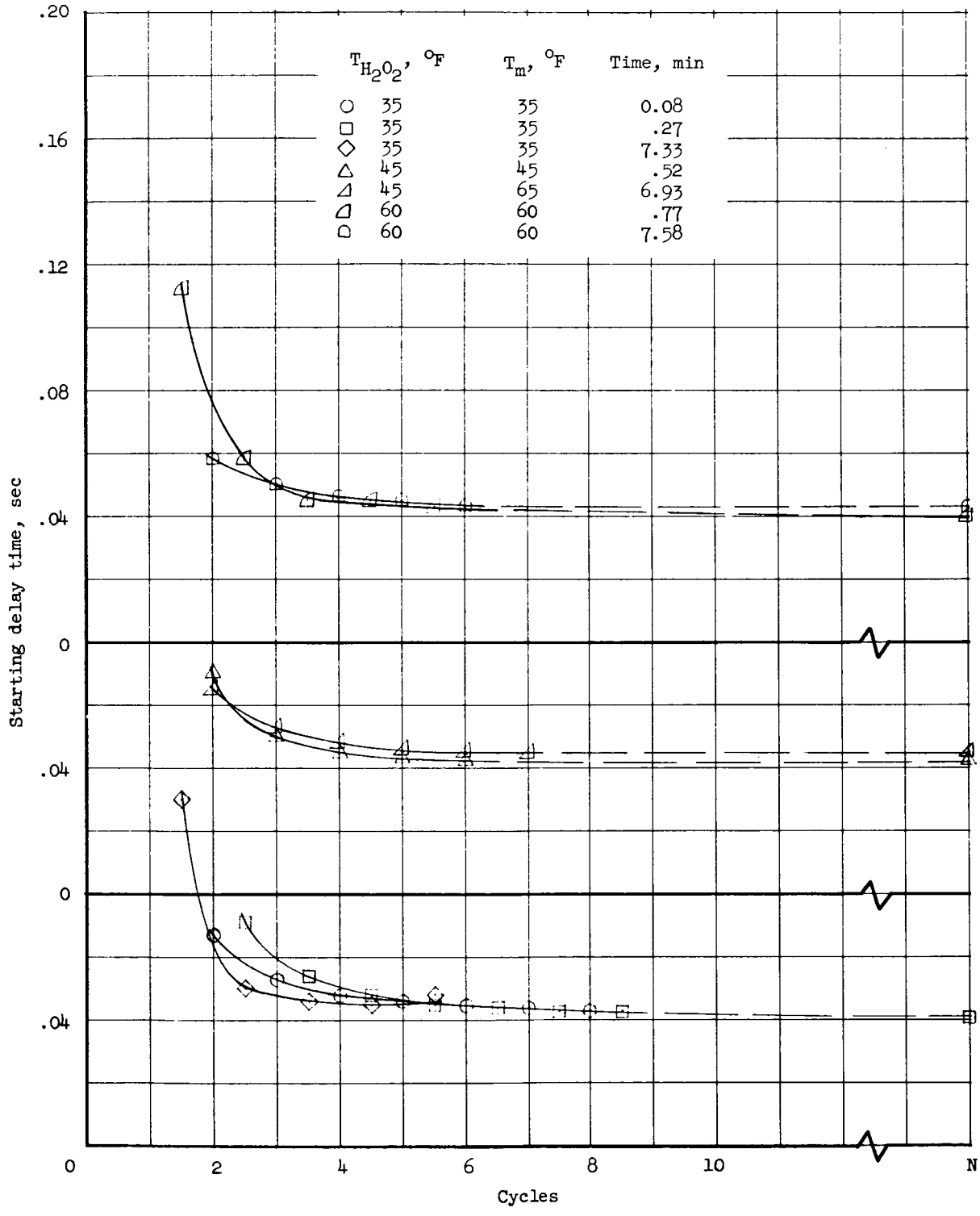

Figure 15.- Starting delay time of catalyst bed 2 during cycling operation.

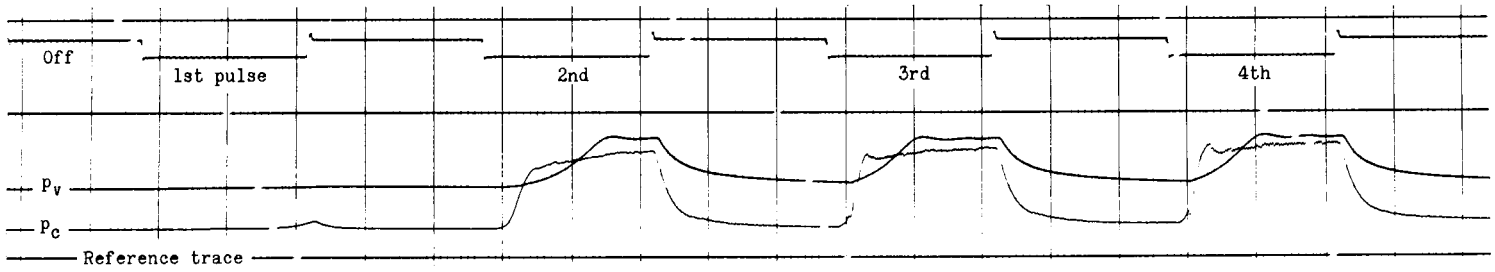

(a) Initial 35° F run.

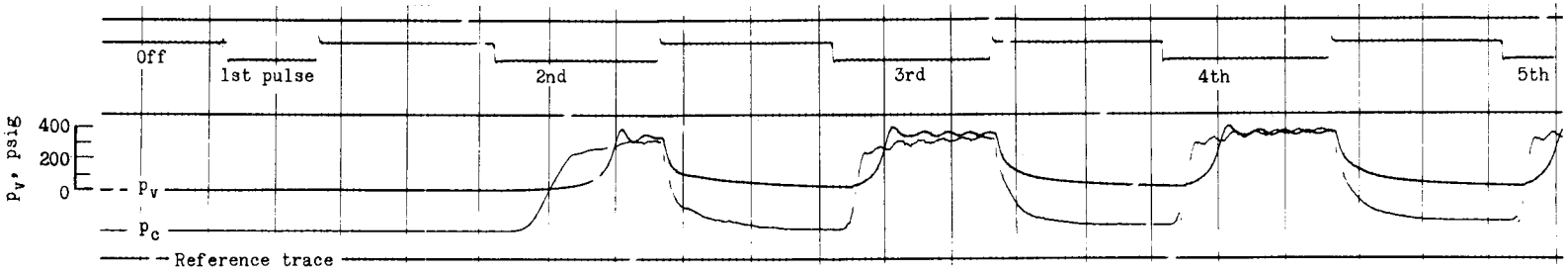

(b) Final 35° F run; t = 7.3 minutes.

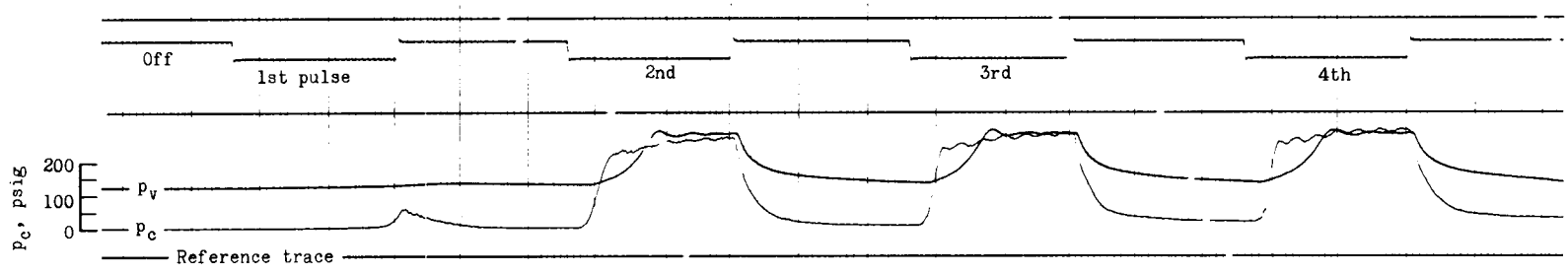

(c) Ambient run; 60° F; t = 7.6 minutes.

Figure 14.- Oscillograph records illustrating delay times for chamber pressure buildup and decay for catalyst bed 2.

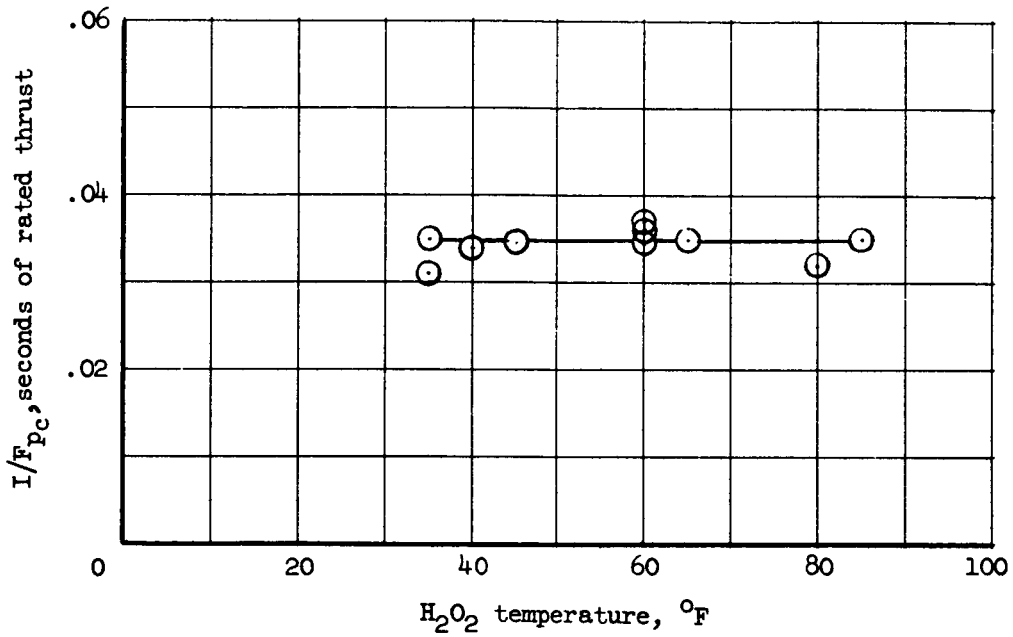

(a) Effect of temperature on tail-off thrust.

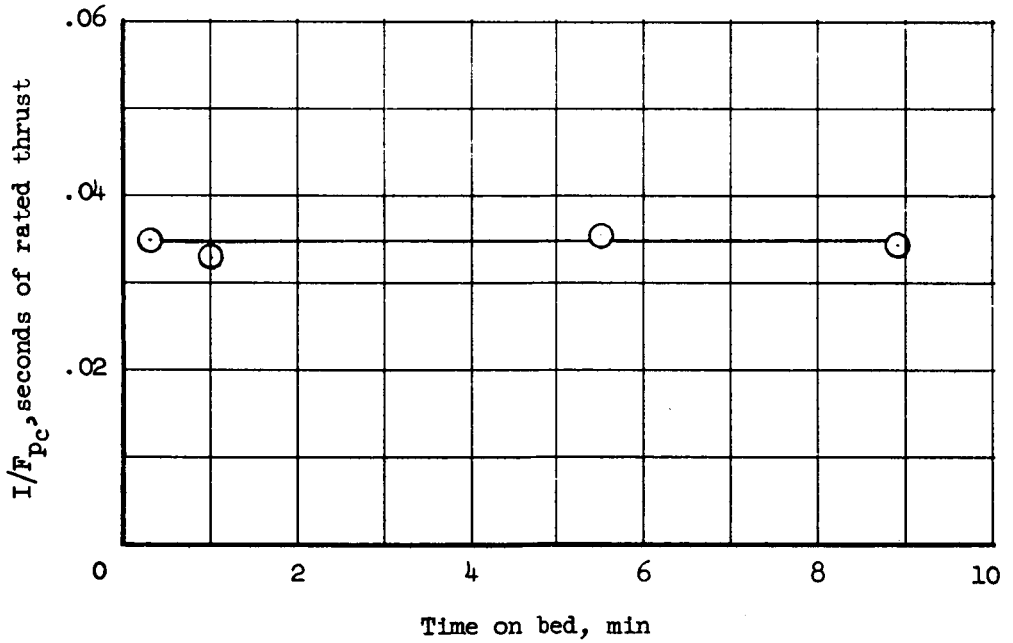

(b) Effect of operating time on tail-off thrust.

Figure 16.- Thrust developed by catalyst bed 2 after valve-closed signal.

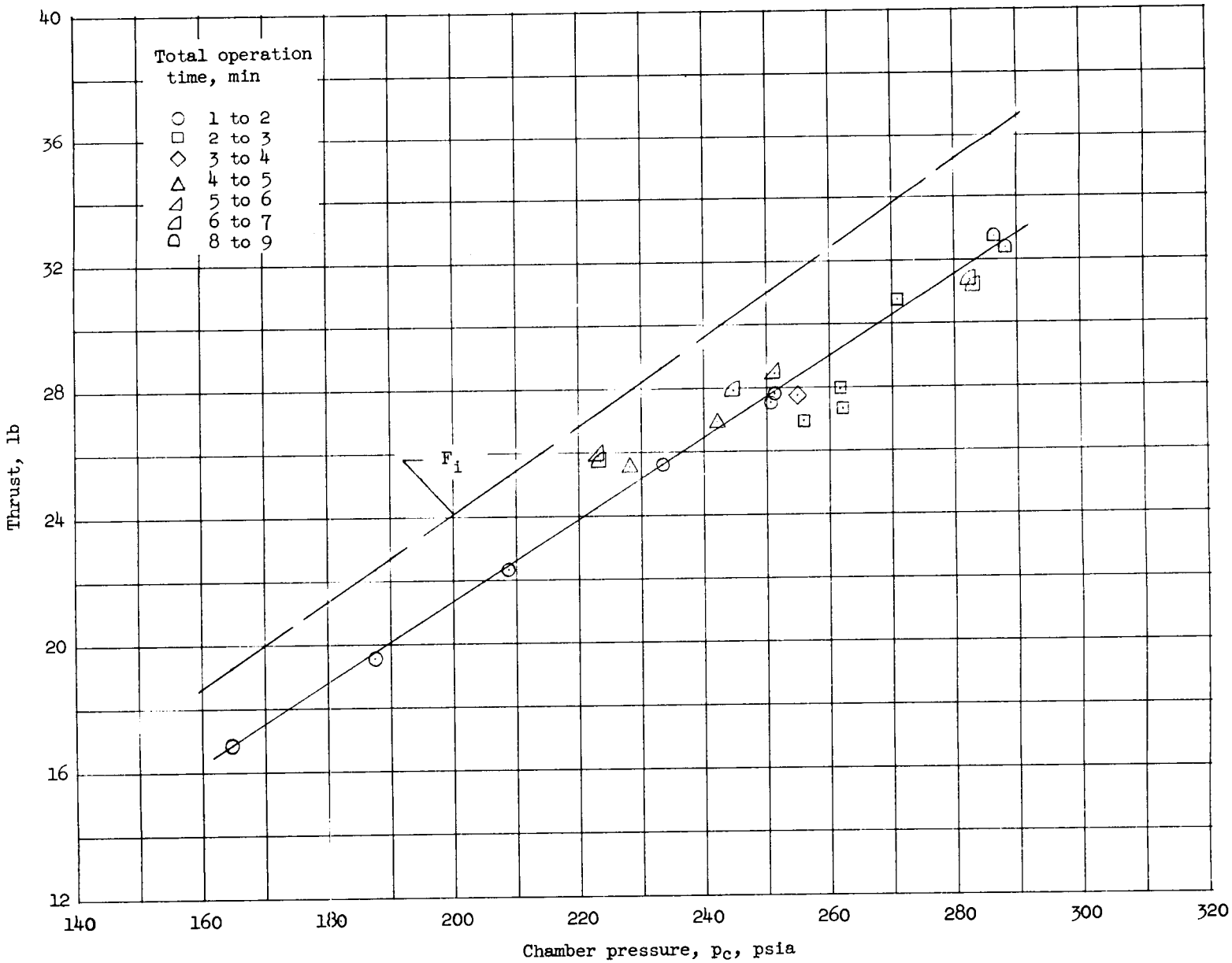

Figure 17.- Variation in thrust with chamber pressure for catalyst bed 2.

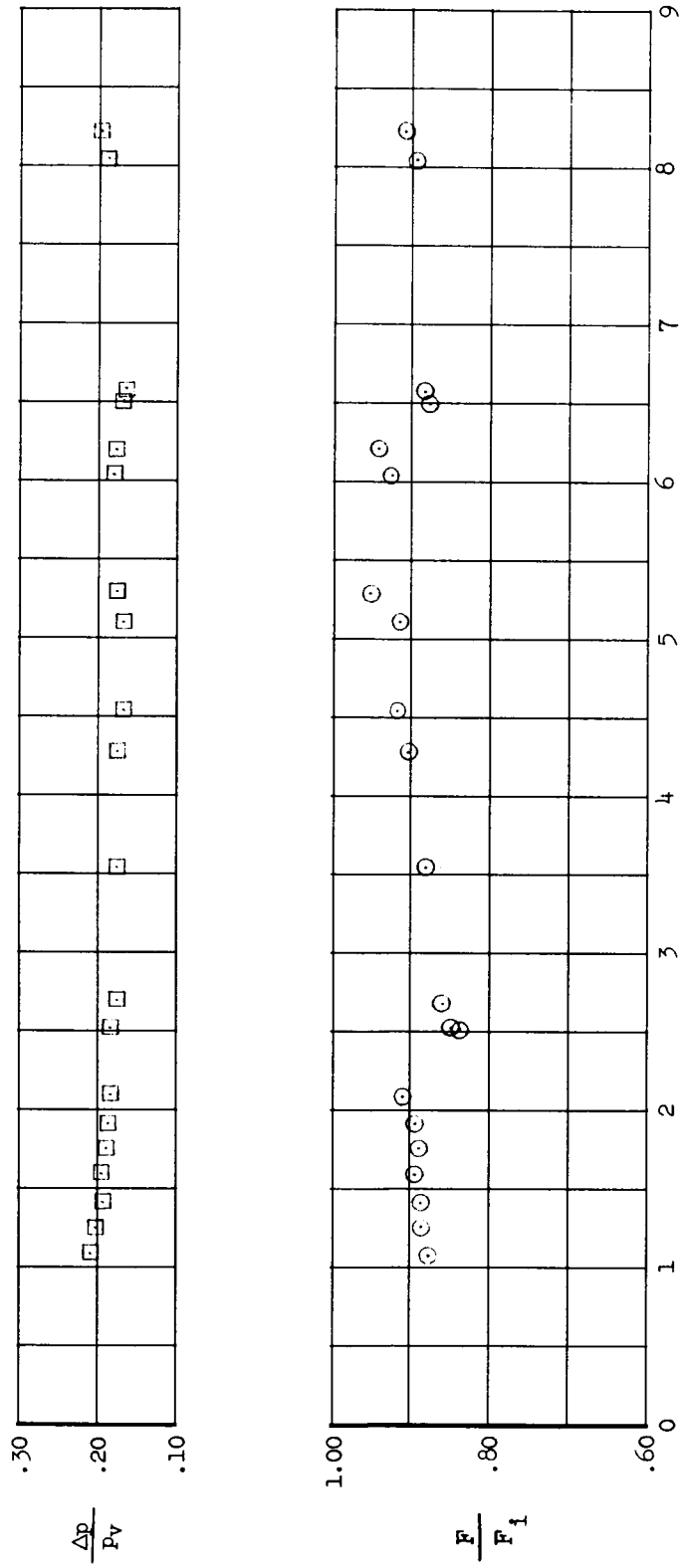

Figure 18.- Variation of thrust ratio and bed pressure drop with operation time for bed 2.

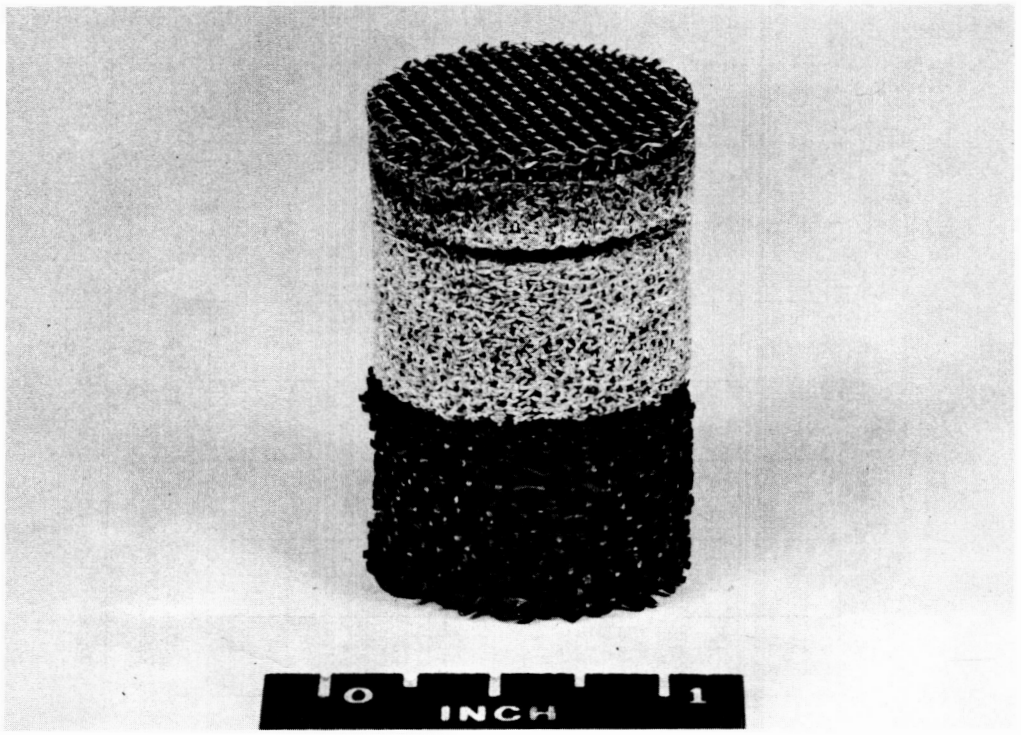

(a) Bed assembly. L-62-568

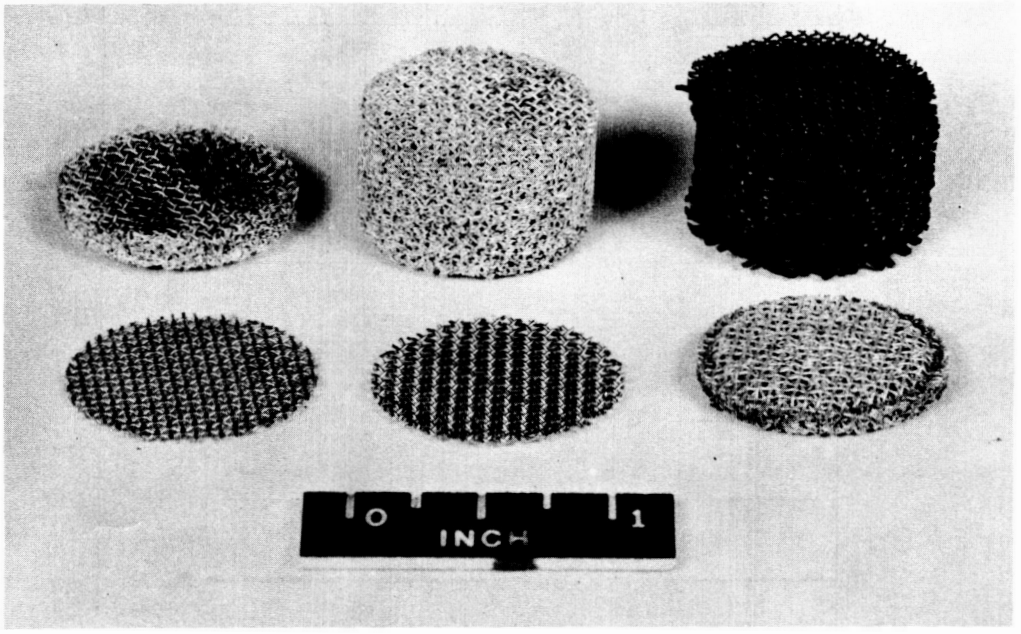

(b) Bed sections. L-62-569

Figure 19.- Catalyst bed 2 after 8.97 minutes run time.

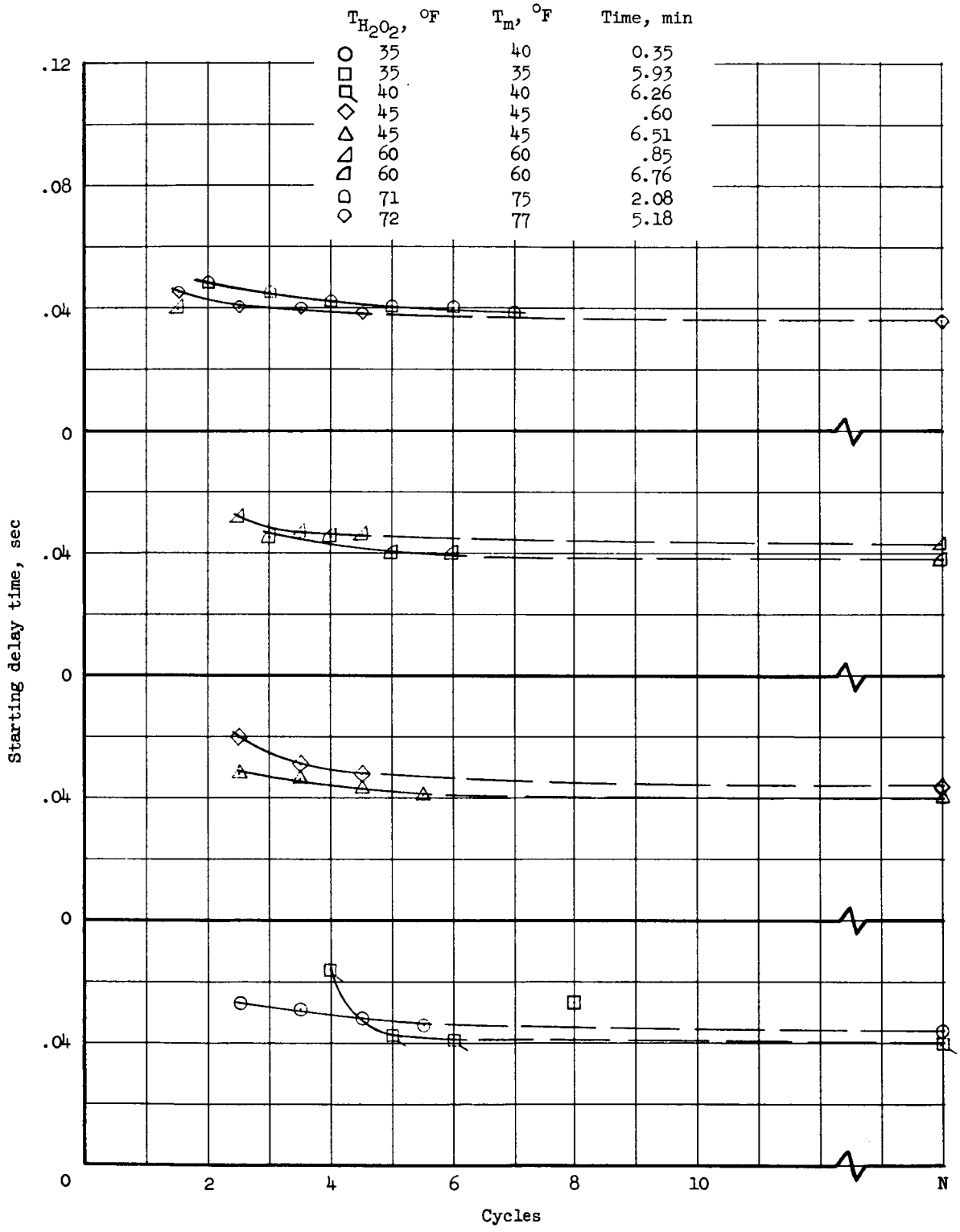

Figure 21.- Starting delay time of catalyst bed 3 during cycling operation.

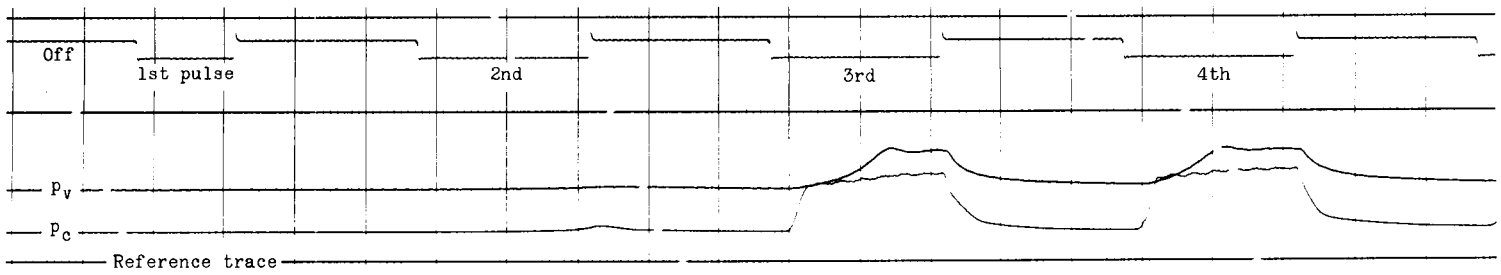

(a) Initial 35° F run.

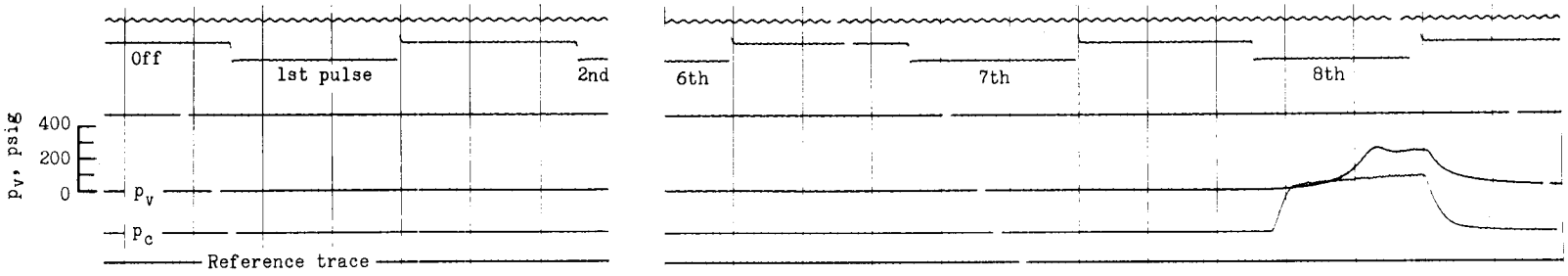

(b) Final 35° F run; t = 5.9 minutes.

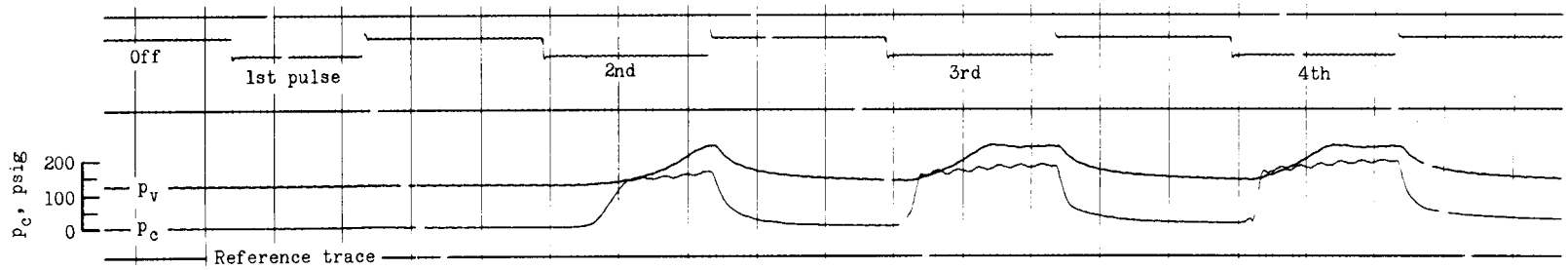

(c) Ambient run; 60° F; t = 0.9 minute.

Figure 20.- Oscillograph records illustrating delay times for chamber pressure buildup and decay for catalyst bed 3.

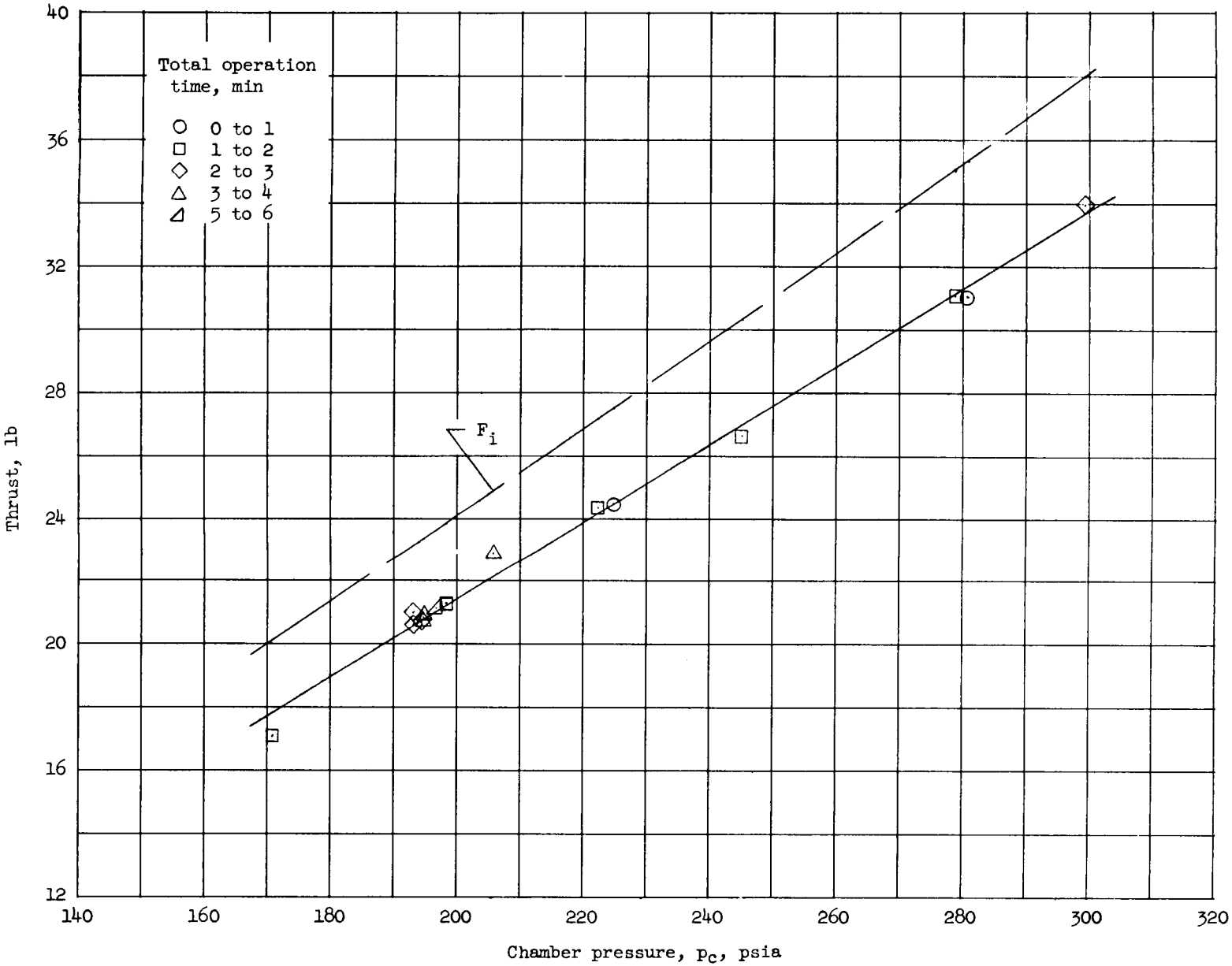

Figure 22.- Variation in thrust with chamber pressure for catalyst bed 3.

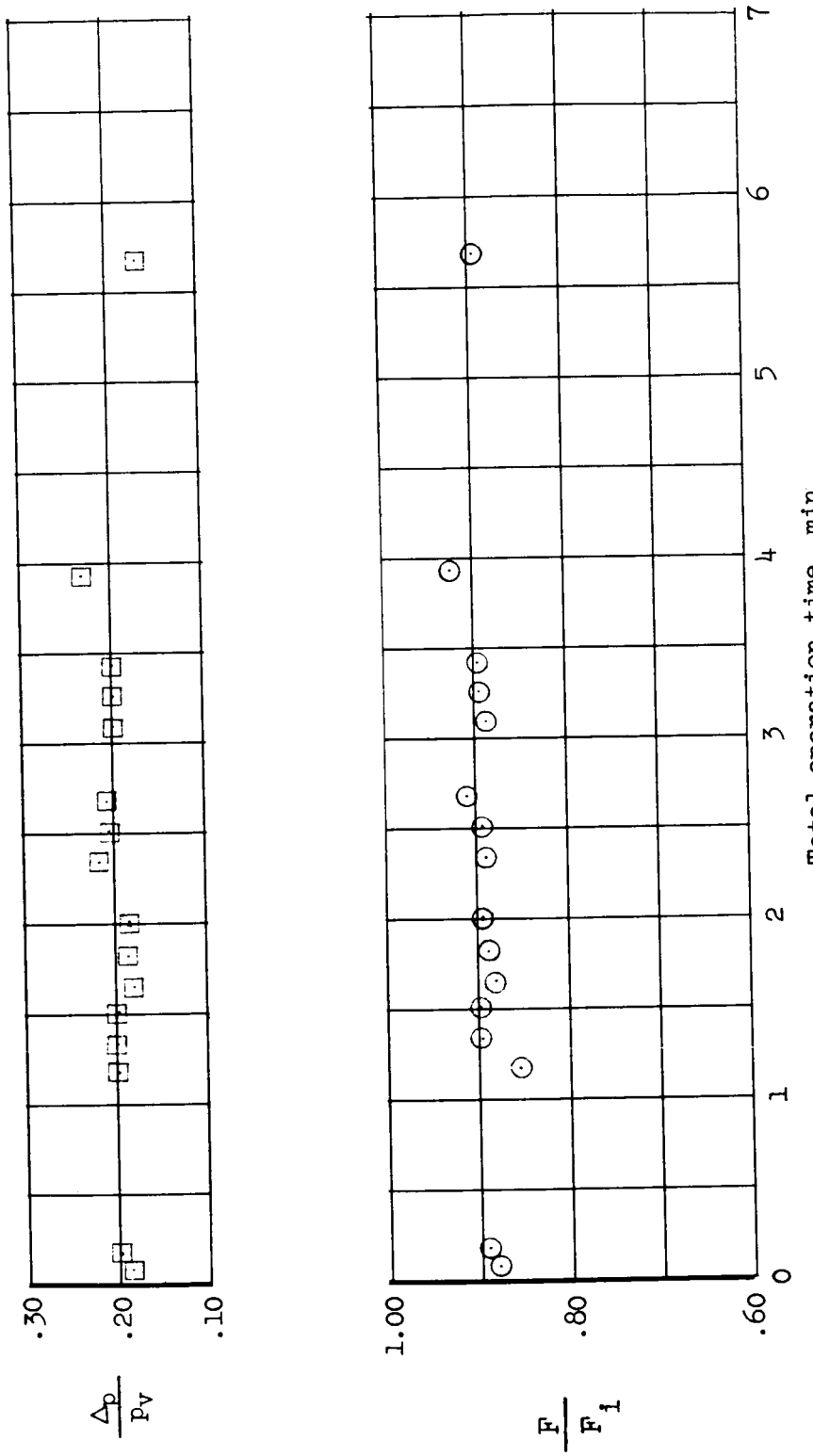

Figure 23.- Variation of thrust ratio and bed pressure drop with operation time for bed 3.

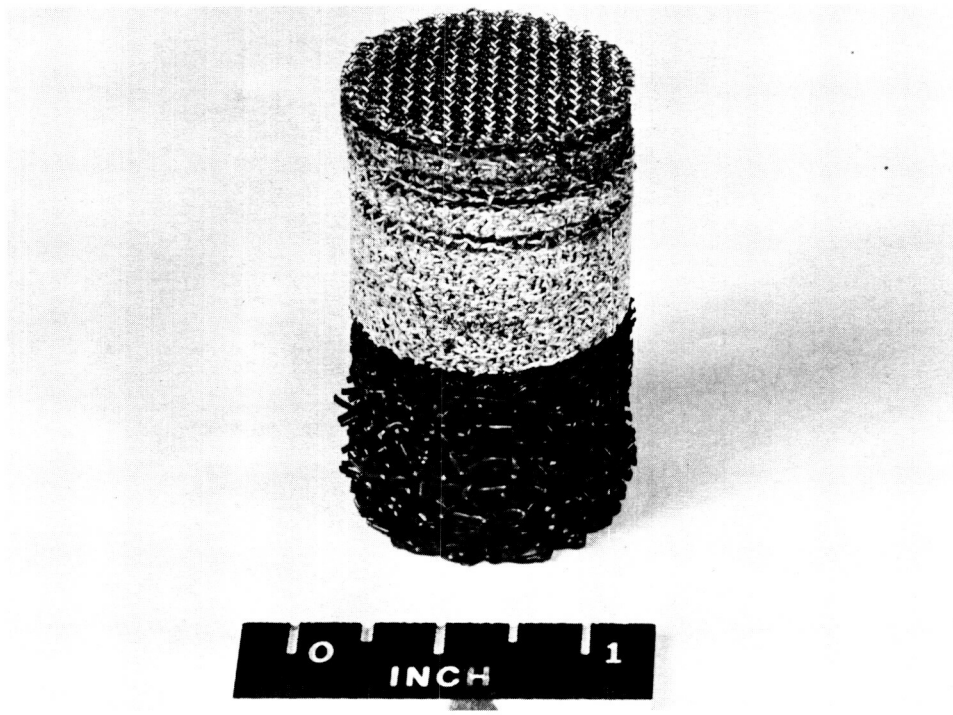

(a) Bed assembly. L-62-570

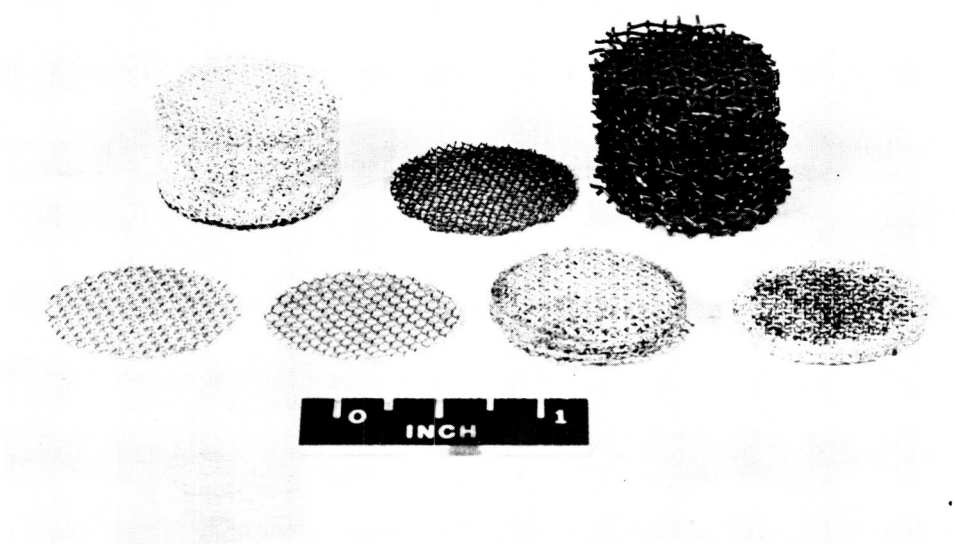

(b) Bed sections. L-62-567

Figure 24.- Catalyst bed 3 after 7.01 minutes run time.

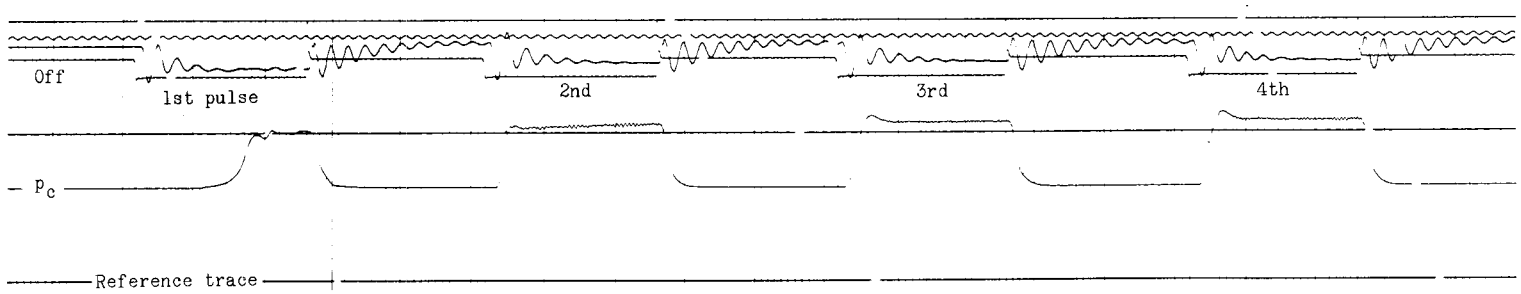

(a) Cold start; H_2O_2 at 35° F; motor warm; t = 20 minutes.

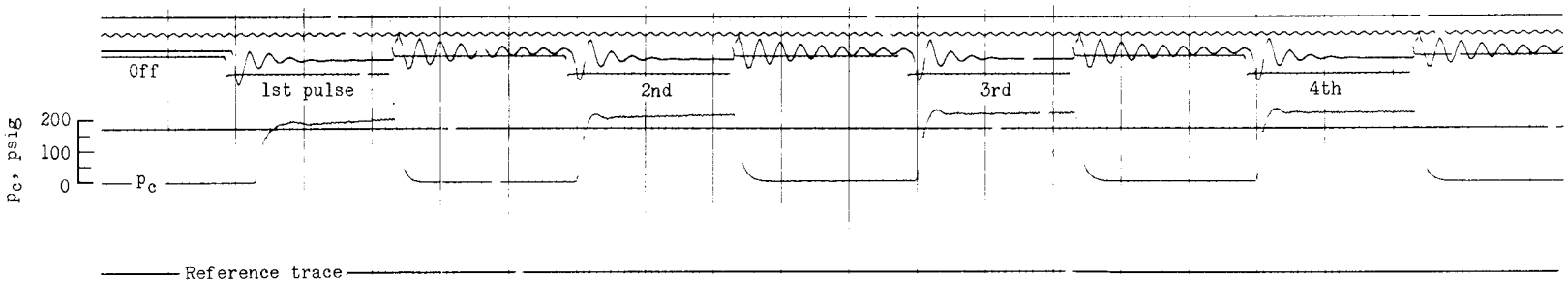

(b) Ambient run; 72° F; t = 21 minutes.

Figure 25.- Oscillograph records illustrating delay times for chamber pressure buildup and decay for catalyst pack of reaction-control rocket.

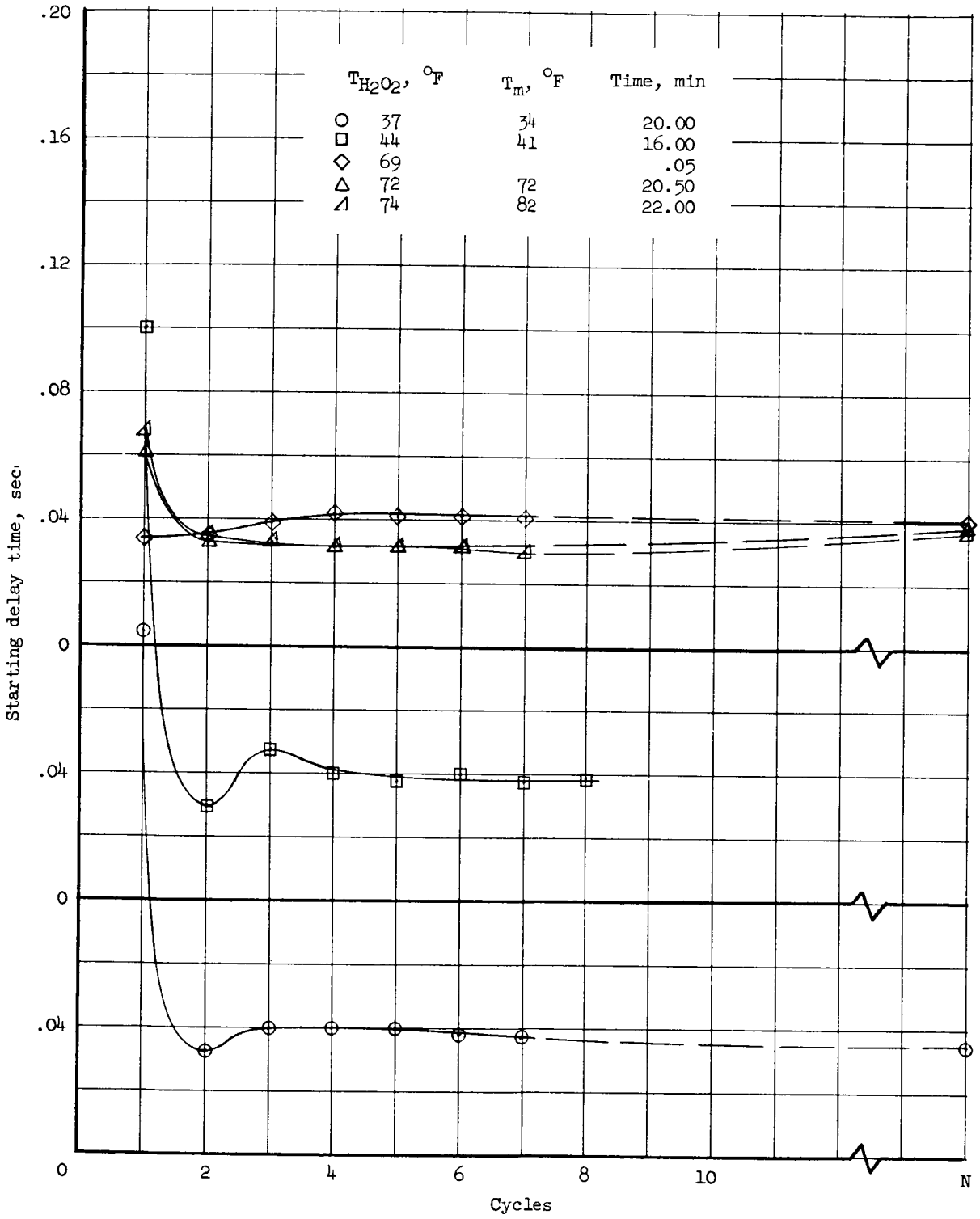

Figure 26.- Starting delay time of reaction-control rocket.

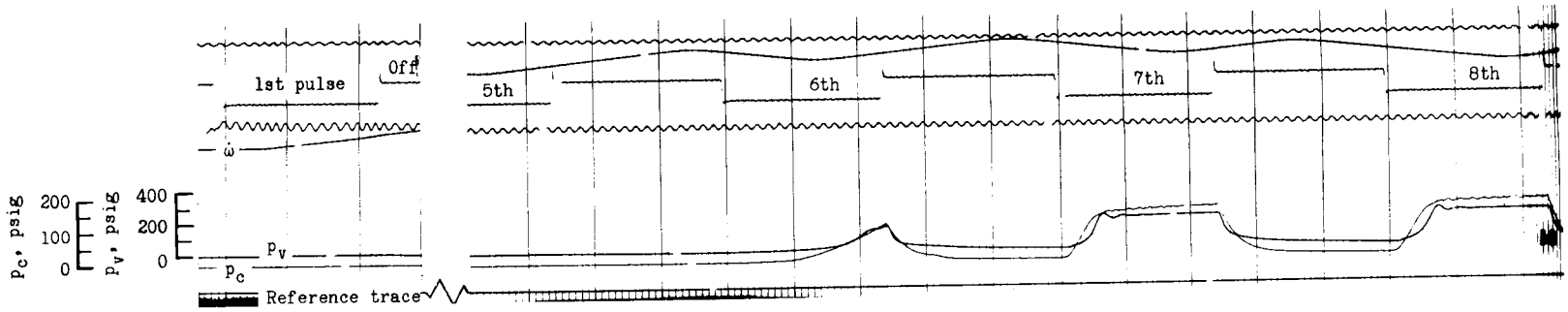

(a) Initial 35° F run.

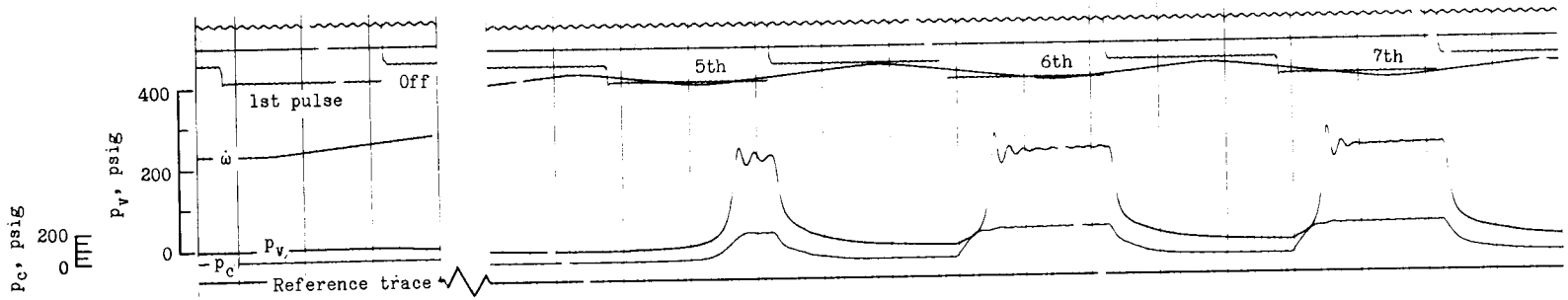

(b) Final 35° F run; t = 6.5 minutes.

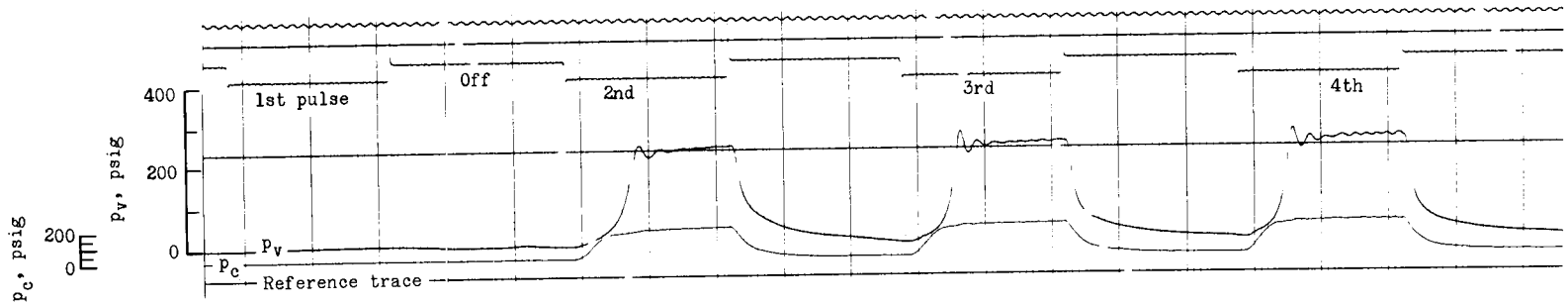

(c) Ambient run; 60° F; t = 7.2 minutes.

Figure 27.- Oscillograph records illustrating delay times for chamber pressure buildup and decay for catalyst bed 4.

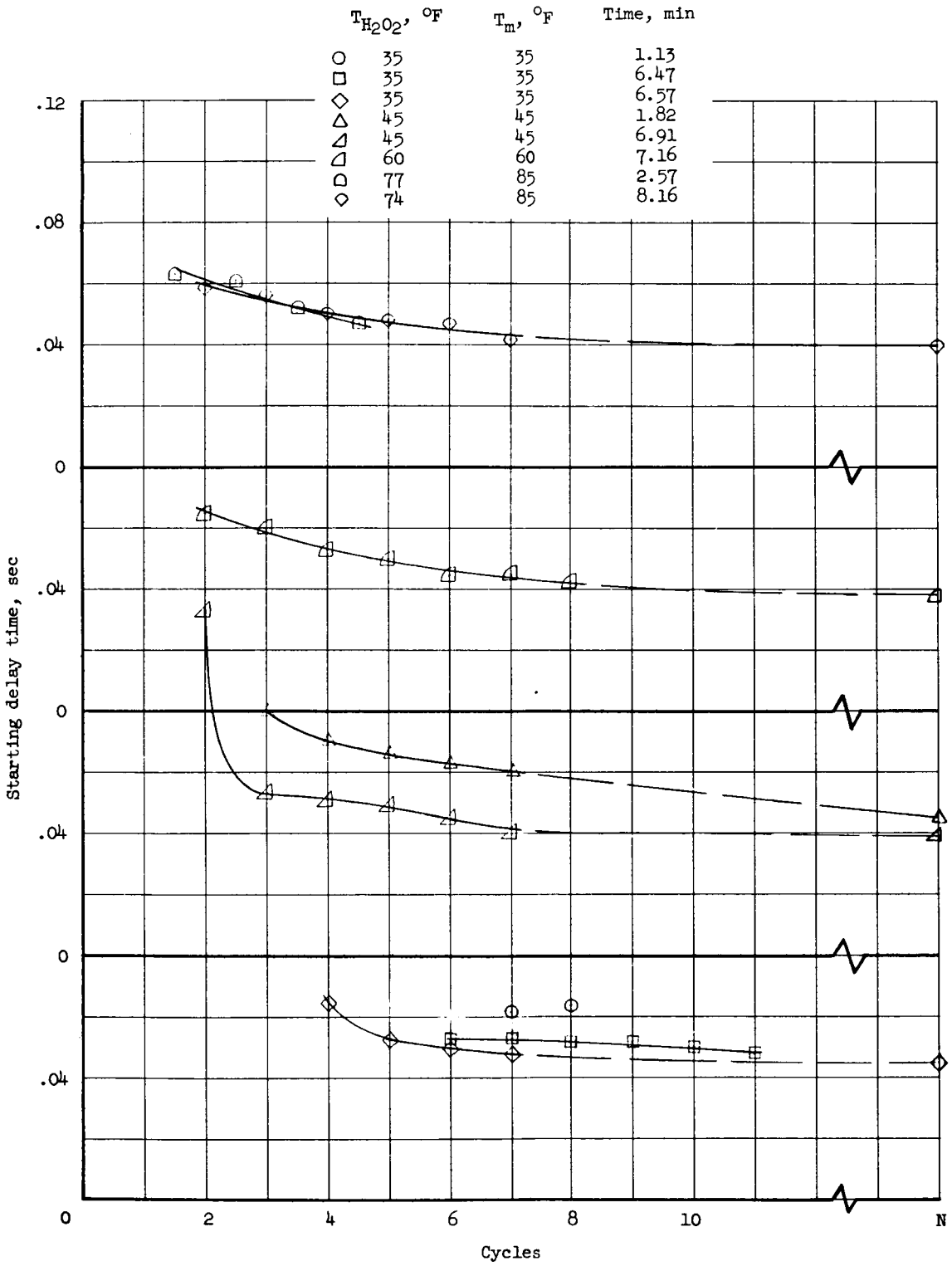

Figure 28.- Starting delay time of catalyst bed 4 during cycling operation.

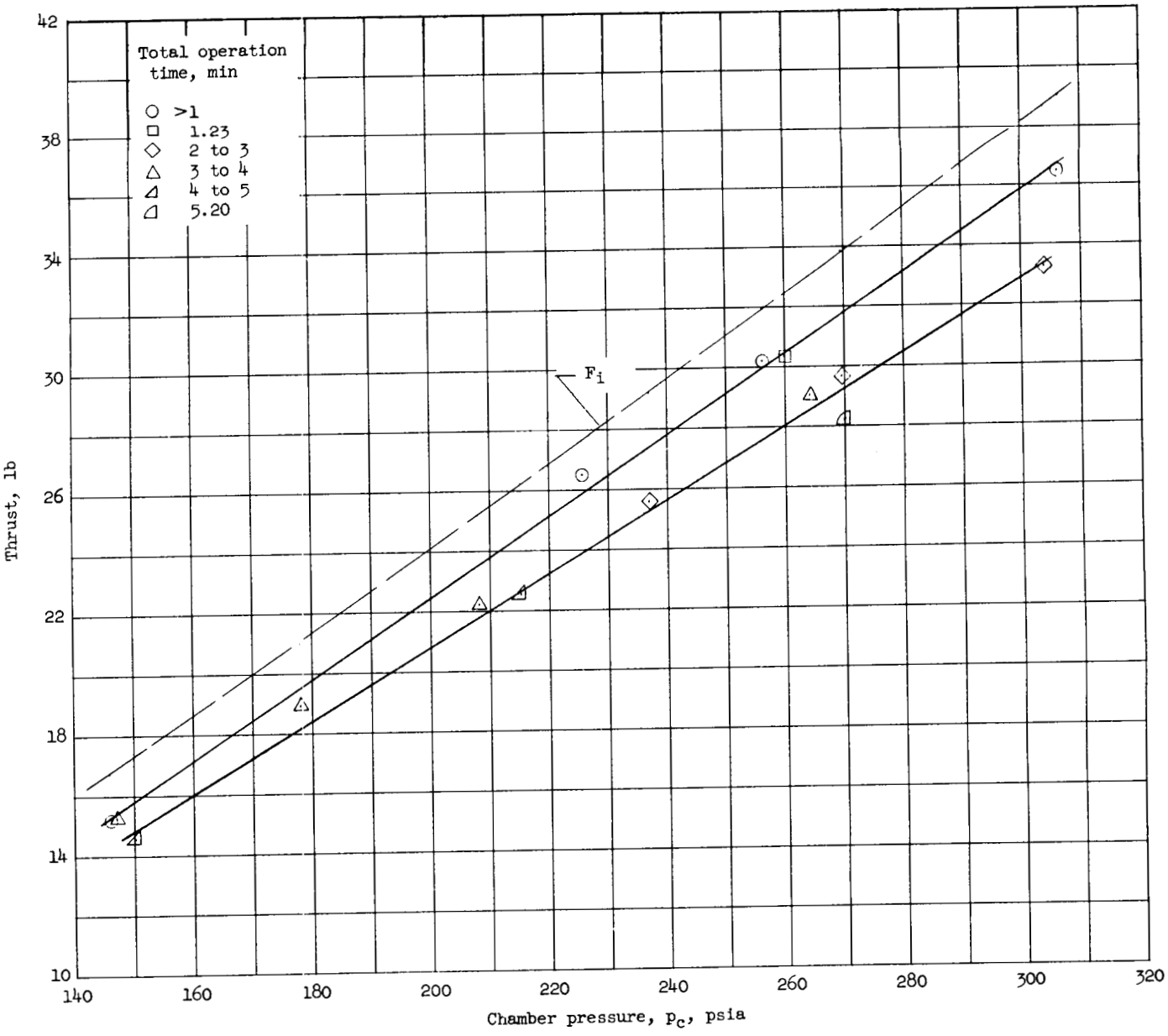

Figure 29.- Variation in thrust with chamber pressure for catalyst bed 4.

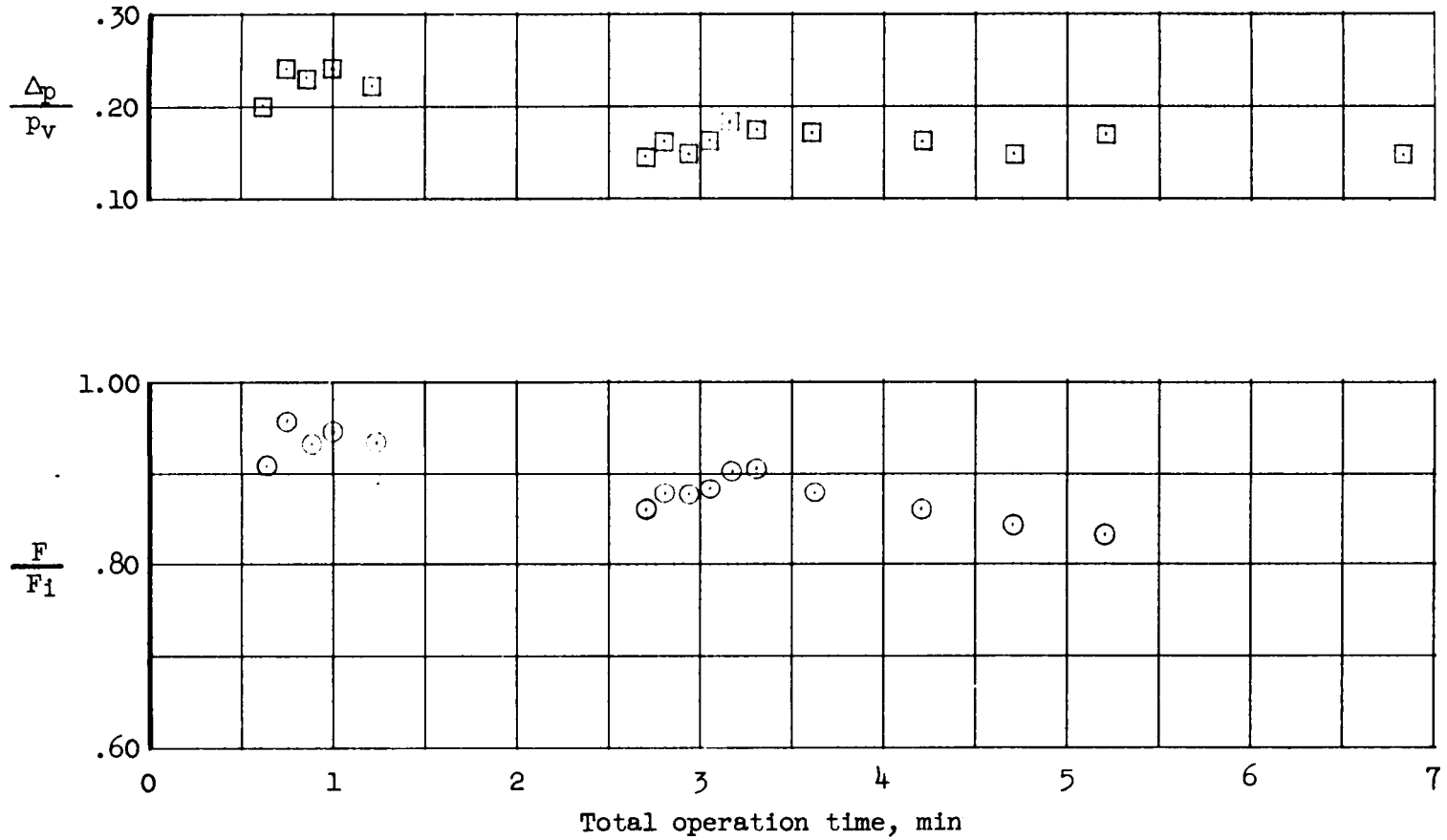

Figure 30.- Variation of thrust ratio and bed pressure drop with operation time for bed 4.

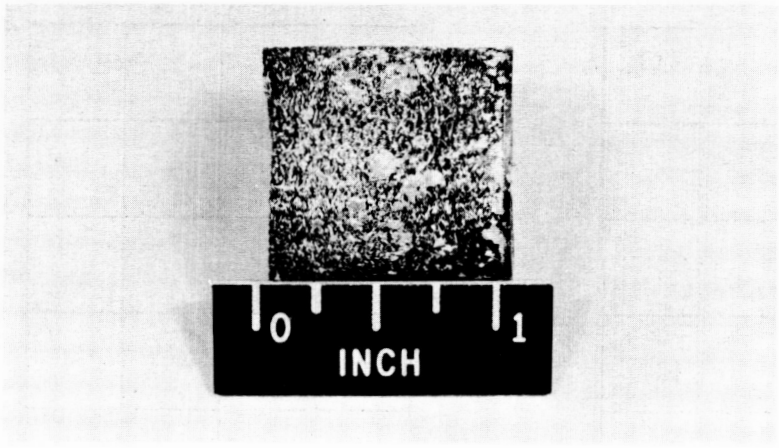

(a) Nickel screen pack. L-61-5042

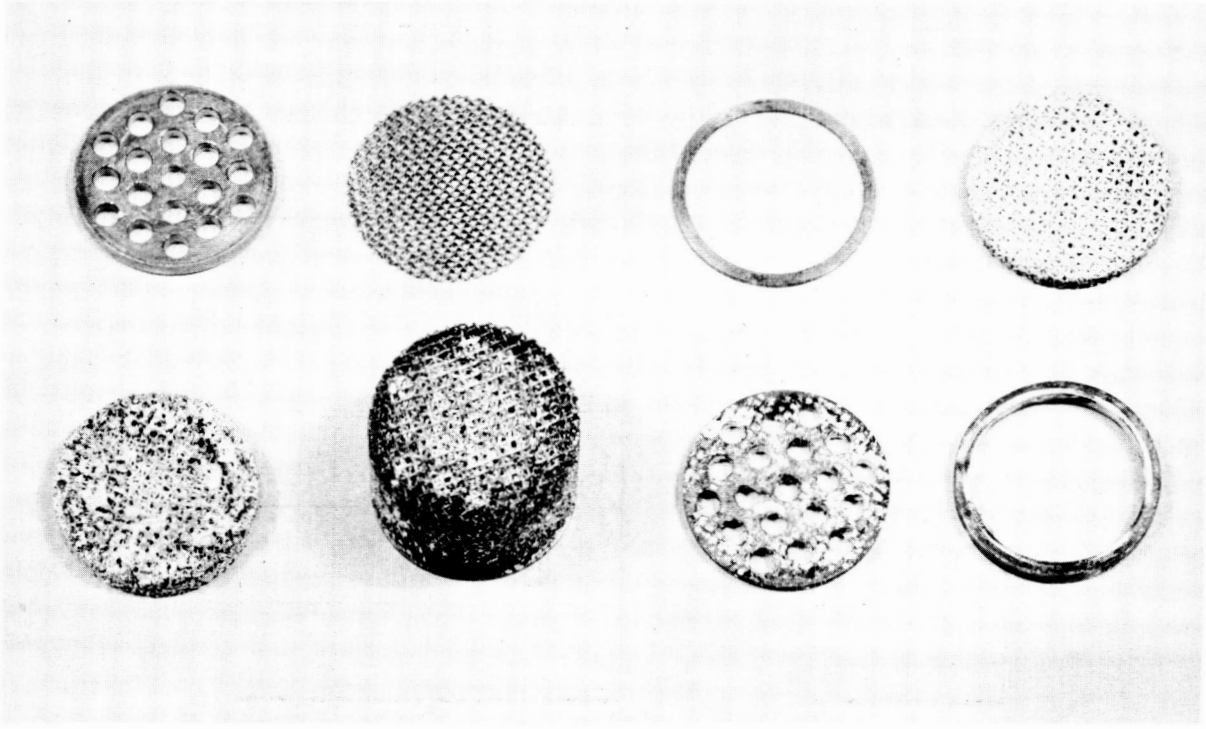

(b) Bed sections. L-61-5041

Figure 31.- Catalyst bed 4 after 2.15 minutes run time.

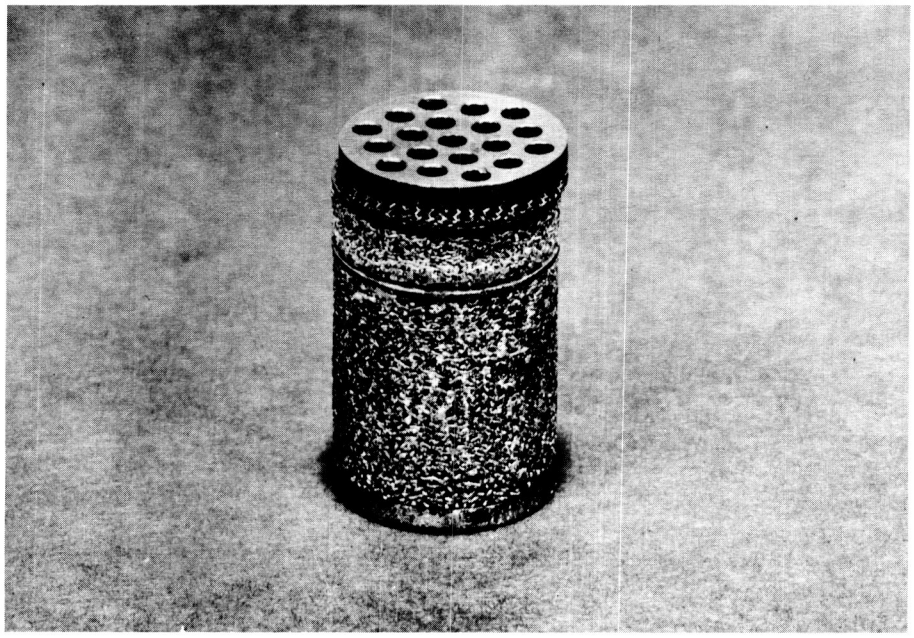

(a) Bed assembly. L-61-6002

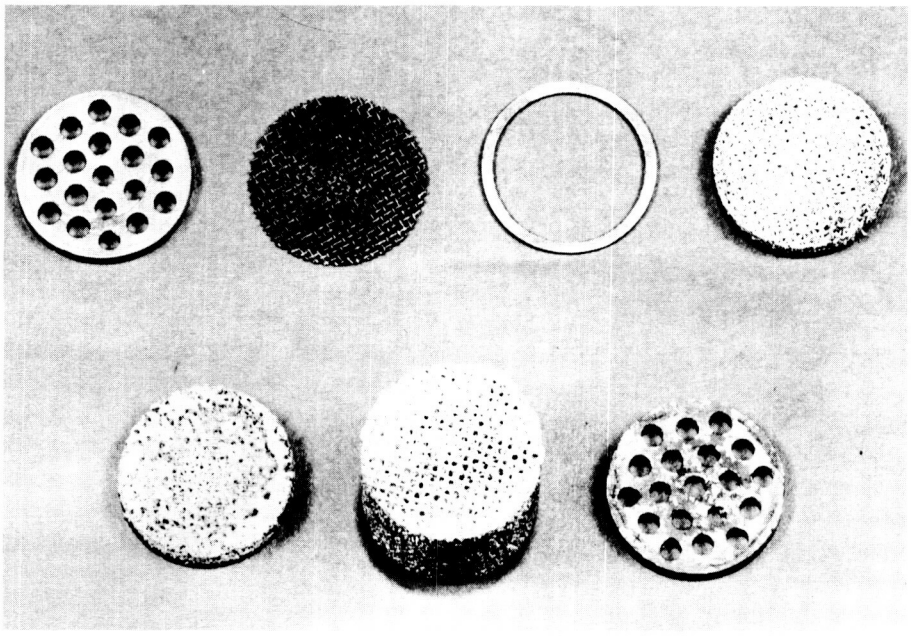

(b) Bed sections. L-61-6001

Figure 32.- Catalyst bed 4 after 10.38 minutes run time.

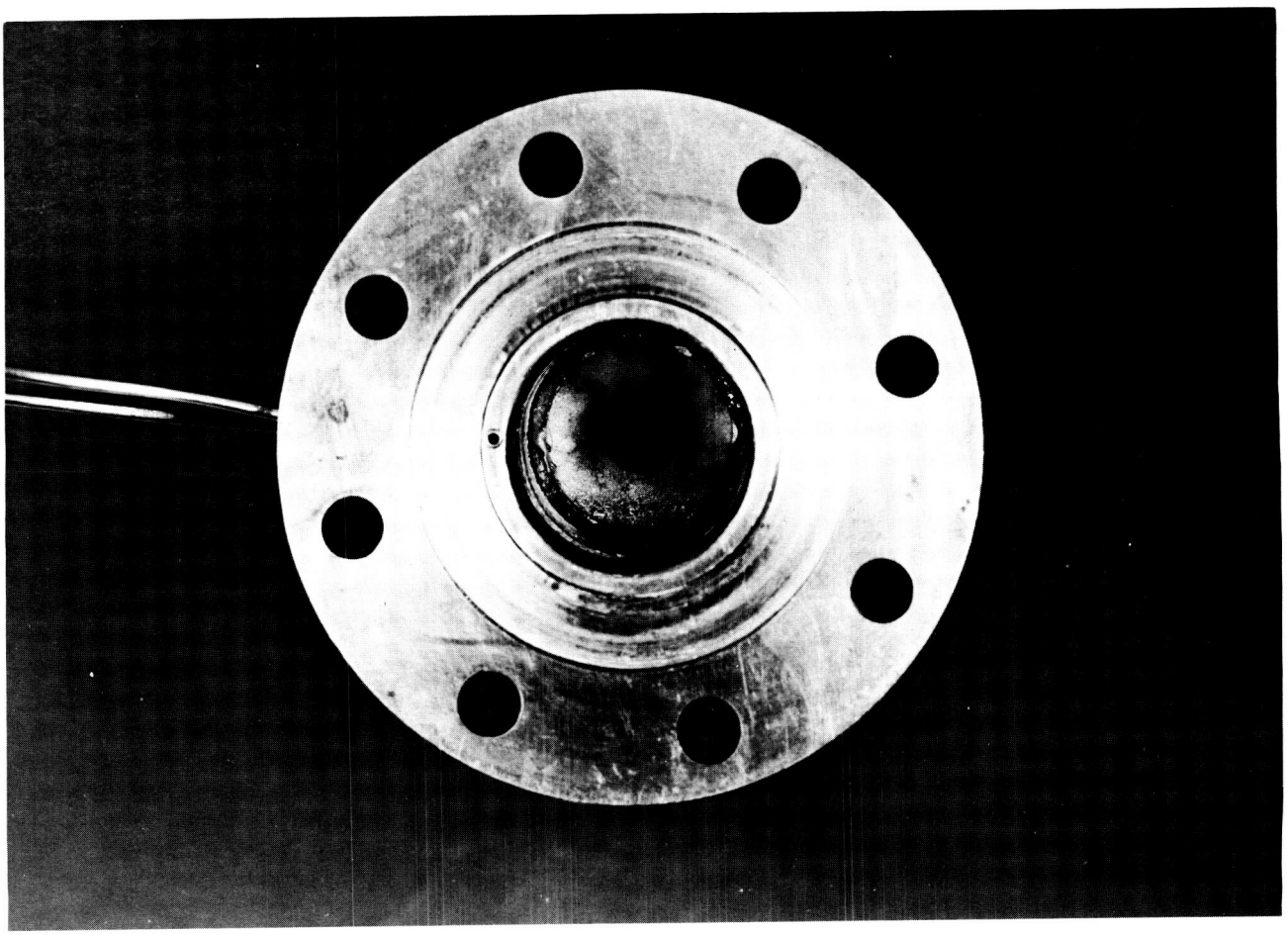

L-61-6003

Figure 33.- Interior of decomposition chamber A after 10.38 minutes run time with catalyst bed 4.

61

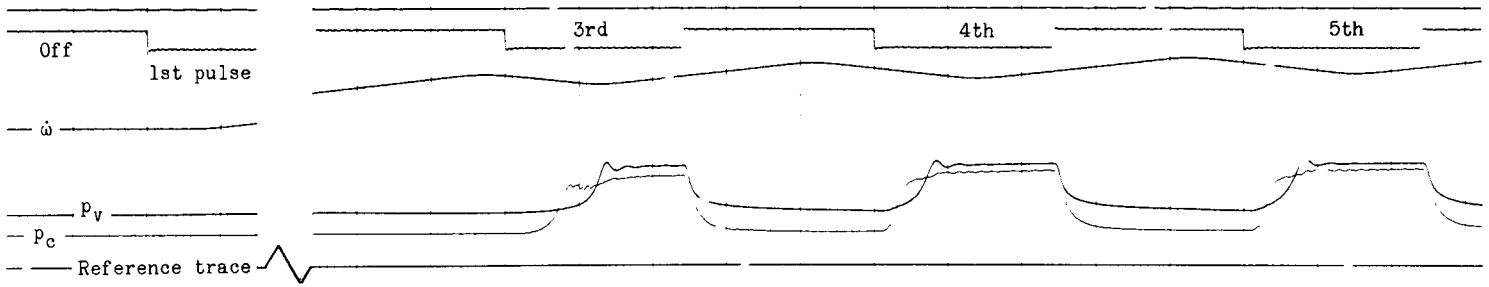

(a) Initial 35° F run.

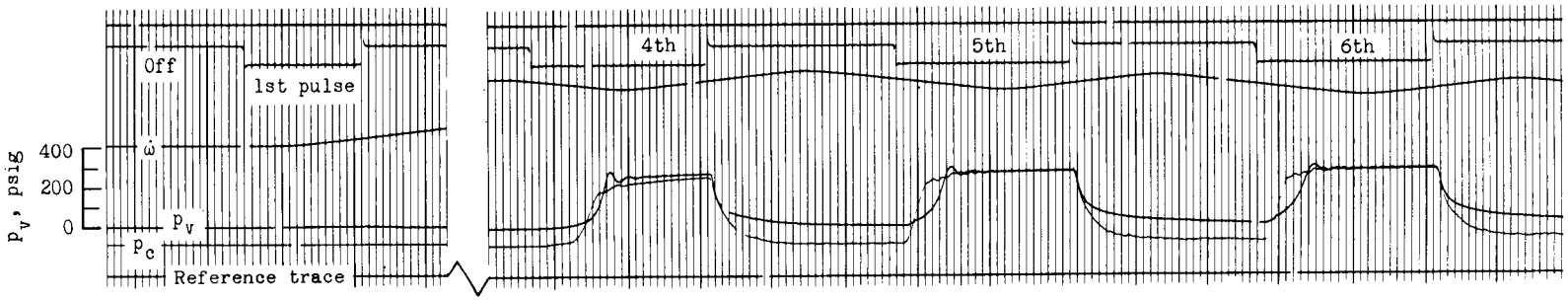

(b) Final 35° F run; t = 7.0 minutes.

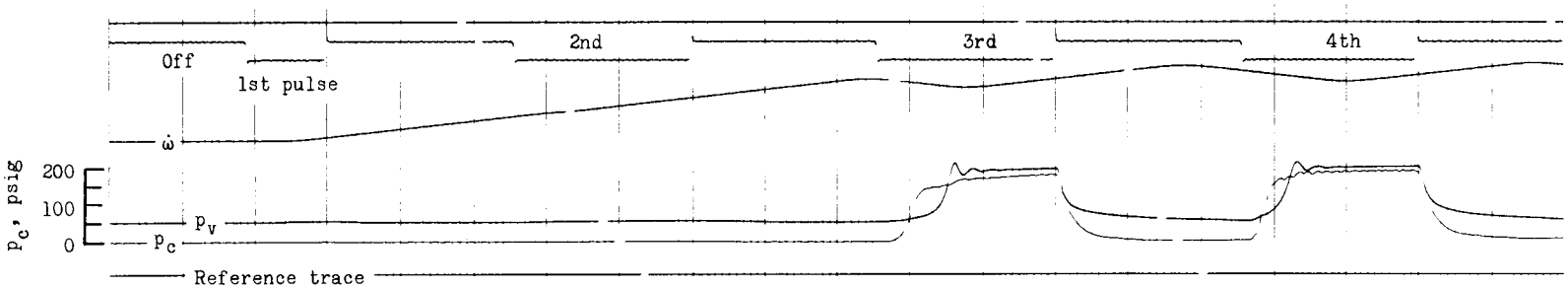

(c) Ambient run; 60° F; t = 1.2 minutes.

Figure 34.- Oscillograph records illustrating delay times for chamber pressure buildup and decay for catalyst bed 5.

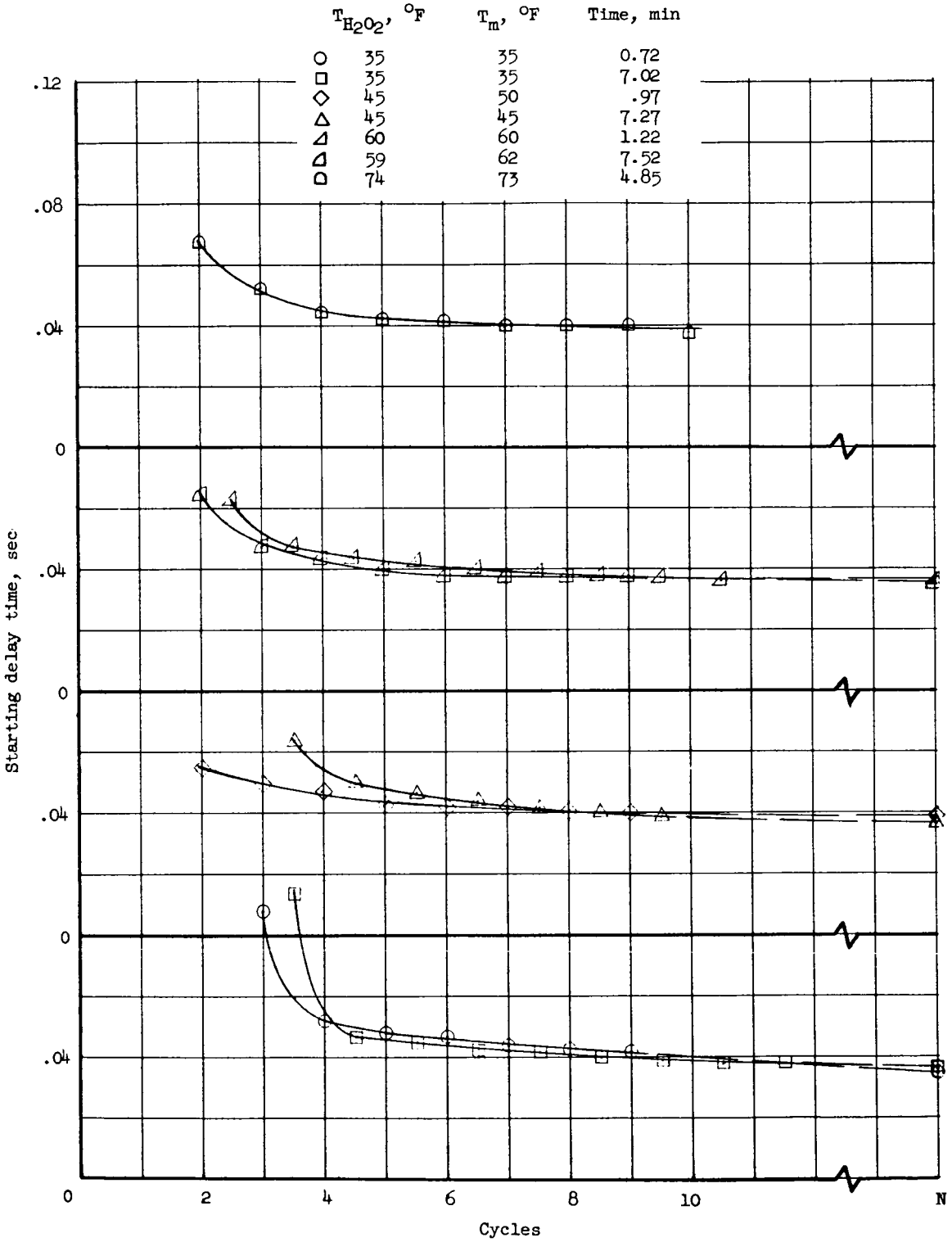

Figure 35.- Starting delay time of catalyst bed 5 during cycling operation.

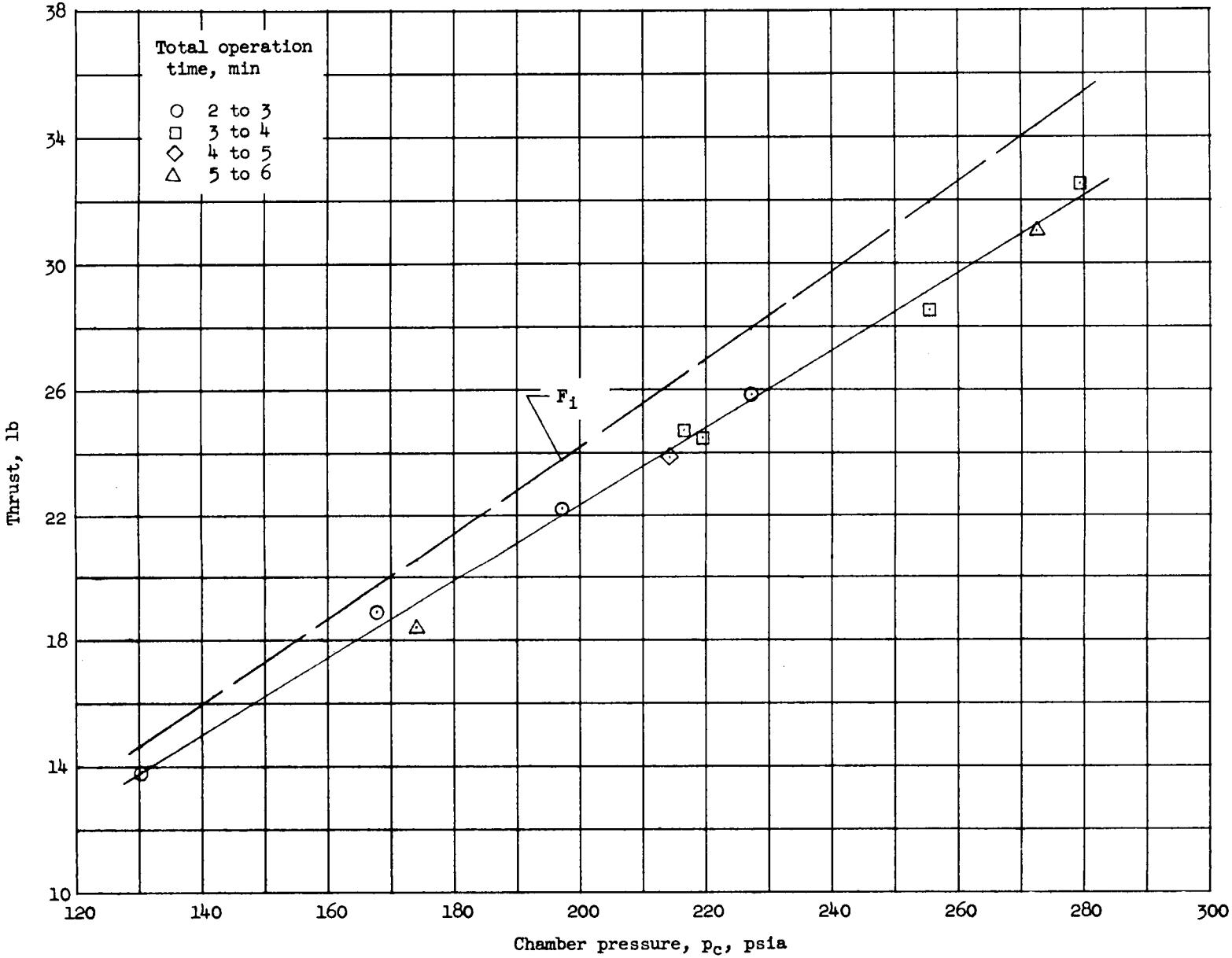

Figure 36.- Variation in thrust with chamber pressure for catalyst bed 5.

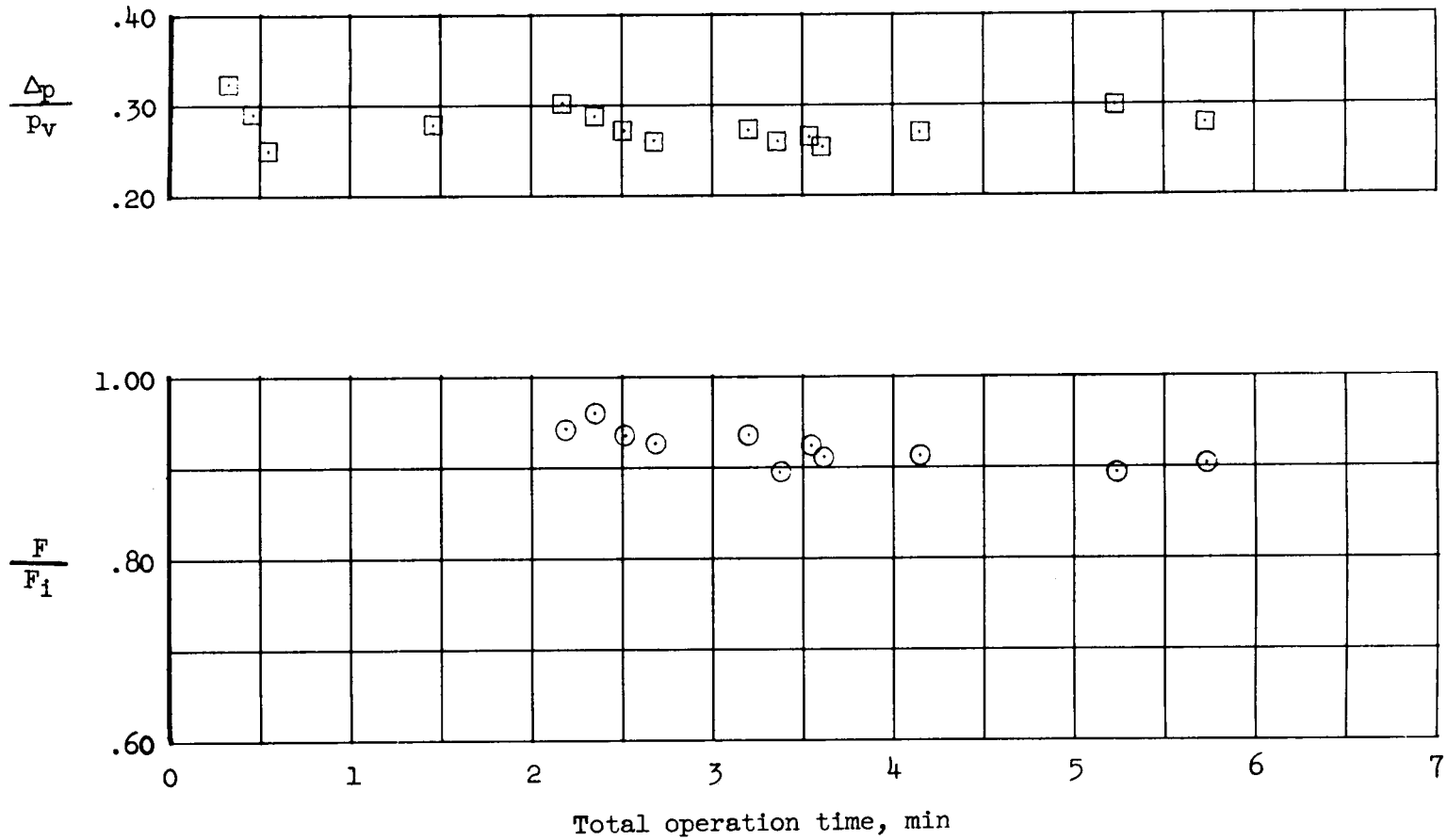

Figure 37.- Variation of thrust ratio and bed pressure drop with operation time for bed 5.

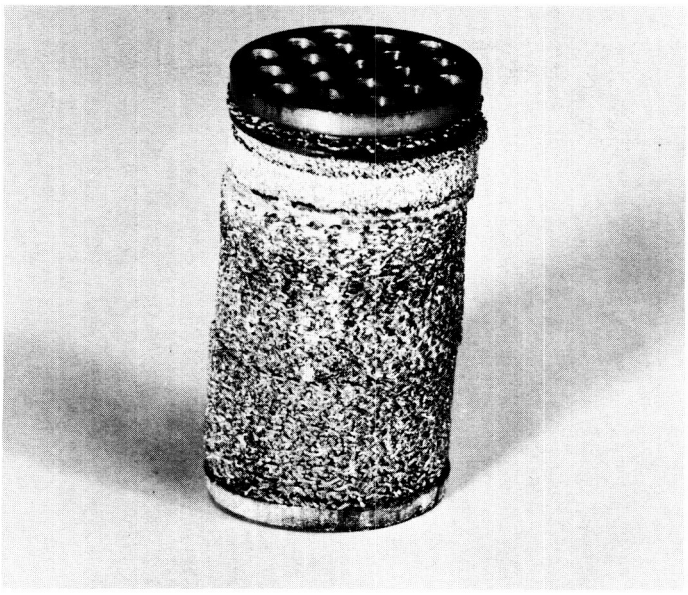

(a) Bed assembly. L-61-7045

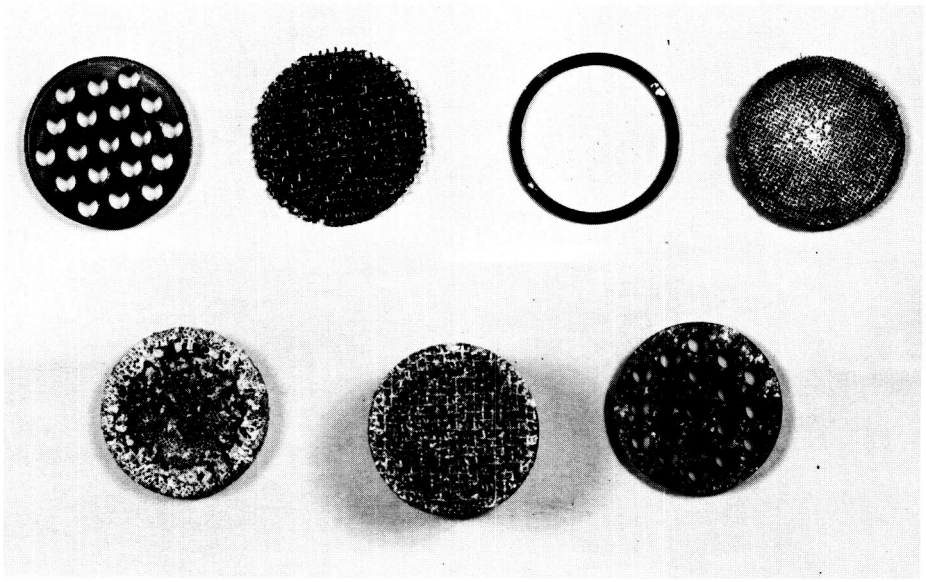

(b) Bed sections. L-61-7043

Figure 38.- Catalyst bed 5 after 8.31 minutes run time.

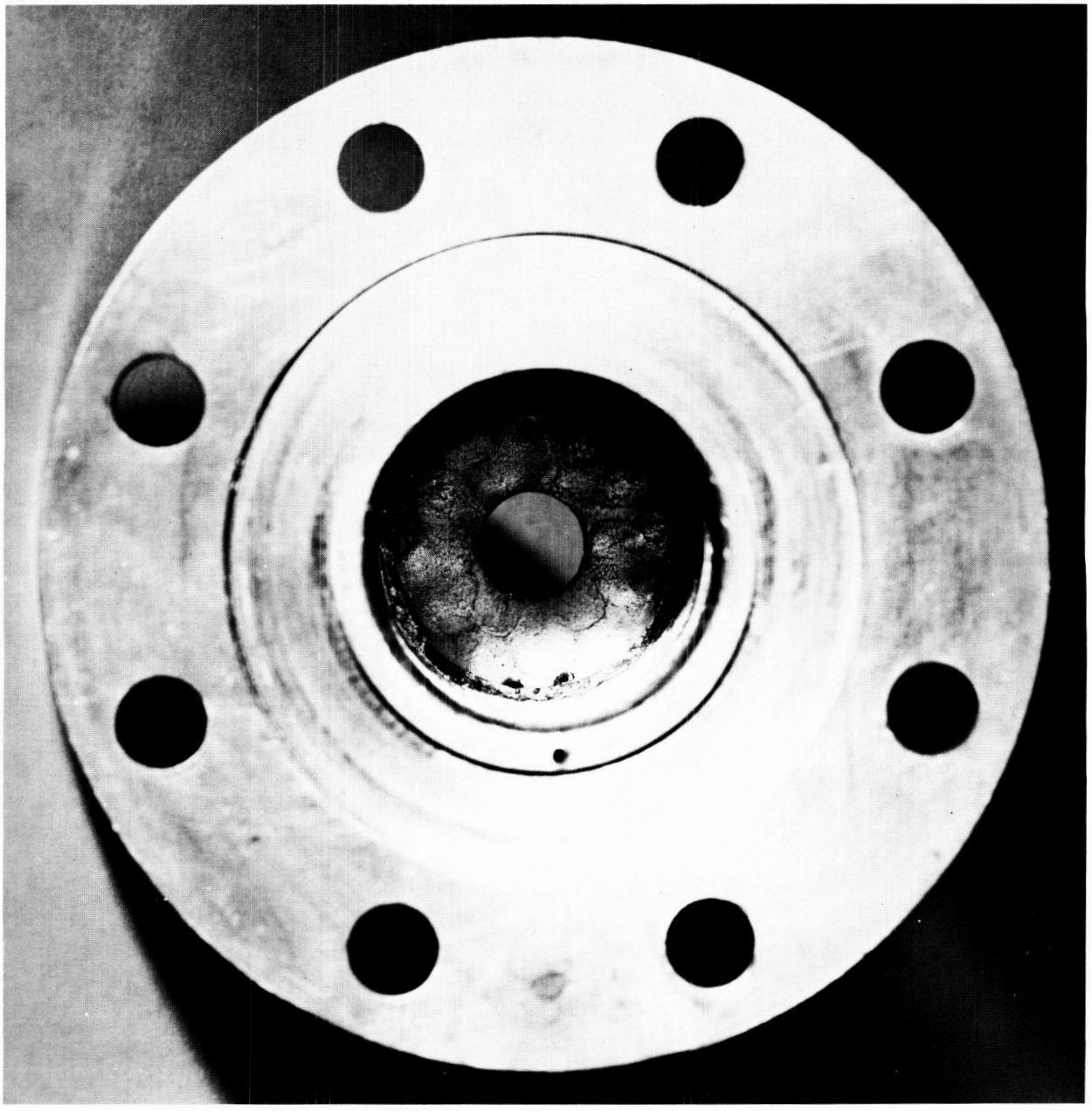

L-61-7044

Figure 39.- Interior of decomposition chamber A after 8.31 minutes run time with catalyst bed 5.

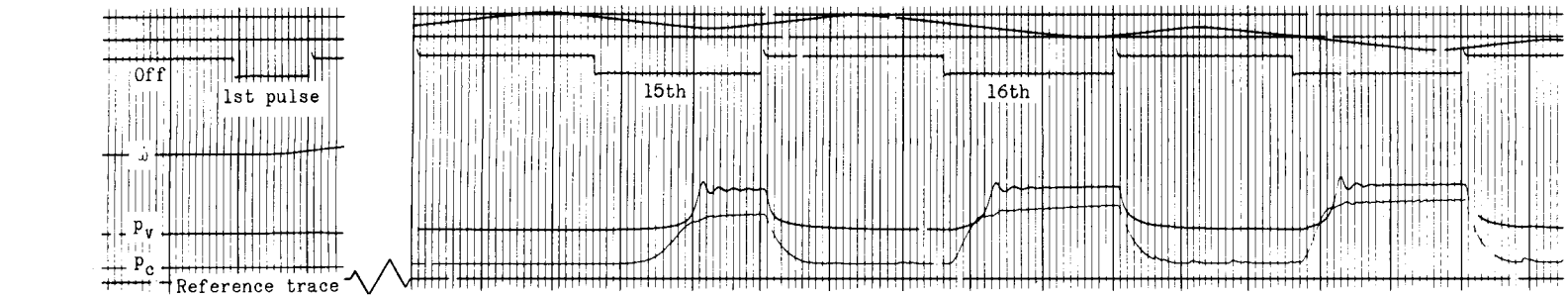

(a) Initial 35° F run.

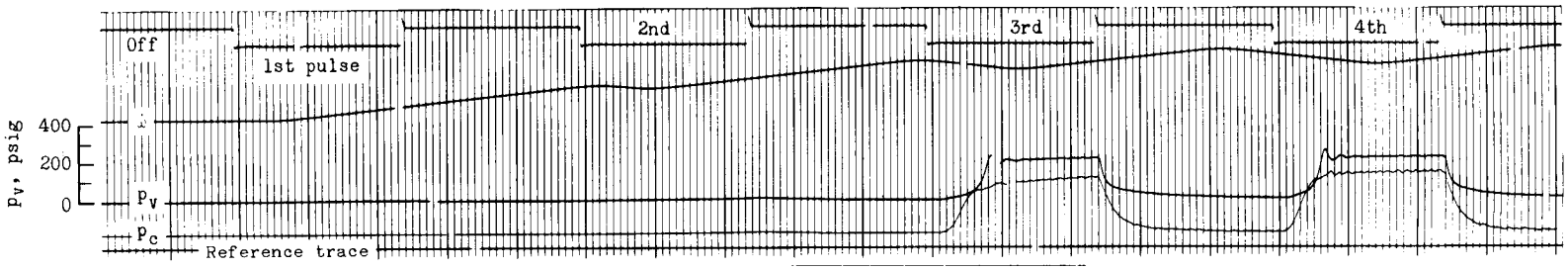

(b) Final 35° F run; t = 7.5 minutes.

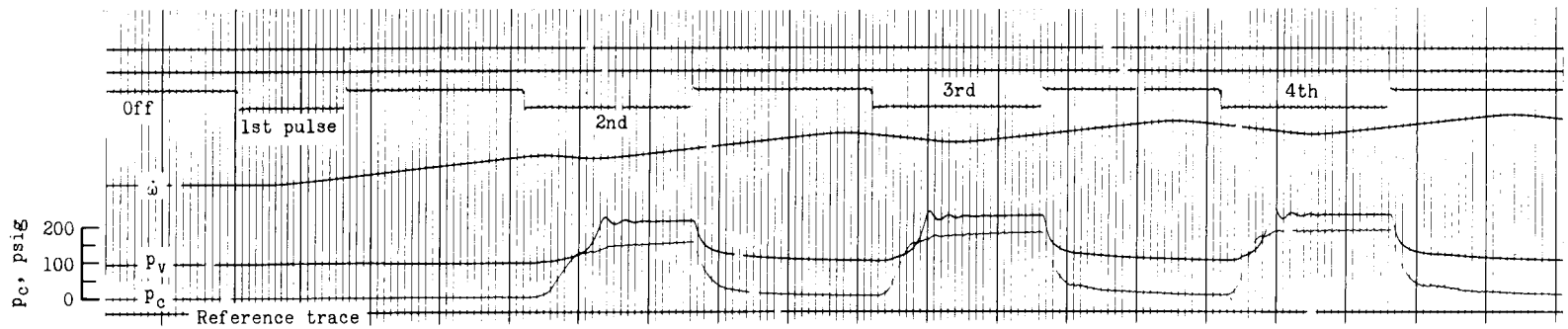

(c) Ambient run; 60° F; t = 2.0 minutes.

Figure 40.- Oscillograph records illustrating delay times for chamber pressure buildup and decay for catalyst bed 6.

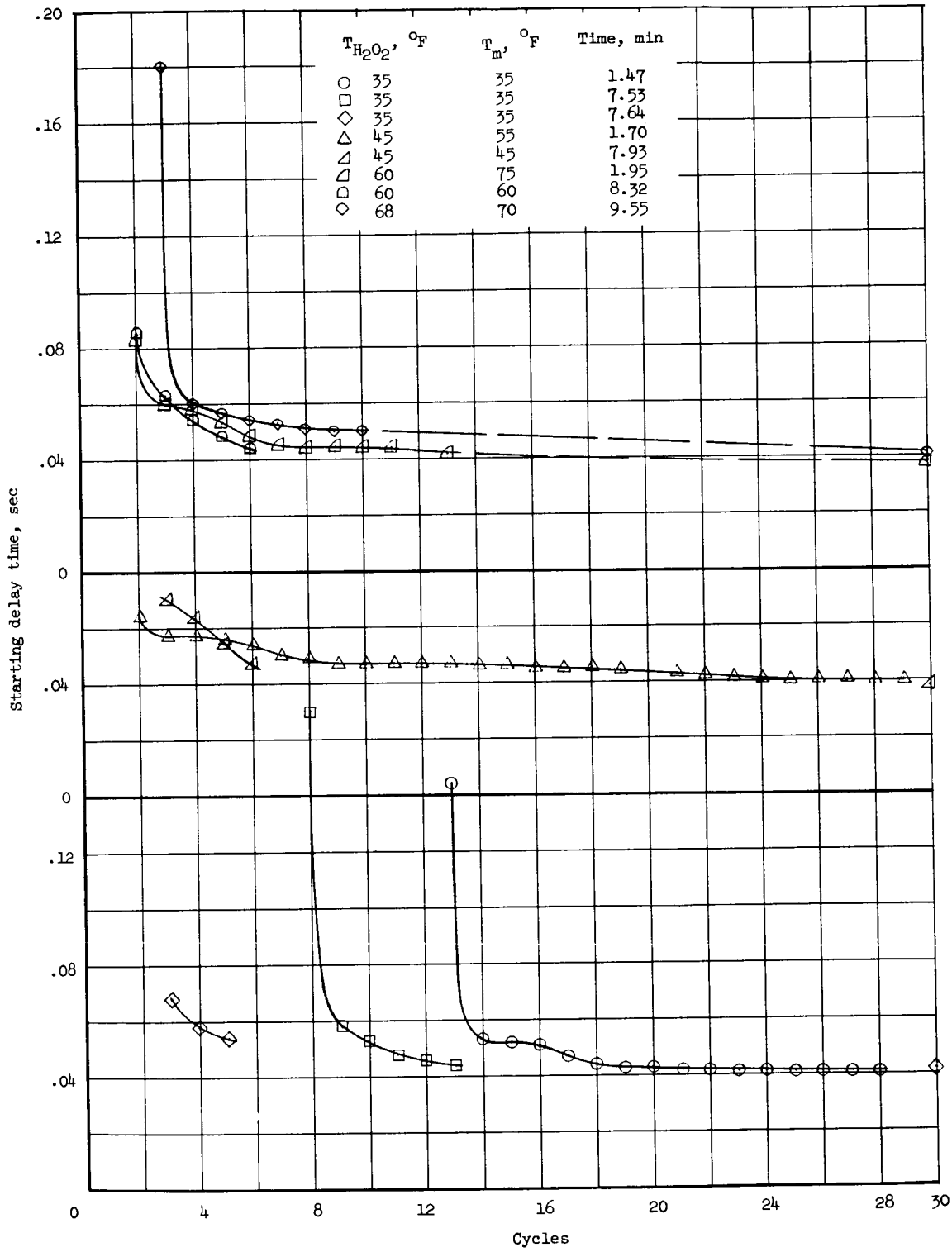

Figure 41.- Starting delay time of catalyst bed 6 during cycling operation.

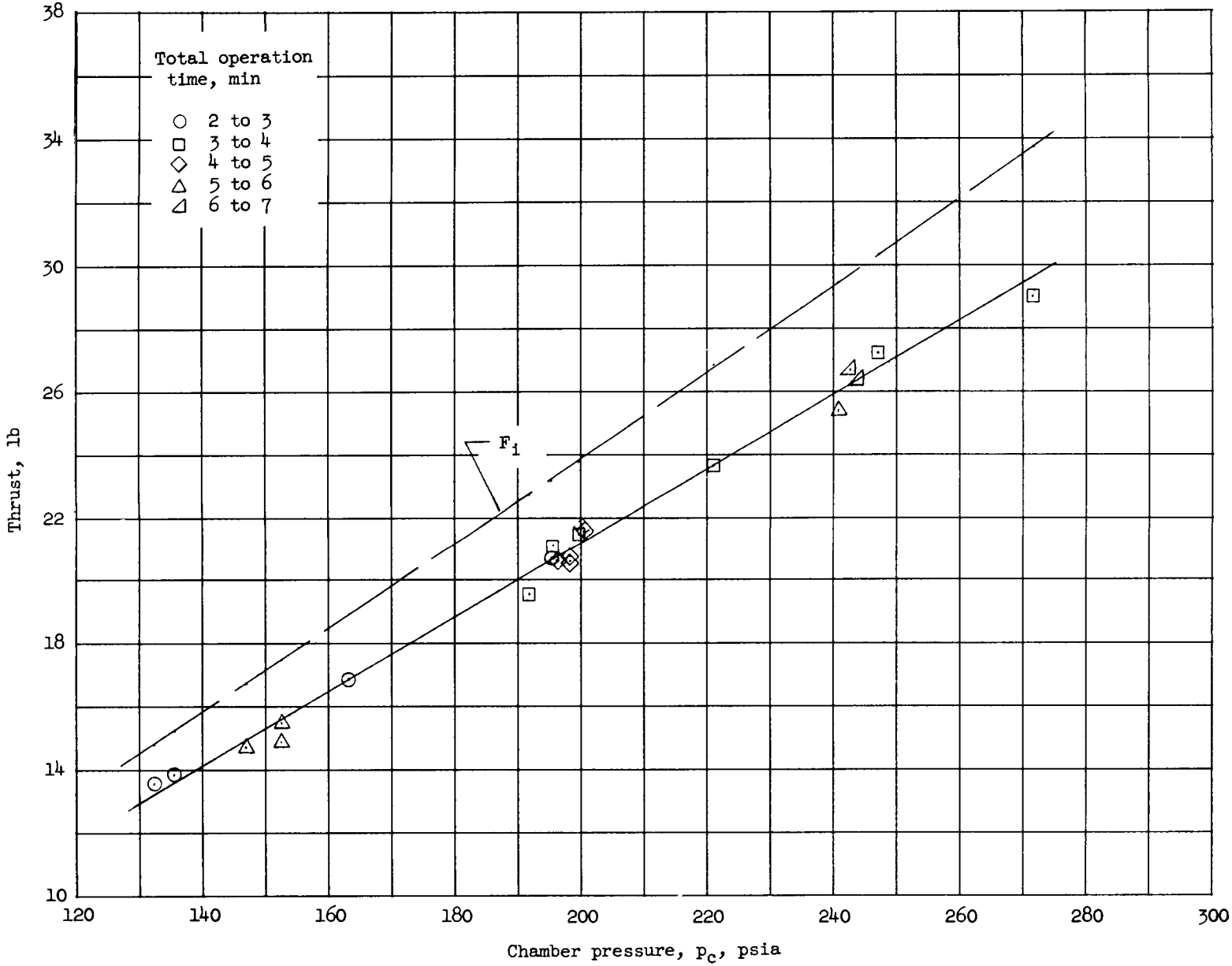

Figure 42.- Variation in thrust with chamber pressure for catalyst bed 6.

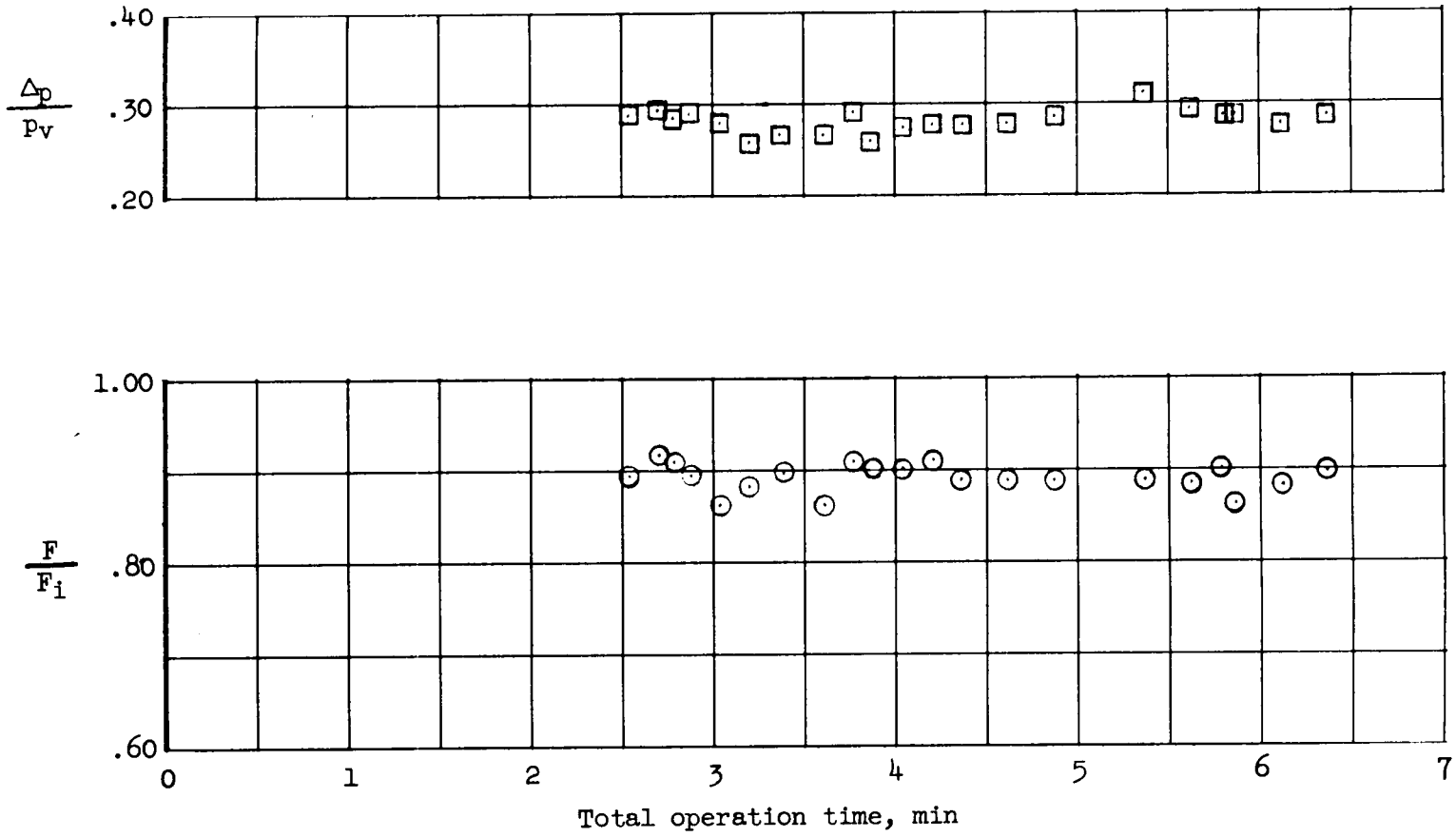

Figure 43.- Variation of thrust ratio and bed pressure drop with operation time for bed 6.

(a) Bed assembly. L-61-7616

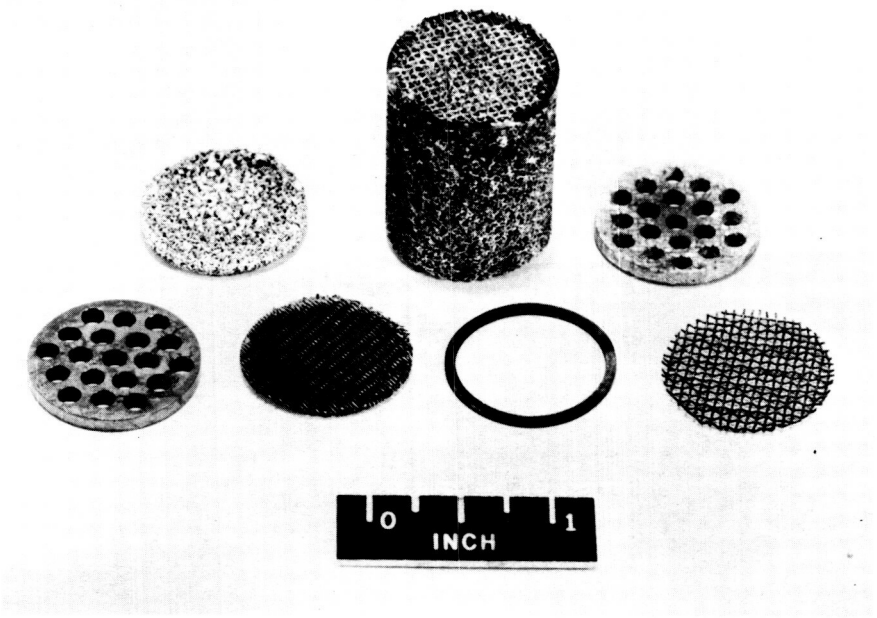

(b) Bed sections. L-61-7617

Figure 44.- Catalyst bed 6 after 9.64 minutes run time.

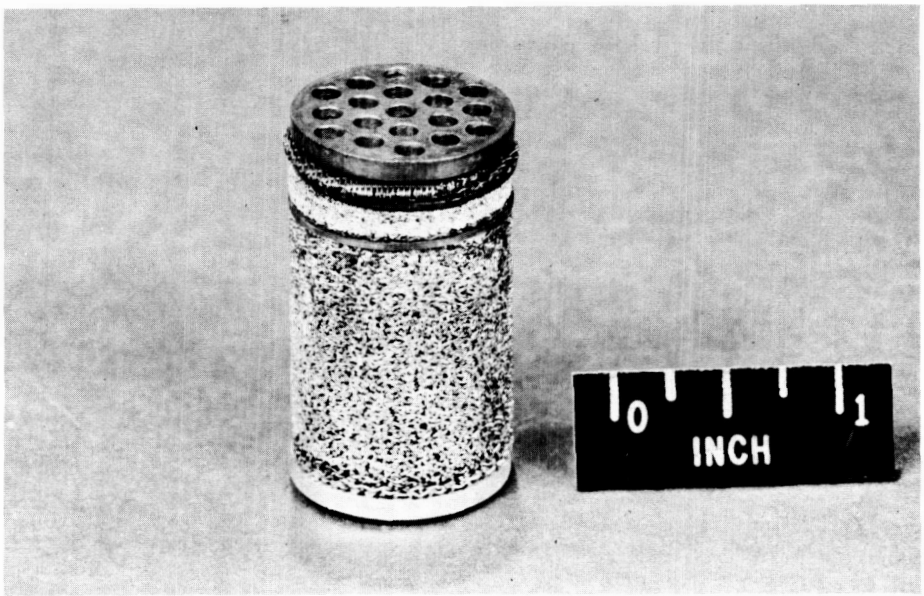

(a) Bed assembly. L-61-8375

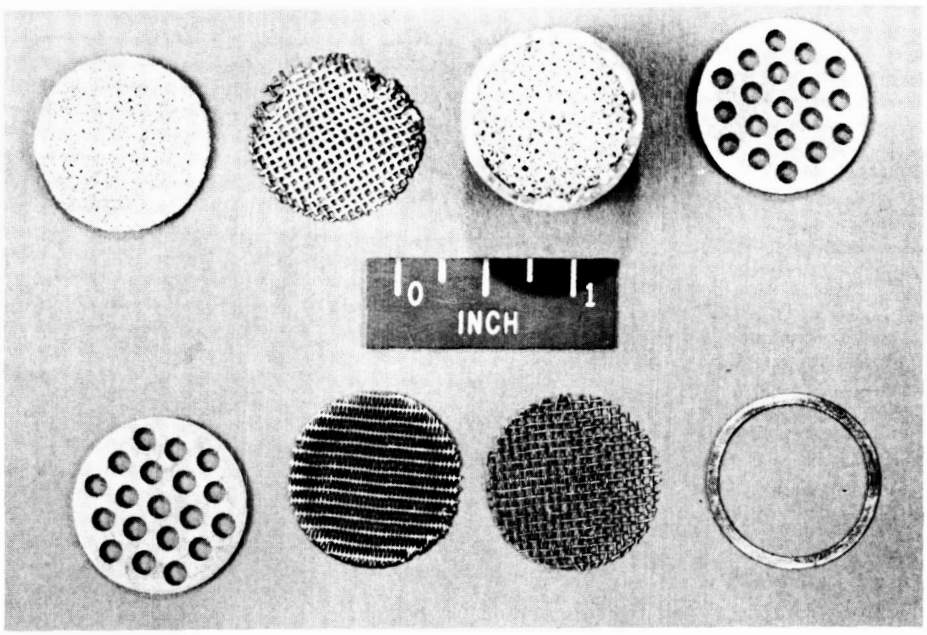

(b) Bed sections. L-61-8374

Figure 45.- Catalyst bed 6 after 12.62 minutes run time.

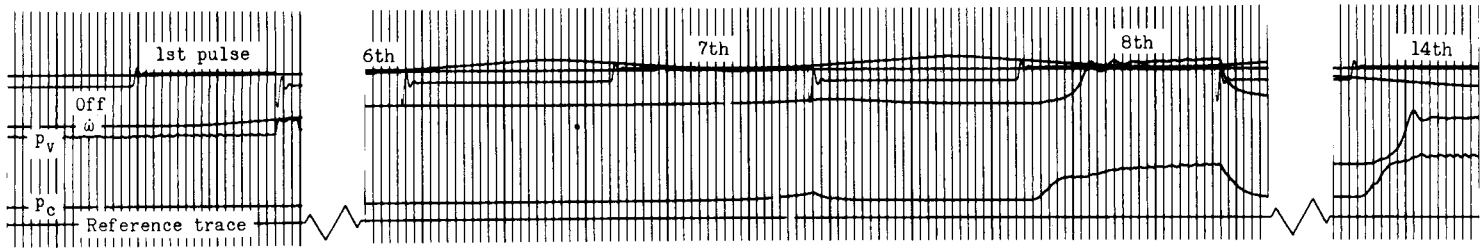

(a) Initial 35° F run.

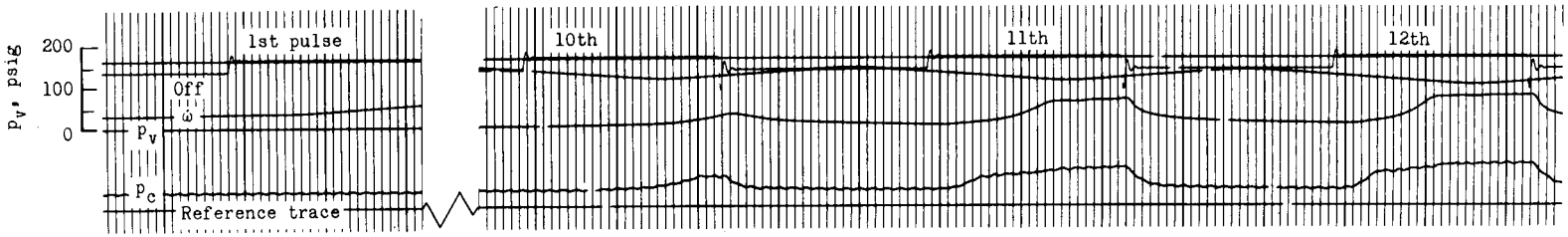

(b) Final 35° F run; t = 4.9 minutes.

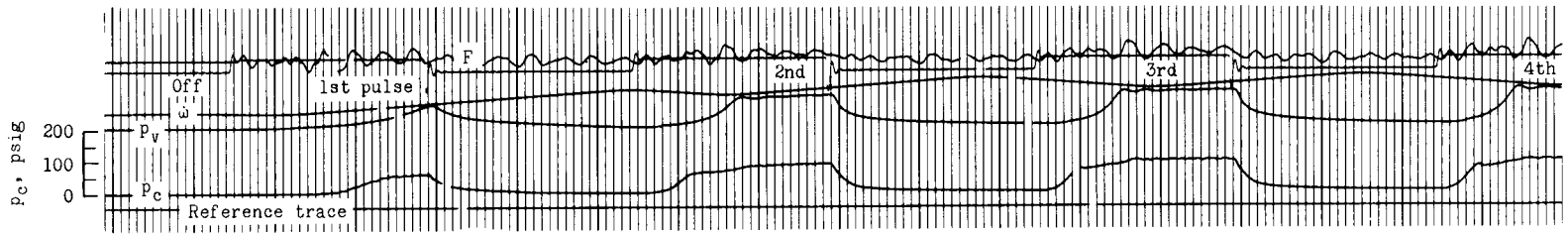

(c) Ambient run; 73° F; t = 4.2 minutes.

Figure 46.- Oscillograph records illustrating delay times for chamber pressure buildup and decay for catalyst bed 7.

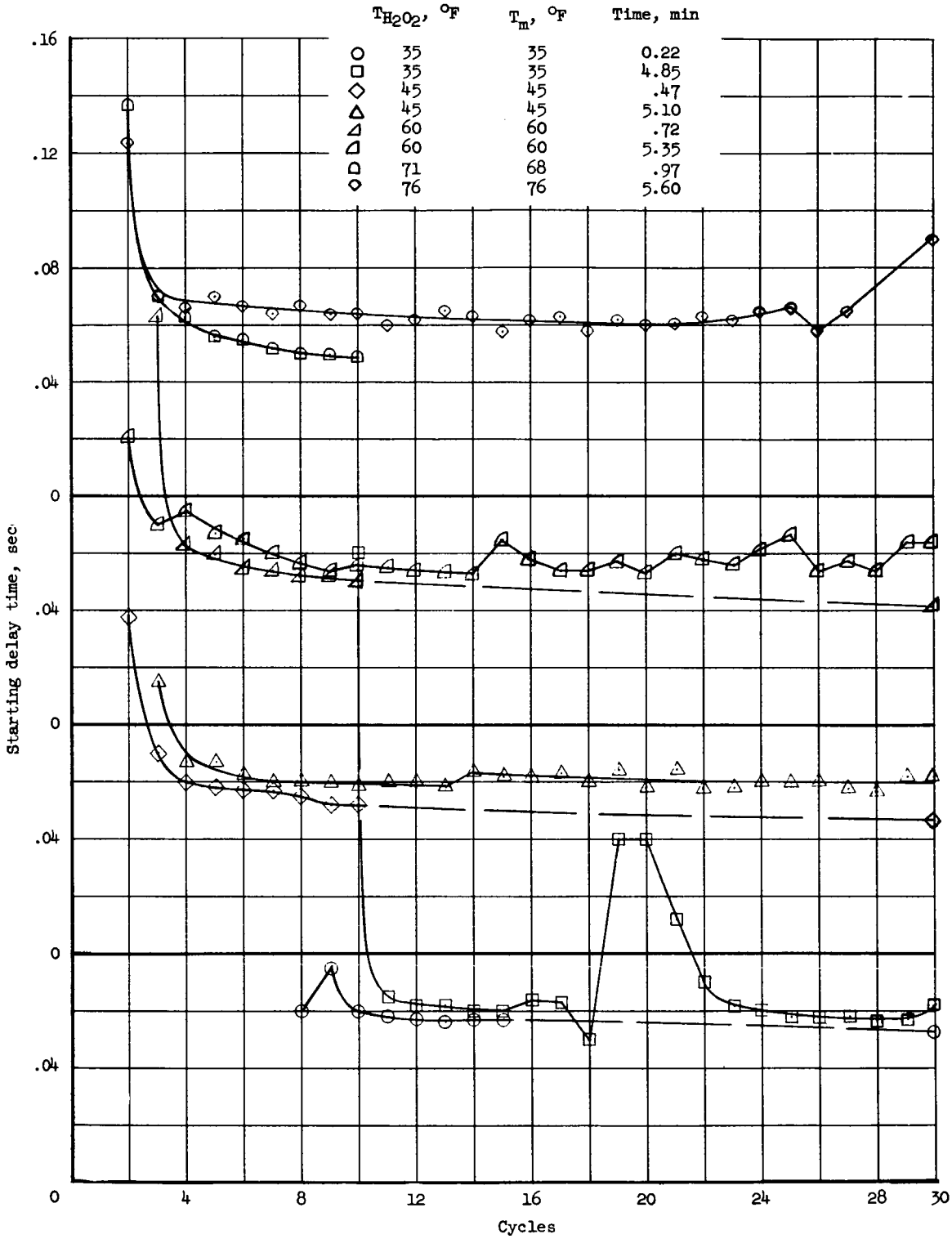

Figure 47.- Starting delay time of catalyst bed 7 during cycling operation.

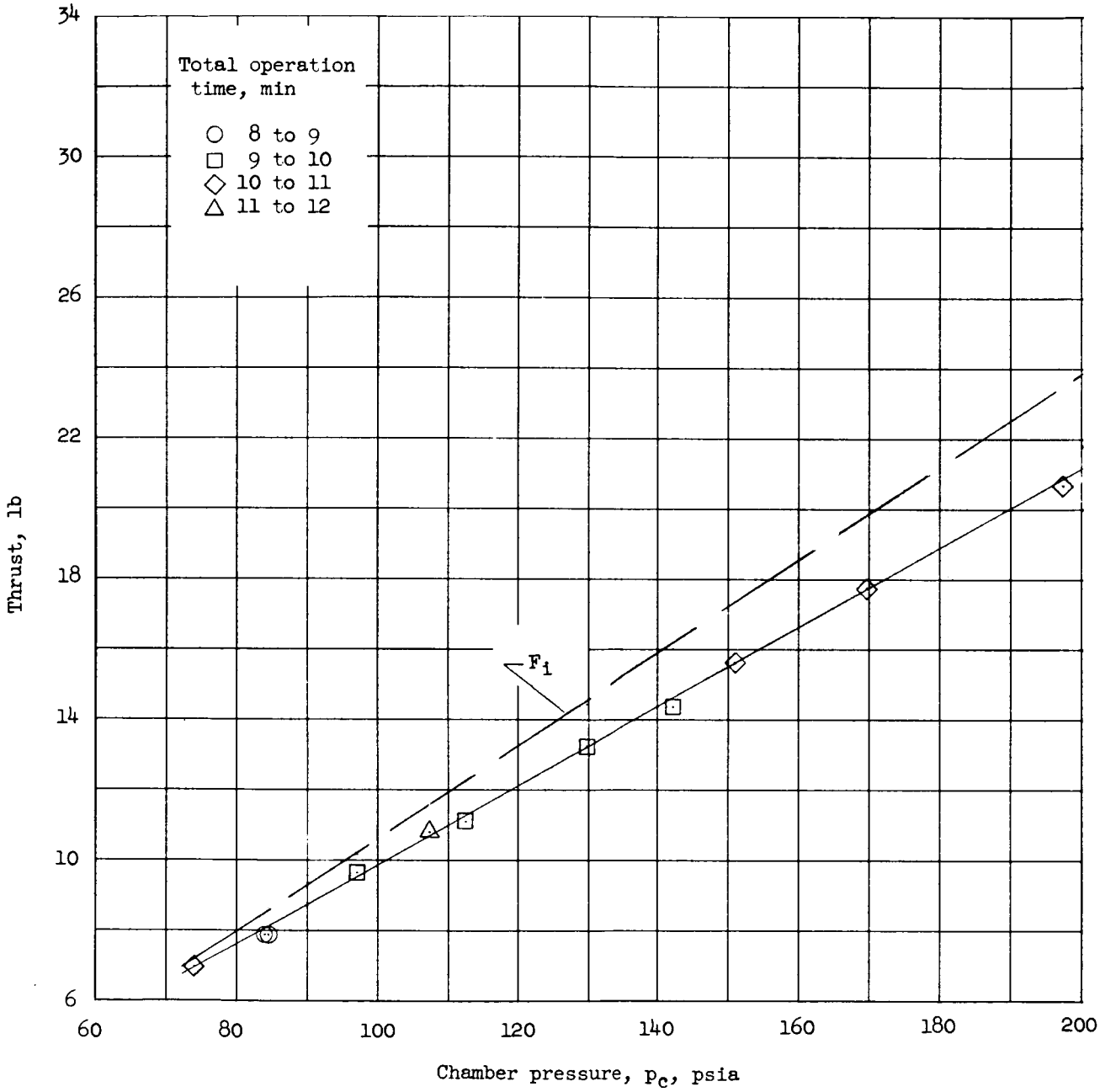

Figure 48.- Variation in thrust with chamber pressure for catalyst bed 7.

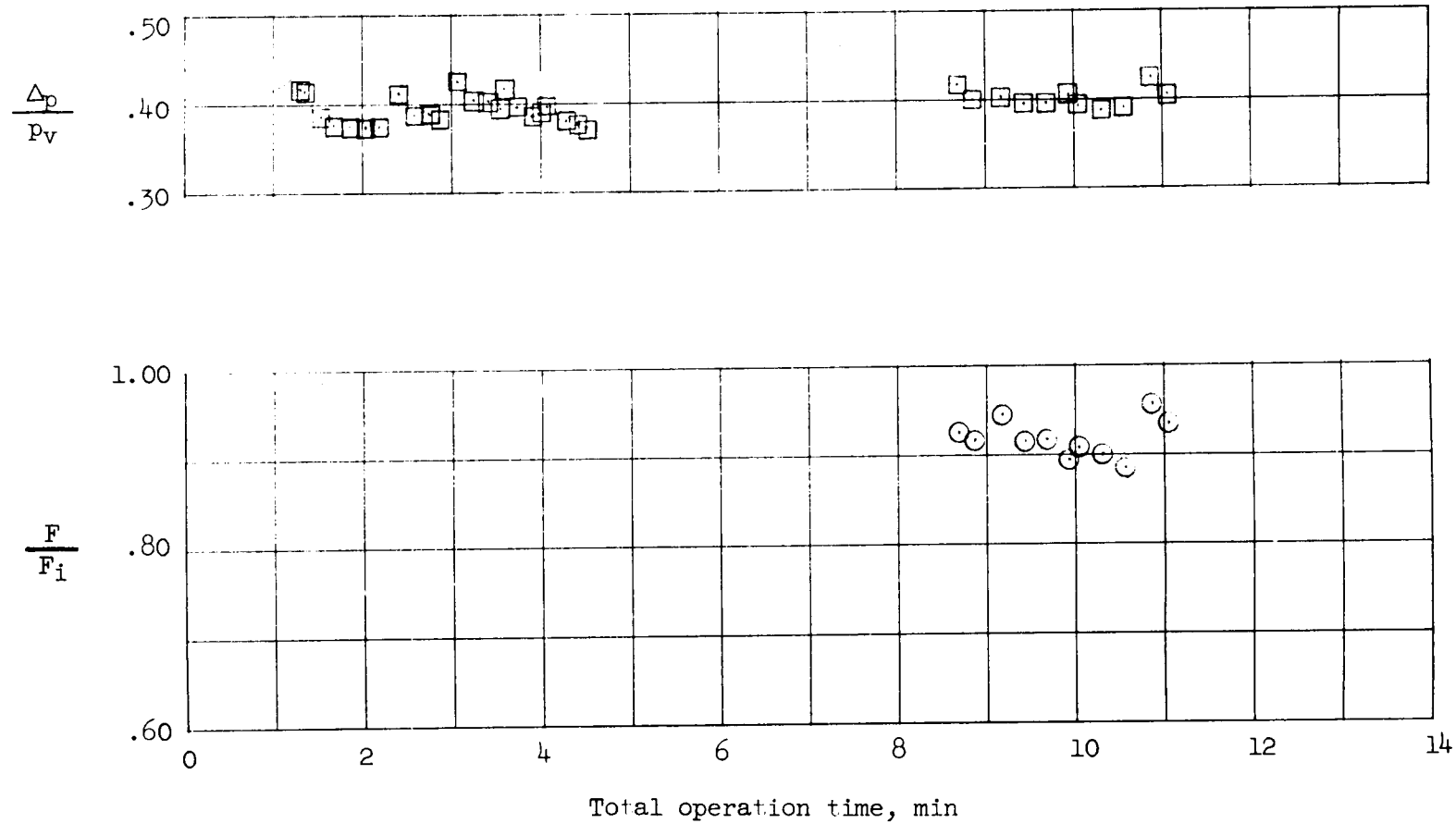

Figure 49.- Variation of thrust ratio and bed pressure drop with operation time for bed 7.

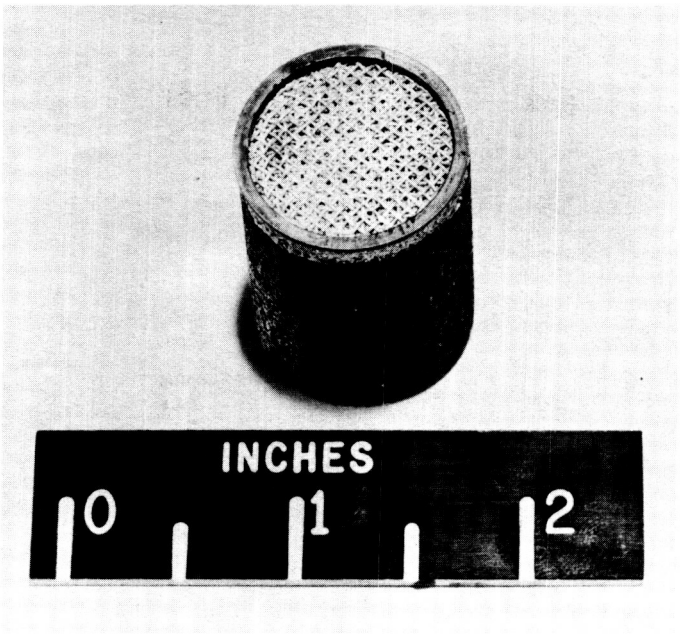

(a) Bed assembly. L-62-5005

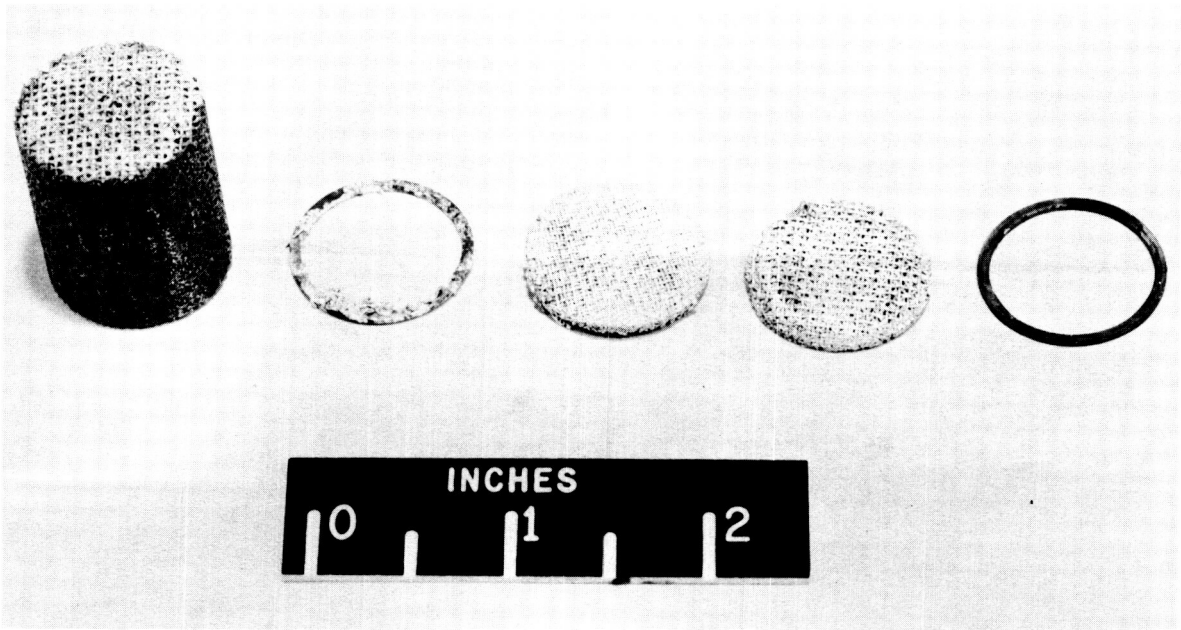

(b) Bed sections. L-62-5006

Figure 50.- Catalyst bed 7 after 8.18 minutes run time.

78

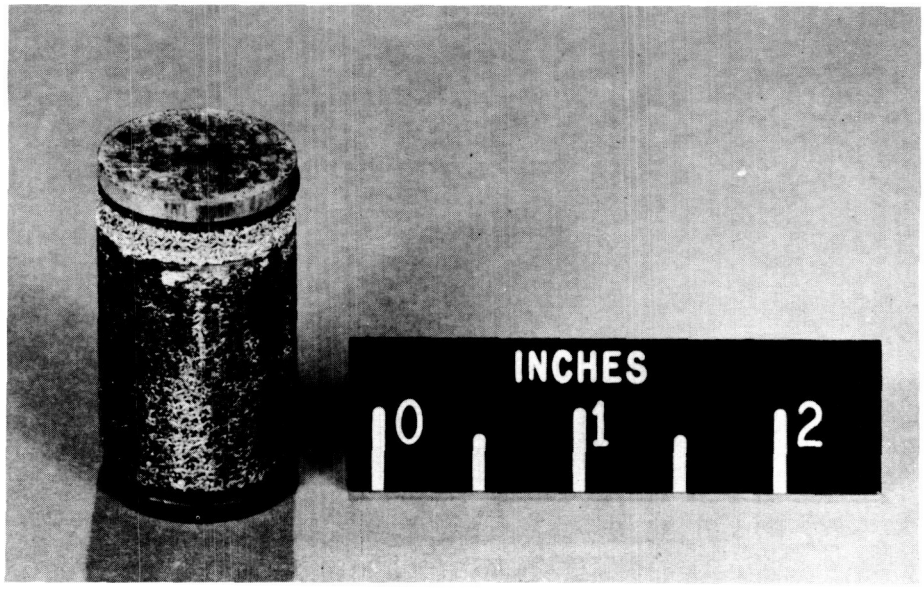

(a) Bed assembly. L-62-5925

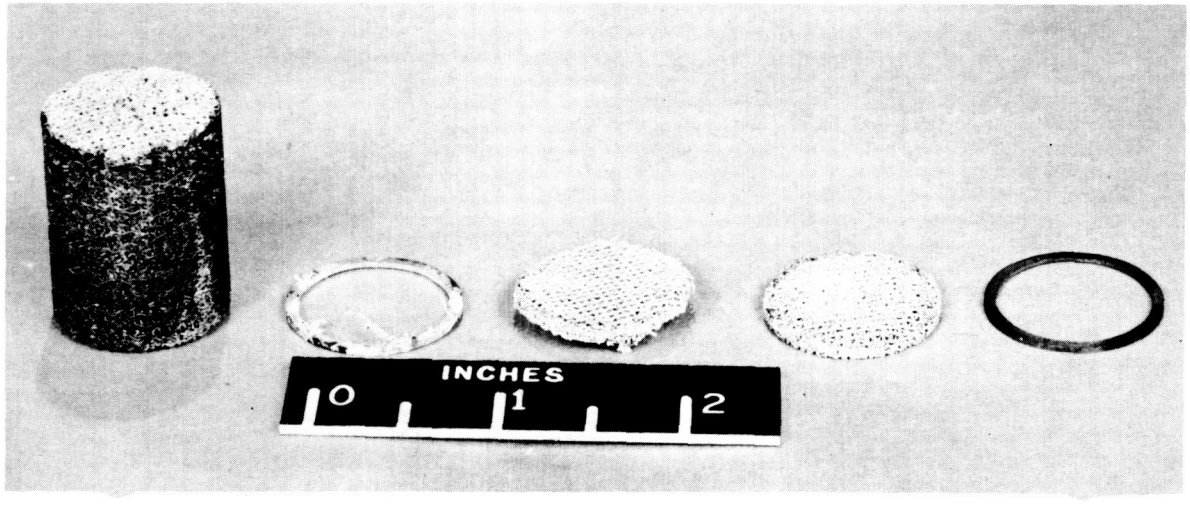

(b) Bed sections. L-62-5926

Figure 51.- Catalyst bed 7 after 16 minutes run time.

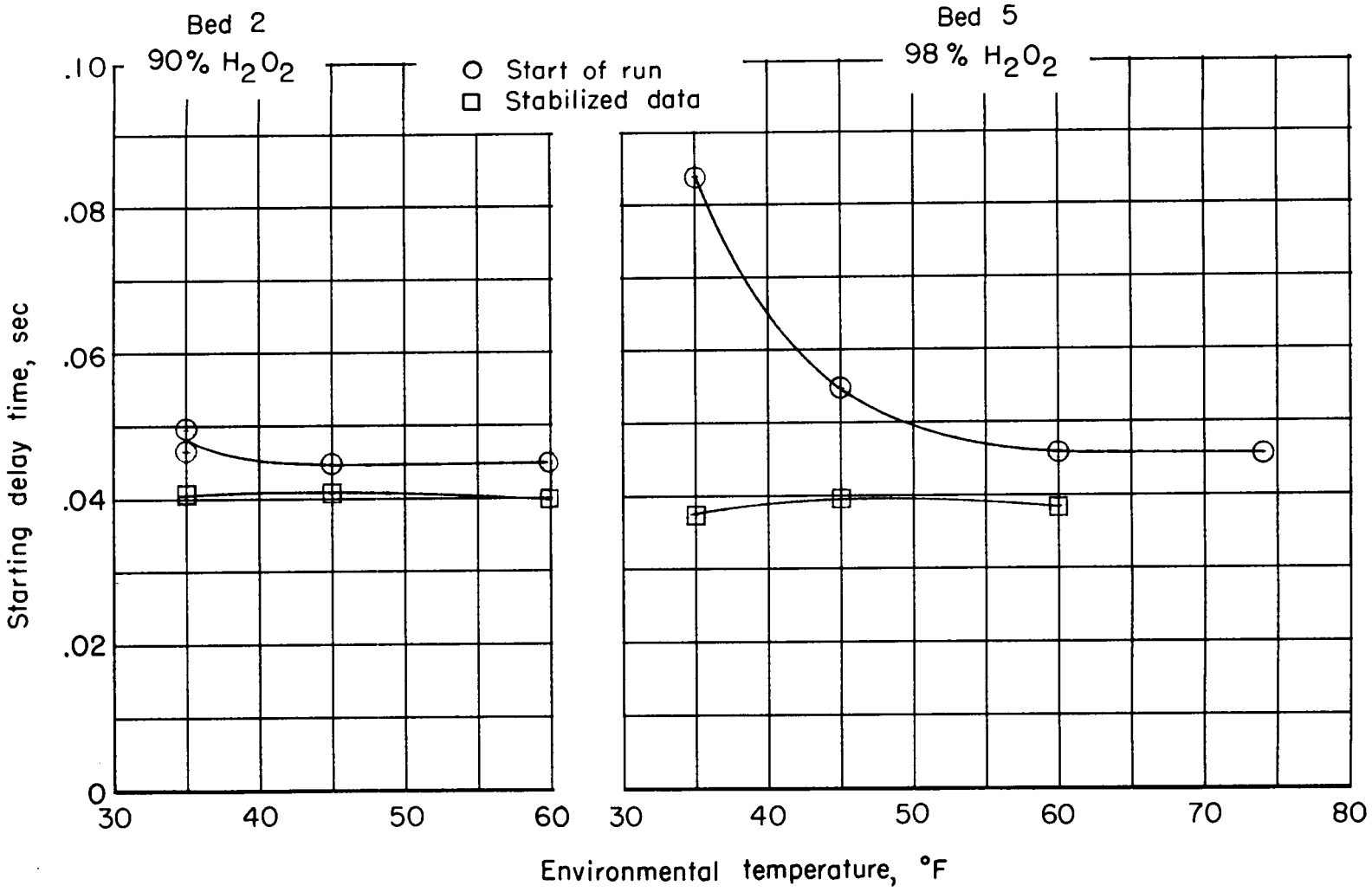

Figure 52.- Comparison of starting delay characteristics of a 90-percent-concentration with a 98-percent-concentration H_2O_2 catalyst bed at various environmental temperatures.

NASA-Langley, 1963